

# Design of a Sternal Fixation Device and Bicortical Bone Model

---

April 2013

A Major Qualifying Project Report:

Submitted to the Faculty of Worcester Polytechnic Institute

In partial fulfillment of the requirements of the Degree of Bachelor of Science

by

---

Aaron Behanzin

---

Brittany Dellasanta

---

Charlene Pizzimenti

---

Prof. Kristen Billiar, Major Advisor

---

Dr. Raymond Dunn, Co-Advisor

## Abstract

Failure to properly close the sternum after a sternotomy can lead to life-threatening complications. Current sternal fixation devices, including screw and plate systems, reduce the risk of complications and promote proper healing but are unable to provide both a flush fit with the sternum and prevent screw loosening, a problem demonstrated by cyclic testing. The first goal of this study was to optimize a screw and plate system that addresses this issue. The system utilizes a lag-lock mechanism that only permits locking of the screws after the plate has achieved a flush fit with the bone. Optimal screw parameters were determined using finite element analysis (FEA). The second goal was to design and characterize a sternal model that mimics the mechanical properties of bone for use in testing such systems. It was characterized using axial and lateral screw pullout tests, and compared to a widely used bone model. The results showed that the custom model performed in a manner similar to how real bone is expected to act, especially when compared to the standard model. From this, it was concluded that the custom bone model is well suited for comparing screw purchase.

## Table of Contents

<b>Abstract</b> .....	<b>2</b>
<b>List of Figures</b> .....	<b>6</b>
<b>List of Tables</b> .....	<b>8</b>
<b>Authorship</b> .....	<b>10</b>
<b>Acknowledgments</b> .....	<b>10</b>
<b>Chapter One: Introduction</b> .....	<b>11</b>
<b>Chapter Two: Literature Review</b> .....	<b>13</b>
<b>2.1 Clinical Statistics and Need</b> .....	<b>13</b>
<b>2.2 Human Sternum Anatomy and Physiology</b> .....	<b>13</b>
<b>2.3 Sternotomy</b> .....	<b>15</b>
2.3.1 Obstacles Related to Sternal Fixation.....	16
<b>2.4 Current Methods of Closure</b> .....	<b>16</b>
2.4.1 Non-Rigid Fixation .....	16
2.4.2 Rigid Fixation .....	18
<b>2.5 Screw and Plate System</b> .....	<b>20</b>
2.5.1 Screw Designs .....	20
2.5.1.1 Cortical and Cancellous .....	21
2.5.1.2 Standard and Locking .....	22
2.5.1.3 Self-tapping and Non-tapping .....	23
2.5.1.4 Screw Purchase.....	24
2.5.2 Plate Designs .....	25
<b>2.6 Previous Design Attempts</b> .....	<b>26</b>
2.6.1 Screw with Cap .....	26
2.6.2 Nested Screw.....	27
2.6.3 Reverse Expansion Screw .....	29
<b>2.7 Sternum Bone Model</b> .....	<b>30</b>
<b>Chapter Three: Project Strategy</b> .....	<b>32</b>

<b>3.1 Client Statement and Project Goals .....</b>	<b>32</b>
3.1.1 Initial Client Statement.....	32
3.1.2 Project Approach .....	33
<b>3.2 Objectives, Constraints, Function and Specifications .....</b>	<b>33</b>
3.2.1 Objectives .....	34
3.2.2 Constraints.....	36
3.2.3 Functions and Specifications .....	37
3.2.4 Revised Client Statement .....	38
<b>Chapter Four: Alternative Designs .....</b>	<b>39</b>
<b>4.1 Needs Analysis .....</b>	<b>39</b>
<b>4.2 Functions and Specifications .....</b>	<b>40</b>
<b>4.3 Design Alternatives.....</b>	<b>41</b>
4.3.1 Reverse Expansion Screw .....	43
4.3.2 Slanted Teeth.....	44
4.3.3 Lag-threaded Plate .....	44
4.3.4 Hexagonal Screw Head .....	45
<b>4.4 Conceptual Final Design .....</b>	<b>45</b>
<b>4.5 Feasibility Study and Experiment Setup .....</b>	<b>46</b>
<b>4.6 Proof of Concept Testing Results .....</b>	<b>47</b>
<b>4.7 Finite Element Analysis Results .....</b>	<b>48</b>
4.7.1 Plate Angle.....	49
4.7.2 Screw Head Height .....	50
4.7.3 Wing-Base Thickness .....	51
4.7.4 Screw Head Radius .....	52
4.7.5 FEA Validation.....	54
<b>Chapter Five: Design Verification .....</b>	<b>57</b>
<b>5.1 Testing Models .....</b>	<b>57</b>
<b>5.2 Testing .....</b>	<b>58</b>
<b>5.3 Testing Results.....</b>	<b>62</b>
5.3.1 Demonstration of Need for Lag-Lock Screw and Plate.....	62
5.3.2 Characterization of the Bicortical Sawbones Model .....	62

<b>Chapter Six: Discussion .....</b>	<b>65</b>
<b>6.1 Reverse Expansion Screw and Plate Design.....</b>	<b>65</b>
<b>6.2 Bicortical Bone Model.....</b>	<b>65</b>
6.2.1 Axial Pullout Testing .....	66
6.2.2 Lateral Pullout Testing.....	66
<b>6.3 Study Limitations .....</b>	<b>67</b>
<b>6.4 Impacts of Device .....</b>	<b>67</b>
<b>Chapter 7: Final Design and Validation .....</b>	<b>71</b>
Introduction.....	71
Methods .....	71
Results .....	73
Discussion .....	75
<b>Chapter Eight: Conclusions and Recommendations.....</b>	<b>77</b>
<b>References.....</b>	<b>78</b>
<b>Appendix .....</b>	<b>83</b>
<b>Appendix A: Sternal Fixation Device Pairwise Comparison Charts .....</b>	<b>83</b>
<b>Appendix B: List of Alternative Designs .....</b>	<b>86</b>
<b>Appendix C: Sternal Fixation Device Design Selection Matrix .....</b>	<b>88</b>
<b>Appendix D: Finite Element Analysis Data .....</b>	<b>89</b>
FEA Calculations .....	89
FEA Reports .....	90
<b>Appendix E: CAD Drawings of Final Plate and Screw Design .....</b>	<b>123</b>
<b>Appendix F: Protocol for Cyclic Loading and Failure Testing Preparation .....</b>	<b>125</b>
<b>Appendix G: Protocol for Cyclic Loading .....</b>	<b>129</b>
<b>Appendix H: Protocol for Axial Pullout Testing .....</b>	<b>130</b>
<b>Appendix I: Protocol for Lateral Pullout Testing.....</b>	<b>133</b>
<b>Appendix J: Cyclic Testing Displacement at Each Cycle .....</b>	<b>134</b>
<b>Appendix K: Axial Pullout Testing Maximum Force Sustained .....</b>	<b>135</b>
<b>Appendix L: Lateral Pullout Testing Summary Data.....</b>	<b>136</b>

## List of Figures

Figure 2.1: Sternum.....	14
Figure 2.2: Cross-sectional view of the sternum.....	14
Figure 2.3: Median sternotomy.....	15
Figure 2.4: Single peristernal and figure-eight closure methods.....	17
Figure 2.5: Sternal dehiscence.....	18
Figure 2.6: Single legged and double legged models of Talon device.....	19
Figure 2.7: Cross-shaped and Synthes Transverse Plate systems.....	20
Figure 2.8: Three parts of a self-tapping bone screw.....	21
Figure 2.9: Cortical screw and cancellous screw.....	22
Figure 2.10: Standard non-locking and locking screw.....	23
Figure 2.11: Tip of self-tapping and non self-tapping screws.....	24
Figure 2.12: Sectional view of unicortical and bicortical screws configuration.....	24
Figure 2.13: Example of plate designs for sternal fixation.....	25
Figure 2.14: Screw with cap design.....	26
Figure 2.15: Mechanical process of screw with cap.....	27
Figure 2.16: Nested screw design.....	28
Figure 2.17: Mechanical process of the nested screw.....	28
Figure 2.18: Mechanical concept of reverse expansions screw.....	29
Figure 3.1: Screw and plate system objectives tree.....	34
Figure 3.2: Bone analog objectives tree.....	35

Figure 4.1: Reverse expansion screw .....	44
Figure 4.2: Slanted teeth screw design.....	44
Figure 4.3: Screw used for lag-threaded plate design.....	45
Figure 4.4: Screw with hexagonal head.....	45
Figure 4.5: Custom Sawbone model.....	46
Figure 4.6: Flush fit between rapid prototype and wooden bone analog.....	47
Figure 4.7: Screw head locked into plate.....	48
Figure 4.8: Illustration of the reactions forces on the applied edge of the screw.....	49
Figure 4.9: 2D cross-sectional view of plate and screw, depicting plate angle.....	49
Figure 4.10: Cross-sectional view showing deformation of the screw.....	50
Figure 4.11: Screw head height.....	51
Figure 4.12: Cross-sectional view of screw head height.....	51
Figure 4.13: Wing of the screw.....	52
Figure 4.14: Cross-sectional view showing deformation of the screw.....	52
Figure 4.15: Screw head radius.....	53
Figure 4.16: Isomeric view of deformation.....	53
Figure 4.17: ABS plastic prototyped screw head.....	54
Figure 4.18: Cemented screw head.....	54
Figure 4.19: Load withstood at certain displacements .....	55
Figure 4.20: FEA showing compressive force.....	55
Figure 5.1: Standard Sawbone model.....	57

Figure 5.2: Standard screw and plate systems.....	58
Figure 5.3: Schematic of cyclic loading testing.....	59
Figure 5.4: Prepared specimen for cyclic and tensile testing.....	59
Figure 5.5: Cyclic loading testing set-up.....	60
Figure 5.6: Axial pullout testing set-up.....	61
Figure 5.7: Lateral pullout testing set-up.....	61
Figure 5.8: Displacement over elapsed cycles.....	62
Figure 5.9: Axial pullout testing results.....	63
Figure 5.10: Lateral pullout testing results.....	64
Figure 7.1: Reverse expansion screw concept.....	72
Figure 7.2: Cyclic loading test schematic.....	72
Figure 7.3: Axial pullout test schematic.....	73
Figure 7.4: Lateral pullout test schematic.....	73
Figure 7.5: Displacement over cycles.....	74
Figure 7.6: Finite element analysis.....	74
Figure 7.7: Axial pullout strength.....	75
Figure 7.8: Lateral pullout strength.....	75

## List of Tables

Table 2.1: Summary comparison of cortical and cancellous screws.....	22
Table 4.1: Design selection matrix.....	42
Table 4.2: Function means chart.....	43

Table 4.3: Plate angles and the corresponding force, deformation and stress.....	50
Table 4.4: Screw head heights and the corresponding deformation and stresses.....	51
Table 4.5: Wing-base thicknesses and the corresponding deformation and stresses.....	52
Table 4.6: Screw head radii and the corresponding deformation and stresses.....	53
Table 4.7: Measured and predicted screw head displacements.....	56

## **Authorship**

All Teams members participated in the writing of this paper.

## **Acknowledgments**

We would like to thank KLS Martin Company, especially Rich McLaughlin and Sean Burke for their support and funding for this project. In addition, we would like to thank Maximillian Ardini and Mehmet Kural for their help with the Instron machine.

## Chapter One: Introduction

Recent studies have shown that one third of Americans are affected by cardiovascular disease (CVD), a condition that can often lead to open heart surgery (AHA, 2009). To perform these and other thoracic procedures, the surgeon must first longitudinally bisect the sternum in a procedure known as a median sternotomy. At the end of the surgery, the surgeon fixes the two halves of the sternum together to allow the bone to heal.

In a portion of the population, sternal fixation related complications occur. Often the causes of these complications are the inadequacies of the fixation method used. The standard of care for repairing the sternum post-sternotomy is to wrap stainless steel wires around the sternum through the ribs to hold the hemi-sterna together. The wires tend to be inexpensive, easy to use, and quick to install. Although they can be effective in many patients, they have been linked to such complications as dehiscence and infection, especially in patients with special conditions including osteoporosis, which severely weakens the bone.

With approximately one in two women and one in four men over the age of 50 suffering from osteoporosis, new devices have attempted to address the challenge of fixating osteoporotic bone (National Osteoporosis Foundation, 2012). One of the most promising is the Talon device, which clamps the hemi-sterna together to permit healing; however, it is expensive, complicated to install, and bulky. Thus, it is not widely used. A second group of sternal fixation devices for osteoporotic bone is the screw-plate system. Despite resolving some of the problems with the wire and Talon fixation methods, screw and plate systems, such as the SternaLock Blu by BioMet, have disadvantages as well. These current models of screw and plate systems can only accomplish one of the two necessary functions: either the plate achieves an intimate fit with the bone to prevent movement of the system or the screw locks into the plate to avoid screw loosening.

There are no current devices on the market that successfully achieve rigid sternal fixation in osteoporotic bone. With the prevalence of CVD and osteoporosis, sternal fixation complications are a serious problem in the medical field. For this reason, there is a need for a safe and easy to use lag-lock screw for sternal fixation that can attain a friction fit with the sternum of an osteoporotic patient. While there have been attempts to develop lag-lock sternal fixation

devices in the past, the proposed designs have not been desirable; some contain several parts and as a result have complicated installation and removal procedures during surgery, while others have not been reduced to practice or validated.

In addition, to validate any sternal fixation device, a proper testing model is required. While human sterna show the most realistic properties that the device will experience, human sterna are very difficult to come by and differ greatly from person to person, allowing for a large variability between sterna. Uniform sternum models made of polyurethane foam are the most widely used model for sternal testing, however their main drawback is their uniform density that does not show the difference between the cortical and cancellous layers of real bone. Therefore, there is a need for a sternal model that can present repeatable and comparable results, while also mimicking the anatomy of the sternum more accurately with cortical and cancellous portions.

With this, the purpose of this project was to optimize, validate, and reduce to practice an improved lag-lock screw for sternal fixation and also to create a sternum bone analog for testing sternal fixation devices. This model should provide reproducible results that are representative of the expected performance of human bone.

## Chapter Two: Literature Review

### 2.1 Clinical Statistics and Need

In the year 2009, approximately one in three Americans was affected by cardiovascular disease (CVD), which was the cause of one in six deaths in the United States (AHA, 2009). With the continued prevalence of CVD, the need for open-heart surgery had also risen; the number of patients who received open heart surgeries as a result of CVD reached 646,000 by 2004 and has continued to grow since then (AHA, 2007). As the majority of patients suffering from CVD are over the age of 65, other factors such as osteoporosis, or the weakening of bone, have been taken into account as they have been linked to the possibility of post-surgical complications (AHA, 2009).

### 2.2 Human Sternum Anatomy and Physiology

In order to understand the process of a sternotomy and how the sternum is fixated after surgery, the anatomy of the sternum must first be understood. The sternum is a bone in the human body that lies vertically in the chest cavity. More specifically, it is found in the “median and anterior part of the thoracic skeleton” (Selthofer, et al, 43, 2006). Also known as the breastbone, the sternum runs from the neck area to the abdomen, supporting the ribs and clavicle, or shoulder bone (sternum, 2012). The sternum is divided into three parts: the manubrium, the body, and the xyphoid process (Figure 2.1) (Ferguson, 2012). The sternum is approximately seventeen centimeters long and one centimeter wide in adult humans, with the male sternum being slightly longer than the female sternum (Ferguson, 2012), (Gray, 2009).

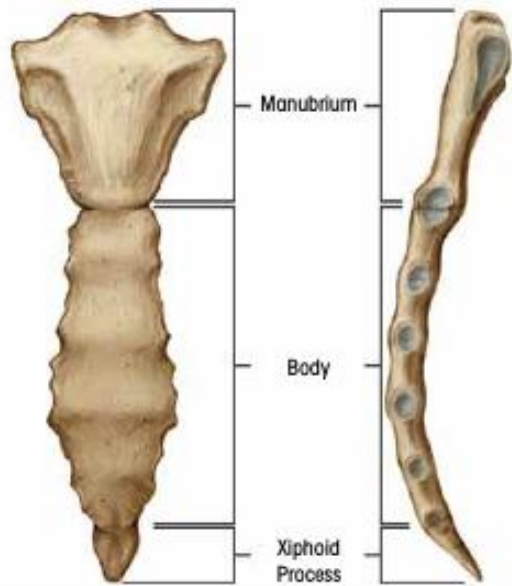


Figure 2.1: Sternum. This image illustrates the three parts of the sternum: the manubrium, the body, and the xiphoid process. (Ferguson, 2012)

There are two types of bone that make up the sternum: cortical and cancellous. Cortical bone is the dense outer layer of bone, acting as a hard shell that envelops the interior of bone. Cancellous bone, also known as the trabecular or spongy bone, is the inner bone layer (Figure 2.2). The cortical layer is stiffer and stronger than the cancellous bone because it is much denser. This difference in density assists the sternum in withstanding the forces that the chest experiences daily during respiration. (Ozkaya, N. & Nordin, M., 1998)



Figure 2.2: Cross-sectional view of the sternum illustrating the two different types of bone. (Ahn et al. 2009)

The sternum not only provides support to the ribs and clavicle (sternum, 2012) but also helps protect the inner chest organs, including the heart and lungs (Ferguson, 2012). As a result of its location in the body, the sternum experiences repetitive motion from respiration. During the act of inhalation, the ribs move upward and outward in the chest cavity, allowing the diaphragm to

contract, resulting in negative pressure. Exhalation then occurs, during which the diaphragm is moved up, and the ribs are moved closer together. The sternum experiences a large force during this process, as it is responsible for holding the rib cage together. (Koeppen, B. & Stanton, B., 2010)

### 2.3 Sternotomy

In order for the surgeon to perform open-heart and other thoracic surgeries, they first complete a median sternotomy. This involves longitudinally bisecting the sternum with a bone saw and then using a sternal retractor to separate the hemi-sterna, revealing the thoracic cavity (Kun & Xiubin, 2009). Figure 2.3 shows a schematic of the cuts made to the sternum in this procedure. Each year, approximately 750,000 median sternotomies are performed (Bek et al, 2010).

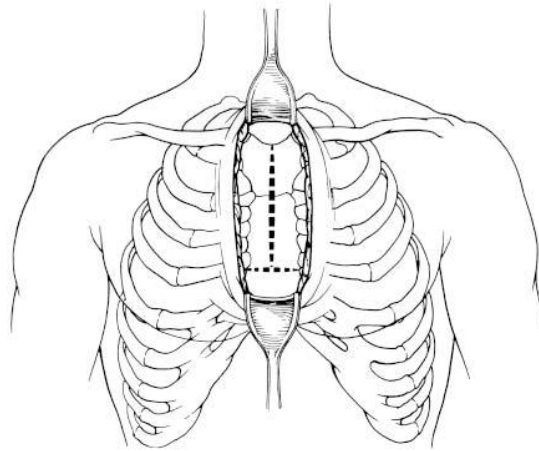


Figure 2.3: Illustration of a median sternotomy. The dotted lines indicate the location of the longitudinal bisection. (Stentless Xenograft Aortic Valve Replacement: Subcoronary insertion of the Toronto SPV valve- Figure 1) (pending copyright approval)

As with any surgical procedure, a significant number of patients who undergo a median sternotomy experience complications. Depending on the complication, the mortality rate of patients varies from 14-47% (Honguero Martínez, 2005). The most common complication is sternal dehiscence, a separation of the sternum before healing is complete. This occurs in 0.5-8.0% of patients and has a mortality rate of up to 40%. Another common complication is mediastinitis, an infection of the tissues near the sternum. Both of these complications are most common in people who are over the age of 75, are morbidly obese, or have a history of osteoporosis. (Bek et al, 2010) Sternal instability, which can cause bone damage and stress, can

be another possible outcome of this procedure (Voss, 2008). These complications are typically caused by ineffective or non-rigid sternal fixation systems.

### **2.3.1 Obstacles Related to Sternal Fixation**

If the sternum is somehow injured, two important factors impact its healing. First, due to the central location of the sternum in the chest cavity, any internal device used to secure the sternum so that it can heal risks damaging neighboring organs. Most critically, the heart and lungs lie directly behind the sternum, making the improper implantation of any device in this region dangerous. Devices used in sternal fixation must allow the surgeon to implant it without damaging other organs and must not cause damage after the surgery as it remains in the body even after the bone has healed. (Dunn. Personal Interview, 2012)

In addition, the sternum and other bones can become weak and harder to fix when affected by osteoporosis, a disease that makes bone brittle and prone to breakage. This condition occurs when the body ceases or reduces bone remodeling. Usually, osteoporosis worsens with time and can affect both males and females. In the United States alone, approximately 10 million people suffer from osteoporosis. (National Osteoporosis Foundation, 2011)

## **2.4 Current Methods of Closure**

There are several current methods of fixating the sternum post-sternotomy. These methods are divided into two groups: non-rigid and rigid.

### **2.4.1 Non-Rigid Fixation**

Non-rigid fixation of the sternum is the oldest and most popular method of sternal fixation. Cables, wires, or polymer sutures can be used to fixate the sternum in a manner that does not completely inhibit motion of the sternal halves after surgery. The non-rigid method of fixating the sternum that involves cerclage wires has been proven superior to other non-rigid fixation methods, and it has been widely accepted among surgeons (Ozaki, 1998).

Wire fixation was first introduced in 1897, and gained popularity in 1957 when it became the standard of care for sternal closure (Ozaki, 1998). Stainless steel wires can be applied to the

sternum in many different configurations, but the most prevalent are the single peristernal and the figure-eight closure method (Figure 2.4) (Chao, 2011) (Losanoff, 2002). During the application of the single peristernal technique, five to eight wires are wrapped around the sternum between the ribs. The wires are then twisted to tighten them around the sternum. The ends are bent and buried in the tissue anterior to the sternum, and the chest is closed. (Losanoff, 2002) Often for better fixation, additional holes are drilled in the manubrium on both hemi-sterna so that the wires can be threaded through them and tightened as described above (Dunn. Personal Interview, 2012).

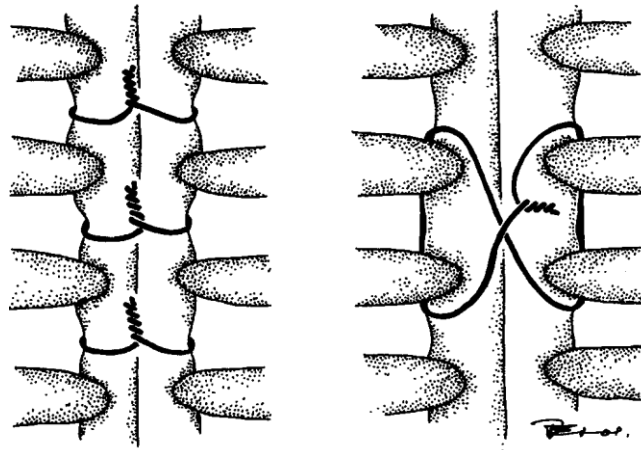


Figure 2.4: Single peristernal (left) and figure of eight (right) closure methods. Note the differences between two wiring techniques. (Losanoff et. al, 2002) (pending copyright approval)

The wire fixation method is widely popular among surgeons. This popularity is largely due to the low cost of wire, the rapid and simple installation, and the relative safety of the process in most patients (Ozaki, 1998). Furthermore, the familiarity of the surgeons with this method, as well as the easy removal of the wires, makes it advantageous (McGregor, 2003).

Despite these advantages, wire fixation complication rates have been reported to range between 0.5% and 8% with high mortality rates up to 40% (Bek, 2010). These complications are most often caused when steel wires cut through osteoporotic bone and sternal dehiscence occurs (Figure 2.5). Sternal dehiscence can then induce other minor and major post-surgical complications (McGregor, 2003), including mediastinitis, chronic sternal instability, and incision pain due to motion (Cohen, 2002) (Ozaki, 1998) (Pai, 2005). Wire failure due to cyclic loading and wire corrosion can also account for these complications on a smaller scale (Chao, 2011).

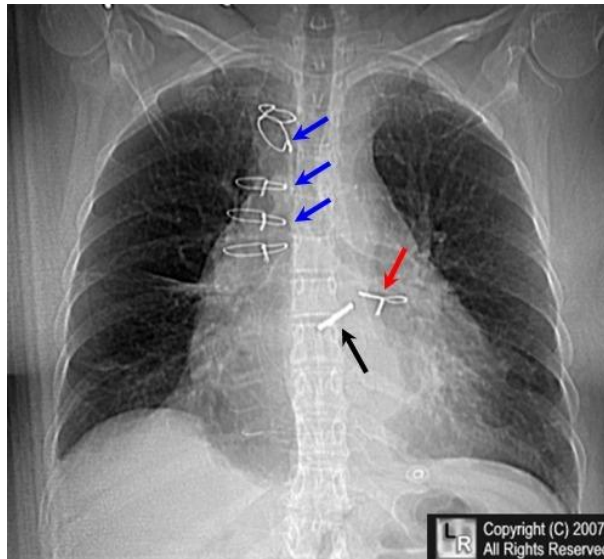


Figure 2.5: Sternal dehiscence. The blue arrows show wires that displaced towards the right side, the red arrow indicates the wire that displaced to the left, and black arrow indicates a prosthetic aortic valve. (Herring, n.d.)

In addition to these problems, cerclage wires can also damage or disrupt blood vessels that pass through the sternum. The wires wrap tightly around the sternum and, as a result, prevent proper blood flow to bone. The damage may induce ischemia, delayed wound healing, and increased complication rates. (Ozaki, 1998)

#### 2.4.2 Rigid Fixation

Several rigid fixation devices have attempted to prevent the complications known to be associated with non-rigid fixation. For injuries in other regions of the body, rigid fixation has replaced wire fixation (Ozaki, 1998). The Talon device produced by KLS Martin is a sternal closure device that provides rigid fixation of the hemi-sterna without any screws or wires. It consists of two mated parts that are locked together using a ratchet mechanism. This device comes in both single- and double-legged models (Figure 2.6) (Levin, 2010). To install the Talon, the legs are placed in between ribs, and the two halves of the device are joined, tightened, and locked. The ratchet mechanism locks and stabilizes the system. (KLS Martin, 2008)



Figure 2.6: Single legged (left) and double legged (right) models of Talon device by KLS Martin. Note the absence of screws and presence of the ratchet mechanism that holds the two parts of the Talon together. (KLS Martin, 2012)

As with any device, the Talon has both advantages and disadvantages. The main advantage is that it can be used in patients with morbid obesity, diabetes, chronic pulmonary disease, and osteoporosis (Martin, 2012) (Levin, 2010) (Baciewicz, 2011). In a recent study of 42 patients with the Talon device, none of the patients developed post-surgical complications nor were there any device-related deaths (Levin, 2010). Although the Talon shows promise, it is not popular among surgeons because of its various disadvantages. The device is extremely expensive; prices for the single- and double-legged Talon are \$1,295 and \$1,495, respectively (Levin, 2010). In comparison, cerclage wire prices range from \$16 to \$41 per ten meters of wire (Cerclage Wire, n.d.). In addition, its bulkiness and complicated installation make the Talon unappealing to surgeons (Buckley et al., 2012).

A second type of rigid fixation is the screw and plate system, which comprises metallic plates and associated screws that tightly fixate the sternum and hinder motion at the wound site. These systems have applications in various orthopedic procedures, such as craniofacial and orthopedic reconstruction. They provide more stability than wires in sternal fixation (Pai, 2005). Two examples of these screw-plate systems can be seen in Figure 2.7.



Figure 2.7: Cross-shaped (left) and Synthes transverse plate (right) systems in human body. Note the drastic differences between the two plate designs. (Raman, 2007) (Plass et. Al, 2006)

## 2.5 Screw and Plate System

There are multiple screw-plate system designs for sternal fixation, each with its own specific parameters and applications. The different designs depend on multiple variables such as bone type, bone geometry, and bone quality.

### 2.5.1 Screw Designs

Screws are widely used in plate fixation devices. They are designed according to their specific clinical functions. A typical screw is comprised of three major regions: the head, the threads or shank, and the tip (Figure 2.8) (Park & Lakes, 1992). The function of the screw, such as the location of its use and the kind of bone into which it purchases, inspires alterations in these parts of the screw (An, Y. 2002).

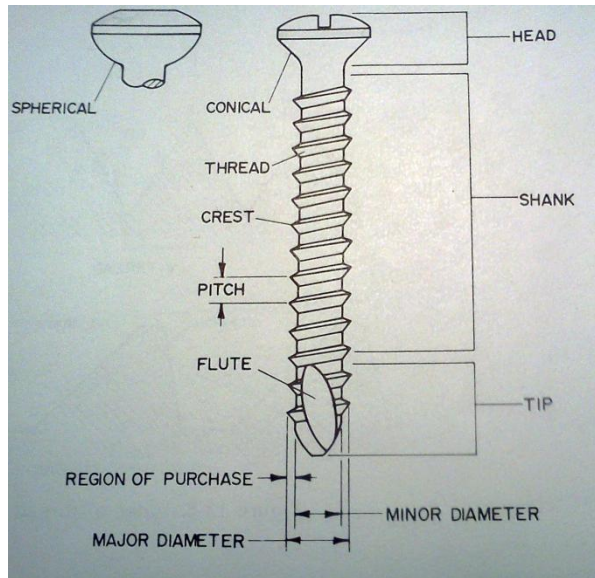


Figure 2.8: Illustration showing the three parts of a self-tapping bone screw. (Park & Lakes, 1992) (pending copyright approval)

In osteoporotic bone, the screw should be placed parallel to the cancellous trabeculae. It should have the largest tolerable major diameter, and it should gain stability from cortical bone rather than cancellous. (An. Y, 2002) Screw designs can be classified as cortical or cancellous, locking or non-locking (standard), and self-tapping or non-tapping.

### 2.5.1.1 Cortical and Cancellous

Due to the different mechanical properties of cortical and cancellous bone, different types of screws are used in each type of bone. Cortical screws have closely spaced, shallow threads and a larger minor to major diameter ratio compared to that of cancellous screws.

In contrast, cancellous screws are typically inserted through one layer of the cortical bone, with the majority extending into the cancellous bone layer. Because of the porous nature and consequent low mechanical properties of trabecular bone, cancellous screw threads have large surface areas in contact with the bone tissue in order to provide and maintain mechanical stability. (Banks et al, 2001) As a result, these threads have greater depth and pitch than cortical screw threads (Figure 2.9). Table 2.1 summarizes the main differences between cortical and cancellous screws.

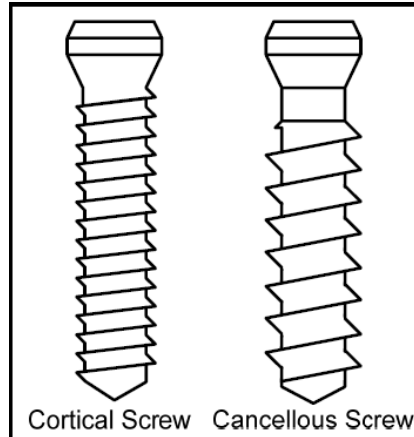


Figure 2.9: a) Cortical screw (left): small pitch and shallow threads and b) cancellous screw (right): large pitch and deep threads. (Decoteau, 2006)

Table 2.1: Summary comparison of cortical and cancellous screws

Parameters	Cortical Screw	Cancellous Screw
Pitch	Small	Large
Thread Depth	Small	Large
Thread Count	Large	Small

### 2.5.1.2 Standard and Locking

Like the threads and length of the screw, the head can be altered for different applications. The two basic kinds of screws are standard (non-locking) and locking (Figure 2.10). Standard screws have no mechanism that allows them to lock to the plate. In contrast, locking screws are equipped with a locking mechanism that fixes the screw tight to the plate and prevents its loosening. The majority of locking screws have heads that thread into the plate, locking it in place.



Figure 2.10: Standard non-locking (left) and locking screws (right). The locking screw has a threaded head, which locks in the plate, while the non-locking screw has no feature on its head. (OrthoHelix Surgical Design, Inc) (pending copyright approval)

### 2.5.1.3 Self-tapping and Non-tapping

The insertion method of the screw into the bone categorizes them into two different groups: self-tapping and non-self-tapping (Figure 2.11). Self-tapping screws bore their own hole while being inserted into the bone and therefore do not require pre-drilling. They tend to have sharp tips, which may vary in shape. In contrast, non-self-tapping screws require a hole to be drilled before it is inserted into the bone. These have a duller tip, which may reduce the risks of excessive tissue damage. One of the disadvantages of using pre-drilled screws is that it requires an additional step when inserting. (Park & Lakes, 1992) Self-tapping screws are commonly used in sternal fixation devices.

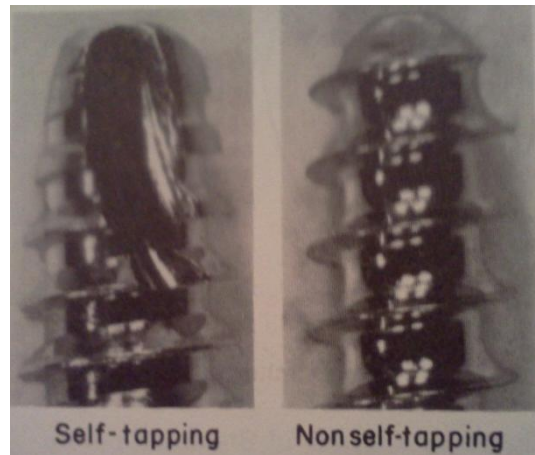


Figure 2.11: Tip of a self-tapping (left) and a non self-tapping (right) screw. Notice that the non self-tapping screw has a duller tip compare to the tip of the self-tapping screw. (Park & Lakes, 1992) (pending copyright approval)

#### 2.5.1.4 Screw Purchase

There are two types of purchase that a screw can achieve in bone: unicortical and bicortical. Fixation where the screw does not extend into the second layer of cortical bone is known as unicortical fixation, while bicortical fixation is that in which the screw penetrates both cortical layers of the bone (Figure 2.12).

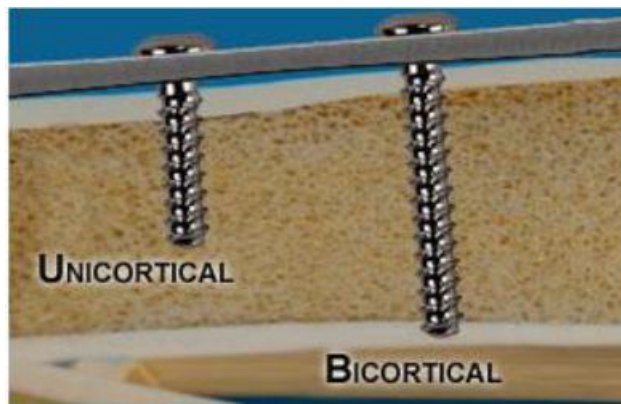


Figure 2.12: Sectional view of unicortical and bicortical screw configuration within the sternum. (Bakalova et. al, 2010)

Although bicortical purchase is desirable because of the added stability, it is not favored for sternal fixation because the screw pierces through the posterior sternal wall. This greatly risks puncturing nearby tissues and vital organs located behind the sternum (Hosam et al., 2009).

Therefore, unicortical purchase is preferred in sternal fixation because it does not pose any risks to the organs near the sternum. The parameters of the two types of screws can be combined to increase the pullout strength.

### 2.5.2 Plate Designs

Sternal fixation plates vary in design to accommodate different sizes and shapes of sternum. The topography, geometry, and locking mechanism of the plates affect the force distribution, amount of pressure on the sternum, and forces exerted on the screw and plate (An.Y, 2002). Plates used in sternal fixation must complement the screws used in the system in order to be effective. Common examples of plate designs are straight plates, X-plates, and H-plates (Figure 2.13).

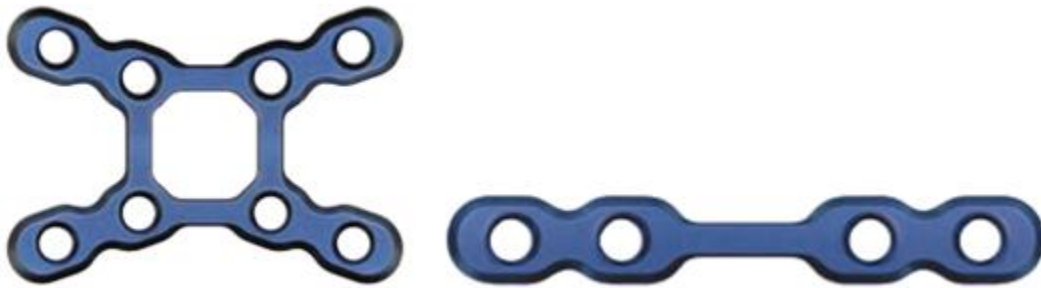


Figure 2.13: Example of plate designs for sternal fixation. Parts of SternaLock® Blu System. a) 8 hole X-plate (left). b) 4-hole straight plate (right). (BioMet Microfixation) (pending copyright approval)

Straight plates are linear fixtures with holes that may differ in size for screw entry. They can be bent to accommodate variations in the sternum shape. Contrastingly, X and H-plates have a similar design concept, but are shaped like an X and H respectively. Both are more effective than straight plates because they distribute the force across a larger area in a stronger and denser region of sternum. A study by Ozaki et al. showed that straight plates do not optimize rigid fixation as well as H-plates. According to the study, the geometry of the straight plate caused the screws to be placed in a less dense area of the bone, which lead to small fractures and loosening. (Ozaki 1998)

Screw placement also has an effect on the healing of bone. Some of the screws are placed near the fracture site, while others are placed as far from the fracture site as possible. Having screws

in both locations minimizes the strain within the plate. In osteoporotic bone, it is recommended that longer plates with widely spaced screws be used in fixation. (An, Y. 2002)

## 2.6 Previous Design Attempts

Because rigid fixation devices currently on the market do not satisfy the needs of the consumer, previous Major Qualifying Projects (MQP) at WPI have attempted to achieve what current devices do not. They aimed to achieve a flush fit between the screw and plate with an easily installed lag-lock screw. Ultimately, these designs were either rejected by the client or never reduced to practice on a clinical scale. The shortcomings of these designs have been considered in the completion of this project.

### 2.6.1 Screw with Cap

One of the MQP designs was a screw-plate system with a two-piece screw: the screw itself, and a threaded cap (Figure 2.14). The screw provides a friction fit between the plate and bone, and then the cap locks into the plate to prevent loosening.

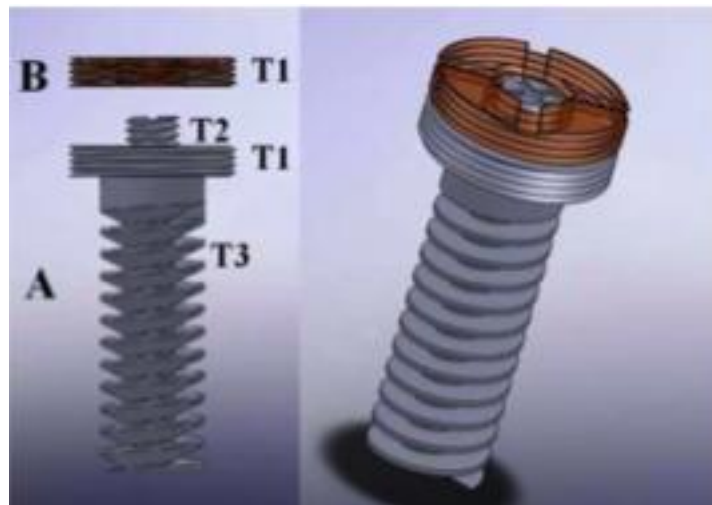


Figure 2.14: Screw with cap design: The screw component is inserted into the plate and then the cap is screwed on top to lock the screw in the plate. (Ahn, et. al, 2009)

During installation, the entire system is first put into the plate, bypassing initial threads, and nestling into an open area. Once the screw presses the plate and bone surfaces tightly together, the cap was then raised into the bypassed threads above the head by reverse tightening. The

interlocking threads then lock the cap into place so that it cannot loosen. An illustration of this system is shown in Figure 2.15. (Ahn et. al, 2009)

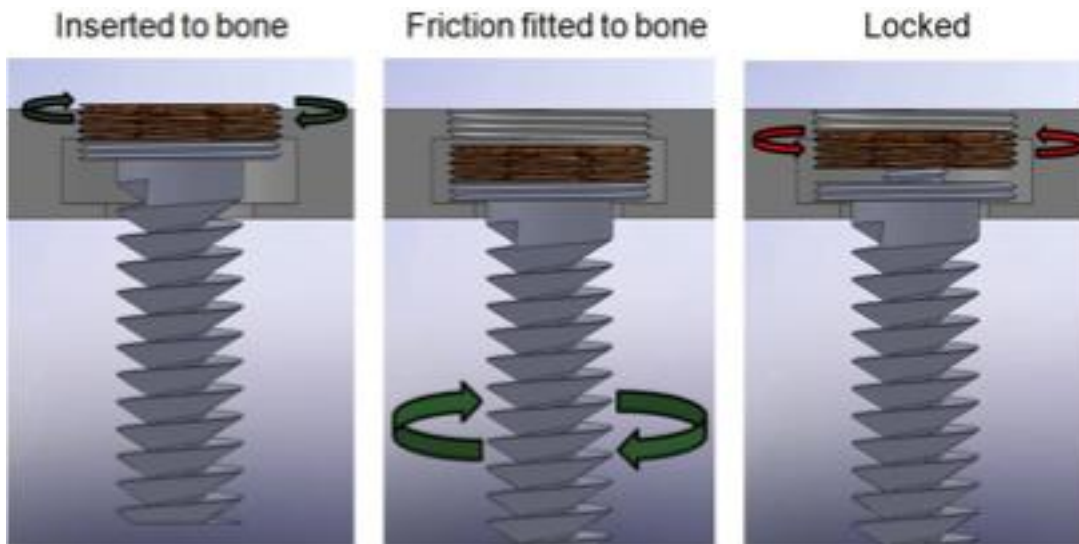


Figure 2.15: Mechanical process of bone fixation device: the screw is first inserted in the bone through the plate (far left). After friction fit is achieved (middle) the cap is then screwed in the plate on top of the screw to lock it to the plate (far right). (Ahn et. al, 2009)

The major disadvantage of this design was having a screw that comprises two pieces. This was unappealing to the clients because extra pieces require more time for installation during a surgery, and the small second piece is difficult to handle during the procedure. Together, these could cause more complications.

### 2.6.2 Nested Screw

The nested screw design comprised a smaller screw nested inside a larger one that provides the friction fit between the plate and the bone. The smaller screw forces the larger one to expand and lock into the plate. As seen in Figure 2.16, the inner screw is much smaller than the outer one.



Figure 2.16: Nested screw design: The smaller, inner screw is inserted in the larger screw, causing the outer to expand into the plate. (Song et. al, 2011)

The screw is provided to the surgeon as one piece, with the inner screw already located inside the outer. Once the unit is placed into the plate, the surgeon tightens the system as they would any other surgical screw, bringing the plate flush with the sternum. To ensure the screw locks into the plate, the surgeon then tightens the inner screw, forcing the ridges in the outer screw to embed themselves into the walls of the plate (Figure 2.17). (Song et. al, 2011)

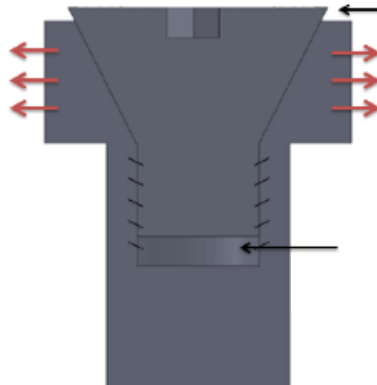


Figure 2.17: Mechanical process of the nested screw expanding due to the insertion of the inner screw. (Song et. al, 2011)

A disadvantage of this design was that it would require a larger force to fully insert the screw into the plate than the surgeon can safely use. This was a result of the titanium material used to manufacture the screw. A second disadvantage was that it would take more effort to remove if a revision surgery were required. The inner screw would first be pried out using extra tools before the outer screw would be removed. (Song et. al, 2011) In addition, the extra part makes it more difficult to handle in the operating room, similar to the screw and cap design.

### 2.6.3 Reverse Expansion Screw

The most recent design was deemed the “Reverse Expansion Screw Head”. This design consisted only of a screw and plate, where the screw head deforms as it is tightened (Figure 2.18). (Buckley et. al, 2012)

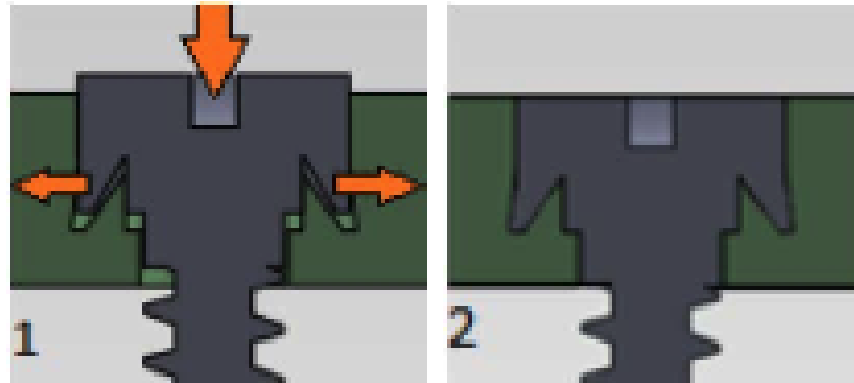


Figure 2.18: Mechanical concept of reverse expansions screw. (1) As the screw is inserted into the plate, (2) it will slowly deform and lock into the plate. (Buckley et. al, 2012)

When the surgeon inserts the screw into the plate, it is tightened like a typical screw. Once the plate lies flat on the sternum, the screw is locked into place via deformation. The custom plate has a ridge over which the screw head must fit in order for it to lock into place. When the surgeon applies pressure to the screw, it deforms into the indentations because the trough in the head is at slightly sharper angle than the ridge on the plate. This locking mechanism showed promise, but was not designed or tested on a clinical scale. (Buckley et. al, 2012)

There are several advantages to this design, including the single-piece screw and the ease of installation. The design does not require any predrilled holes in the sternum and is not bicortical. This design also demonstrated flaws, such as the angle at which the screw must be inserted into the plate. This design was also not tested on a reasonable scale, and no prototypes using appropriate materials were made or tested. (Buckley et. al, 2012) Thus, reliable testing of the design is required in order to validate and reduce it to practice.

## 2.7 Sternum Bone Model

Currently testing of such sternal fixation devices is completed on either human cadavers or standard polyurethane sternum models (Sawbones), both of which have flaws. While human sterna give the most accurate data as to how a system tested on it will act *in vivo*, it is quite difficult to come by. In addition to the small sample size, there is extreme biological variability between each human sternum. Bone also takes extra care when being used and is costly. (Ali et al, 2006) (Trumble, 2002)

As an alternative to human cadavers, polyurethane foam sternal models are widely used for testing studies. These models are created to be consistent in size and shape from model to model, and can also be made to model any density (Hausmann, 2006). The uniformity between models assures that numerous models will have the same mechanical properties for each test, resulting in reliable and comparable data (Ali et al, 2006). In most cases, these standard models cost less than what it takes to obtain human cadavers, and they require no special care when being stored and used, and do not need to be approved by the ethics committee (Hausmann, 2006).

A study comparing the use of human sterna and standard Sawbones yielded results in favor of using the sternal model. The similarity between the biomechanical properties of the model and the cadaver was deemed close enough for these models to be used in place of actual bone for testing purposes. The sternal models were also suggested for other reasons: lower cost, quicker preparation allowing for more tests in shorter period of time, lower variability in the data collected, and the ability to perform different tests on more than one model instead of forcing all tests to be completed on one model. (Trumble et al, 2002)

The main drawback of the standard Sawbones models is that they do not share all of the same properties as human sterna, including the bone structure and viscoelastic properties (Ali et al, 2006). For this reason, standard Sawbones models may not be a good representation of real bone.

With the consistent disadvantages of both human cadavers and standard Sawbone models, it was necessary to create a new sternum model that addresses these problems, representing real bone more accurately and yielding reproducible results.

## Chapter Three: Project Strategy

The purpose of this project was to design a screw and plate system that could be tested, evaluated, and put into practice and to design a sternal bone analog that could provide reproducible results similar to human sterna. There are 750,000 median sternotomies performed each year, most resulting from open-heart surgeries (Bek et al, 2010). As a result, a sternotomy is performed. To repair the sternum post-surgery, a screw-plate system must be put into place on the sternum, effectively holding the two hemi-sterna together and assuring the sternum heals correctly. The current standard of care is not suitable for osteoporotic bone, and therefore a new screw-plate system must be designed. In addition, there is no testing model available that can easily provide reproducible results similar to the data that may be collected using human sterna.

### 3.1 Client Statement and Project Goals

The most logical approach to create a new screw and plate system was to optimize the reverse expansion screw and plate system. This design included the delayed locking of the screw to the plate upon screw tightening during closure of the sternum. Past projects that focused on this problem were also analyzed. These provided information about and strategies for improving the anti-wobble idea and rigid sternal fixation, as well as minimizing bone stripping. To create a new bone model, the problems associated with human sterna and other common bone models were analyzed.

The two major clients of this project were Dr. Dunn, Chief of Plastic Surgery at the University of Massachusetts Medical School (UMMS), and KLS Martin, a company that specializes in making surgical products, specifically sternal fixation devices. In addition, the bone analog could be used by various researchers whose research required testing on sternal models.

#### 3.1.1 Initial Client Statement

*Repair of a sterna following sternotomy can be accomplished with a variety of wire or rigid plate fixation methods. However, with osteoporotic bone of elderly individuals, a significant issue is that wire closures can cut through the bone making wires less desirable. With rigid plate fixation,*

*the screws used for plate fixation may loosen and put out of the sterna as natural loading occurs. The objective of this project was to determine optimal screw design parameters for stable rigid sternal fixation. More specifically, a novel screw designed last year, but never reduced to practice. Your challenge was to iterate the design as necessary, create prototypes, and validate the design.*

### **3.1.2 Project Approach**

The first goal of this project was to improve and validate the previous screw and plate design so that it would fulfill the needs of the clients. In examining the literature, the main objectives, constraints, specifications, and functions were identified. In order to accomplish this task, the reverse expansion screw design was first analyzed and critiqued. Next, the design was iterated to optimize it using finite element analysis, and a final design sent to be manufactured by KLS Martin.

In planning for testing of this screw and plate design, a second goal arose to create a better bone analog from which reproducible data could be gathered, and that mimicked the anatomy of human sterna better than sternal models currently on the market. To create this model, the current bone analogs were compared against the expected behavior of human sterna for anatomical differences. Based on these differences, a new model was then designed; it consisted of two layers, each of different densities and thicknesses to mimic the cortical and cancellous layers of human bone. These models were then created by Sawbones Company, and tested in axial and lateral pullout to characterize their performance. Tests were completed using unicortical locking and non-locking screws, as well as bicortical locking and non-locking screws. All tests were completed and compared against tests in the standard bone model that has a uniform density.

### **3.2 Objectives, Constraints, Function and Specifications**

When beginning the project, several factors that would influence the design were considered and sorted into four categories: objectives, constraints, functions, and specifications. The factors associated with each category are discussed below.

### 3.2.1 Objectives

The main objectives that the screw and plate system design needed to meet were manufacturability, ease of use, effectiveness, and safety, while the bone analog needed to possess bone properties and give easily replicated results. The objective trees in Figure 3.1 and 3.2 are a visual representation of these objectives and their contributing factors.

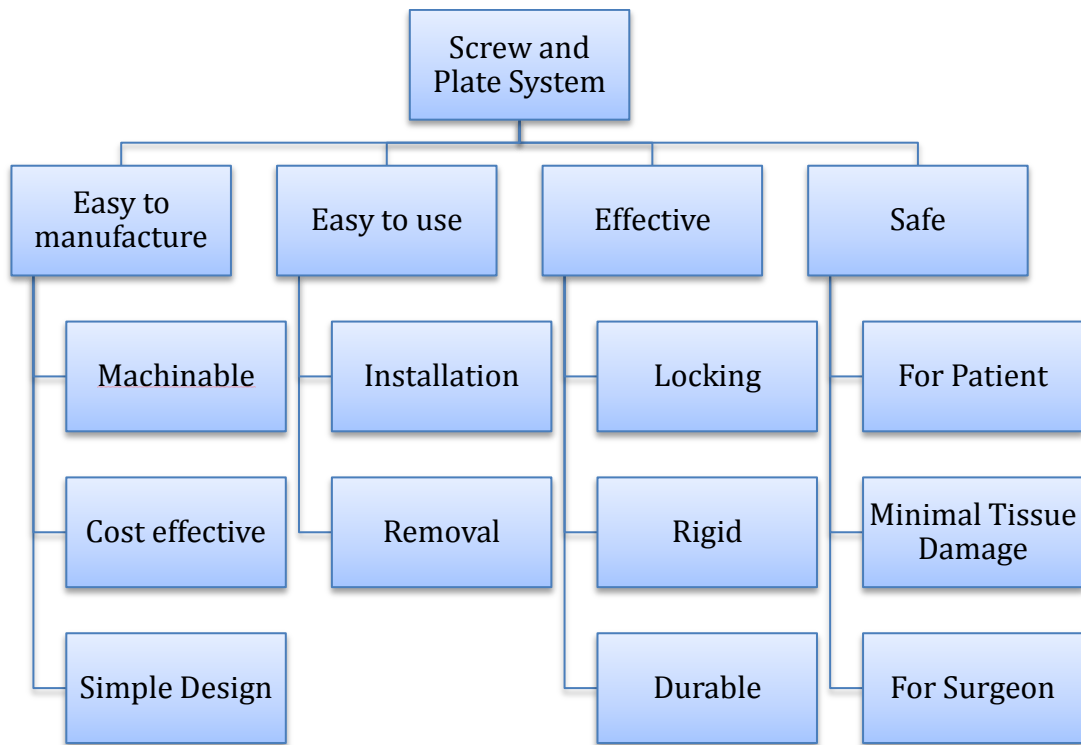


Figure 3.1: Screw and plate system objectives tree

**Easy to manufacture:** Our rigid sternal fixation device had to be manufactured efficiently. To achieve this, it had to be possible to fabricate the device using standard machinery and readily available materials. The manufacturing process also had to be cost effective, as we did not have access to unlimited resources for this project.

**Easy to use:** The device had to be easy for the surgeon to use. The most important factor in the usability of this device was in its installation. The surgeon must be able to install the system quickly to avoid complications and costs associated with a longer surgery. In addition, it should be possible to easily remove the device in a case a second surgery is required.

**Effective:** The sternal fixation device had to be effective in holding the hemi-sterna together post-sternotomy. For the device to be effective, the screw should be able to lock into the plate, preventing the screws from loosening due to the cyclic loading during respiration. The device also had to be rigid to prevent dehiscence and allow the bone to heal. The plate was to lie flat on the sternum to both reduce bulkiness and prevent the plate from shifting, which could apply excessive shear stress to the screws and bone. Finally, the device had to be durable so that it could remain in the body for the entirety of the patient’s life. Therefore, it had to be able to withstand loading from respiration, movement, and delivered impacts without deteriorating or shifting.

**Safe:** The sternal fixation device had to be safe for both the patient and the surgeon. Any screws used in the device had to be unicortical. This type of screw does not extend into the posterior layer of cortical bone, eliminating the risk of damage to the heart and other vital organs located directly behind the sternum. It was also vital that the use of the device and its parts pose no risks to the surgeon during both installation and removal.

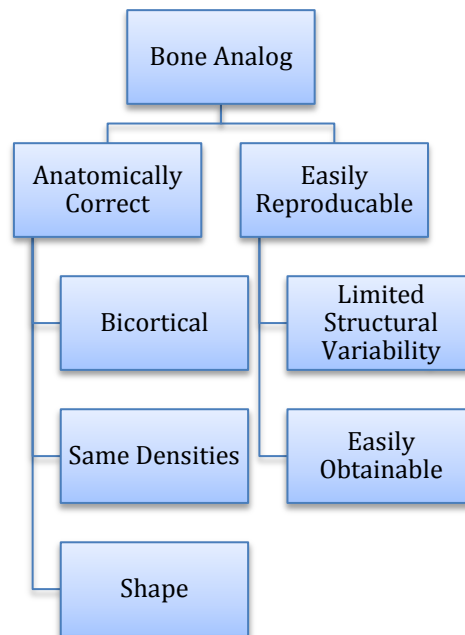


Figure 3.2: Bone analog objectives tree

**Anatomically Correct:** The bone model had to be anatomically correct in modeling the sternum in order to produce results similar to what would be collected with real sterna. To accomplish

this, the model had to be bicortical, consisting of both cortical and cancellous layers, as well as have densities of these layers similar to human bone. Finally, the shape of the model needed to be similar to best reproduce the changes in the sternum.

**Easily Reproducible:** The sternum model had to be easily reproducible in order to use numerous samples for testing. To do this, the model had to have a minimal amount of structural difference between each sample, meaning the layers must consistently have the specified densities. The samples also had to be easily obtainable so that a large sample size could be obtained.

To rank the objectives for the first goal of this project, pairwise comparison charts were completed by the design team, the clients, and the project advisor. These charts are found in Appendix A. It can be seen in all four pairwise comparison charts regarding the screw and plate systems that the most important objective was safety. If the device was not safe, it could not have been implanted or used. The next highest-ranking objective was effectiveness. All clients, as well as the advisor and group were in agreement that if the product was not effective, it would serve no purpose. The final two objectives had different rankings. While the team thought that the ease in manufacturing should have the same importance as the ease of use, the advisor had felt that the ease in manufacturing was more important. In contrast, one client, KLS Martin, had felt that ease of use was less important than the ease in manufacturing, because the ease of use varies with the skills and experience of each surgeon. In contrast, no pairwise comparison charts were completed to rank the objectives of the bone model. This was because there were only two major objectives, and it was felt that both these objectives were equally as important and could both be met.

### 3.2.2 Constraints

The following constraints are the conditions that the designs had to meet in order to be successful.

**Budget:** The sternal fixation device and bone analog had to be created using no more than \$450 contributed by Worcester Polytechnic Institute. In addition, Dr. Raymond Dunn and KLS Martin were able to provide additional funds and materials to complete the project. The budget was a factor in limiting not only the materials and costs associated with fabricating the device, but also those associated with testing.

**Time:** The sternal fixation device and bone analog had to be produced within 26 weeks.

**FDA standards:** The screw and plate system had to comply with FDA regulations, as it is a medical device.

**Biocompatible:** The sternal fixation device had to be biocompatible. Because the device will be implanted into a patient and remain in the body for the rest of their lives, the device had to be made of inert materials. The materials are not to cause an inflammatory response, degrade over time, or hinder the healing process.

**One piece screw:** The screws used in the screw and plate system had to be made of a single part, as additional parts make the device too difficult to handle and require extra time to install.

### 3.2.3 Functions and Specifications

The sternal fixation device had to be able to perform several functions and fulfill certain specifications in order to be useful. The functions were:

- Achieve a tight, locking fit between the screw and the plate
- Provide a friction fit between the plate and the sternum
- Minimize tissue damage by reducing bone stripping and preventing dorsal puncture of the sternum
- Withstand the forces generated during respiration and chest impact

In order to fulfill these functions, as well as the previously mentioned objectives and constraints, certain specifications had to be met. These specifications were based on prior research in this field. The specifications were as follows:

- Screw length must be between 11 and 15 mm
- Must withstand 0.4 - 43.8 N, the forces generated during respiration
- Torque used to apply the screw must be lower than 0.048 N-m, the maximum tolerable torque in the human sternum  
(Pai et al, 2008)

The bone model also had to accomplish the following functions and specifications:

- Provide reproducible results
- Produce results similar to human sterna

In addition, the specifications that were chosen for this analog were based upon the anatomy of human bone and the properties of bicortical models of other bones. They were as follows:

- Inner cancellous bone layer of 10 pcf
- Outer cortical bone layer of 20 pcf
- 1.5mm cortical bone layer surrounding cancellous area

(Pacific Research Laboratories, 2012)

#### **3.2.4 Revised Client Statement**

*The first objective of this project was to optimize a rigid, locking sternal fixation device that provides a friction fit between the sternum and the plate surface. This device should be able to withstand prolonged cyclic loading due to respiration. It should be safe for both the patient and surgeon, easy to use, and easy to manufacture. The second objective was to design and characterize a sternum model with similar structure to human bone that can demonstrate the difference in properties between bone layers. It must also be able to yield reproducible results that are indicative of the expected performance of bone.*

## Chapter Four: Alternative Designs

From the revised client statement, several alternative designs for the screw-plate systems were generated and evaluated. In doing so, the constraints, objectives, functions, and specifications of the project were taken into account, and a final design was selected. It was not pertinent to create alternative designs for the human sternum model, as specific properties, such as density and thickness, were sought after and could only be displayed one way.

### 4.1 Needs Analysis

Each year, approximately 750,000 median sternotomies are performed (Bek et al, 2010), mostly as a result of open heart surgery. The most common sternum closure method is wire fixation; however, this is inappropriate for osteoporotic bone, as it can cut through the bone easily. A sternal fixation method for patients with osteoporosis is the Talon device, but it is too expensive and bulky for widespread use. The other method for fixating osteoporotic bone is the screw and plate system, which is more widely used due to its easy installation and removal. Unfortunately, these screw and plate systems do not simultaneously achieve the two functions needed to be maximally effective: having a friction fit between the plate and the sternum and securely locking the screw into the plate.

In order to create a useful screw-plate system for osteoporotic bone in the sternum, the design had to meet both of the above criteria. In addition, the system had to be able to withstand the forces provided during respiration and any other anticipated chest impact. It also needed to be safe for the patient so that it minimized tissue damage caused during implantation and over time. In addition, it would be ideal if the system prevented any bone stripping in the sternum.

Other requirements for our sternal fixation device included being easy to use in installation and removal, as well as being durable for long-term use on constantly degrading osteoporotic bone. It also was to be easily manufactured, meaning it had to be machinable, cost effective, and have a simple design. Finally, it was decided that the screw should be unicortical in order to prevent possible safety issues associated with bicortical screws, such as possible chest organ punctures.

In addition, there is a lack of anatomically correct sternum bone models on the market. While testing completed with human sterna would seem the most ideal, it actually proves problematic due to the limited samples available for testing, the extra care when testing, and extreme biological variability. As an alternative, polyurethane foam sternal model (Sawbones) are widely used, as they are easy to obtain and can give reproducible data. However, these models do not represent the morphology of real bone, as they are a uniform density, whereas real bone has two distinct bone layers of different densities.

To address these problems, the new bone analog had to be anatomically correct to demonstrate the difference between the two bone layers. It also had to be easy to make so that numerous samples could be obtained, allowing for a large sample size with minimal differences between samples to provide repeatable and reproducible results.

## 4.2 Functions and Specifications

The main function of the screw and plate system was to hold the hemi-sterna together to permit proper healing of the bone by providing rigid stability. For optimal performance, the device had to achieve four different functions.

First, it had to provide a friction fit between the plate and the sternum. It was important for the system to do this because a gap between the plate and the sternum may result in sternal dehiscence and other complications. One such complication can arise when the plate shifts with respect to the bone, causing the screws to move inside the bone and destroy the tissue.

Secondly, the system had to achieve a tight, locking fit between the screw and the plate. This locking not only prevents screw loosening, but also minimizes separation of the two hemi-sterna during cyclic loading caused by respiration. Furthermore, the locking mechanism had to prevent the screw from pivoting within the plate, ensuring that the screw remains perpendicular to the plate, reducing bone stripping and further minimizing bone separation (Ahn et. al, 2009).

To lock the screw effectively into the plate and assure the plate and sternum achieve a friction fit simultaneously, a torque that was lower than 0.048 N-m was required. This torque is the maximum tolerable torque that the human sternum can withstand.

Next, the screw-plate system had to minimize tissue damage by reducing bone stripping and preventing dorsal puncture of the sternum, caused by bicortical purchase of the screw. To perform this function, the screw had to provide unicortical purchase, which has shown to be more effective in minimizing bone separation and avoiding dorsal puncture than bicortical purchase (Bakalova et al, 2010).

In order to achieve a unicortical purchase, the screw had to be long enough to reach the cancellous bone, but no longer than the width of the sternum. This required the screw length to be between 11 and 15 millimeters.

Finally, the system had to withstand the forces generated during respiration and impact. To avoid failure of the device, the system had to be able to withstand between 0.4 N to 43.8 N, the forces generated during cyclic loading due to respiration (Pai, 2008).

In addition, the main goal for the bone model was to anatomically represent the sternum while providing reproducible results. To do this, two functions had to be achieved. First, the model had to be designed in a manner that makes it easily producible so that multiple samples could be manufactured for testing. This would allow for a large enough sample size in testing. The second function was to give results that were similar to those expected when testing on cadaveric bone. This is important because the bone model should yield results accurately representing the behavior of fixation systems *in vivo*. In order to produce results similar to real bone, the model had to consist of two different layers representing both cortical and cancellous layers. The densities had to be 20pcf and 10pcf, respectively. In addition, the thickness of each layer had to be similar to real bone, with the outer cortical layer having a width of 1.5mm.

### 4.3 Design Alternatives

We developed several different conceptual screw and plate designs to achieve stable, rigid sternal fixation for osteoporotic bone. The complete list of designs can be found in Appendix B with complementary pictures. Initially, the designs that did not meet the project constraints were eliminated. The remaining concepts were then compared using a design selection matrix, shown in full in Appendix C and for the top ranking designs in Table 4.1.

To complete this chart, each design was scored on a scale from one to ten for each of the four objectives of the project. The following weights were assigned to each of the objectives:

- Easy to use- 0.075 out of 1
- Easy to manufacture- 0.075 out of 1
- Effective- 0.40 out of 1
- Safe- 0.45 out of 1

These values were based on the pairwise comparison charts (PCC) completed by the team, the advisor, and our two clients. As shown, a higher value was given to safety and effectiveness over the other two objectives, as ease of use and ease of manufacturing were deemed less important but equal on an average of the PCCs. The above weights were then multiplied by the score given to the design for each objective. The values for the four objectives were then totaled to calculate the final score of each design.

Table 4.1: Design selection matrix. The table shows the evaluation of the top four designs with respect to the weighted objectives. The highlighted row shows the top-ranked design.

	Easy to use	Easy to manufacture	Safe	Effective	Total Points
<b>Weighting based on PCC</b>	0.075	0.075	0.45	0.40	1
<b>Reverse expansion screw and custom plate</b>	8	4	8	9	8.1
<b>Slanted teeth in screw and plate</b>	7	2	8	8	7.475
<b>Lag-lock threaded plate and custom screw</b>	8	6	8	7	7.45
<b>Hexagonal screw head with custom plate</b>	6	7	8	5	6.575

These scores yielded four high-ranking designs: the reverse expansion screw, a screw with slanted, ratchet-like teeth, a lag-threaded hole with a threaded screw head, and a screw with a

hexagonal head. Each of these four designs and how they perform the required functions are described below in Table 4.2.

Table 4.2: Function means chart. This table describes how each of the top four alternative designs achieves the four functions.

	<b>Reverse expansion screw and custom plate</b>	<b>Slanted teeth in screw and plate</b>	<b>Lag-lock threaded plate and custom screw</b>	<b>Hexagonal screw head with custom plate</b>
<b>Achieves a tight, locking fit between the screw and the plate</b>	Wedges lock into custom spaces in plate	Screw teeth lock into plate teeth by turning in one-direction	Screw threads lock into plate threads	Screw head locks into hexagonal hole in plate
<b>Provide a friction fit between the plate and the sternum</b>	Expansion of wedges into their designated plate slots	Locking of screw teeth to plate teeth at bottom of plate	Screw locks into lower threaded plate	Screw presses plate to sternum as it is threaded
<b>Reduce bone stripping</b>	Once wedges fit into plate spots, screw can no longer be tightened	Once screw teeth locked into plate teeth, can no longer tighten screw	Minimal plate threads makes it easier to observe when the screw is completed inserted	Hexagonal head prevents further insertion of the screw
<b>Withstand the forces generated during respiration and chest impact</b>	Sturdy design and screw wedges prevent movement between screw and plate	Teeth in one direction prevent screw from moving in plate	Screw and plate threads match up, minimizing screw movement in plate	Locking between hexagonal head and plate

#### 4.3.1 Reverse Expansion Screw

The reverse expansion screw featured a screw head that deformed upon tightening to lock it into the plate and can be found in Figure 4.1. The screw head has an angled trough along the bottom with a complementary ridge in the plate. The angle of the ridge, however, is wider than that of the trough. This discrepancy forces the outer edges of the screw head to deform. Not only does this allow the screw to lock and prevent loosening, but it also lets the surgeon tighten the screw to the fullest to achieve a friction fit with the bone. An extensive patent search did not return any results that behaved in a similar manner to the reverse expansion screw.

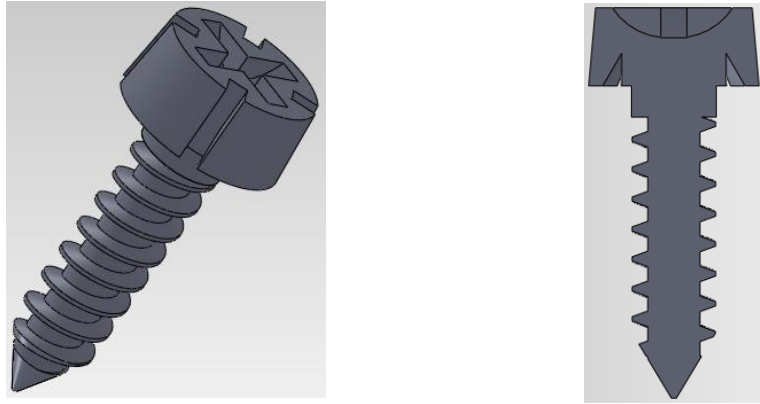


Figure 4.1: Reverse expansion screw. The reverse expansion screw deforms as it is inserted into the plate. On the right, you can clearly see the edges of the screw head that will deform.

### 4.3.2 Slanted Teeth

The second design alternative (Figure 4.2) was a screw and plate system that had complementary, angled teeth that mimic a ratchet mechanism. Their angle allows the teeth to slip over each other as the screw is tightened to the plate to attain a flush fit with the bone. However, it prevents the screw from rotating in the opposite direction, thus locking it in place. Although it shows promise in effectiveness and safety, this design does not demonstrate great potential for ease of use. This is due to the difficulty of removal because of the nature of the locking mechanism. Like the reverse expansion screw, the patent search did not reveal any existing ratchet inspired locking screws.

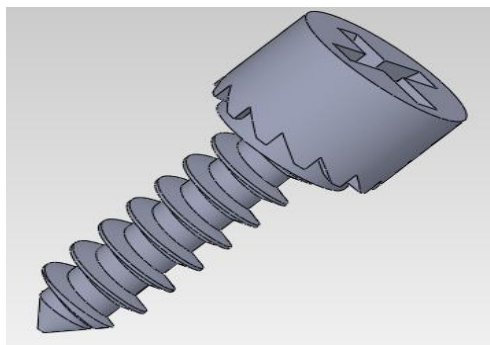


Figure 4.2: Slanted teeth screw design.

### 4.3.3 Lag-threaded Plate

The lag-threaded plate design was inspired by standard locking screws, which have threaded heads that screw directly into the plate (Figure 4.3). However, existing locking screws, such as

the self-locking bone screw presented in US Patent #7322983, lock into the plate before they have the opportunity to press the plate to the bone. In an attempt to avoid this problem, the plate threads for this design alternative would only be present in the bottom portion of the screw hole. If successful, this would allow the screw to produce a friction fit between the plate and the bone. This design had slightly lower scores for effectiveness because while it is locking and durable, the rigidity of the system was questioned, as testing would be necessary to determine whether or not a friction fit was possible. However, it was clear that it would still be safe, easy to use, and easy to manufacture.

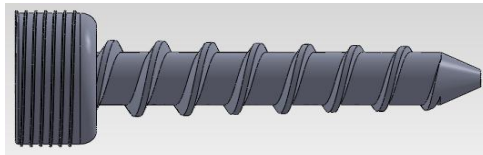


Figure 4.3: Screw used for lag-threaded plate design. This screw with different threads for both the top and bottom will screw into a plate where the threads start further from the top.

#### 4.3.4 Hexagonal Screw Head

The last alternative design considered was a hexagonal screw head and hole (Figure 4.4). The angles of the screw head would prevent the screw from loosening once it is tightened because it would require much more force to rotate the screw that is already in place. However, this was also a fault with this design; the force to insert and remove the screw would be incredibly high, making it difficult to use. On the other hand, the design illustrated potential in the categories of effectiveness and safety.

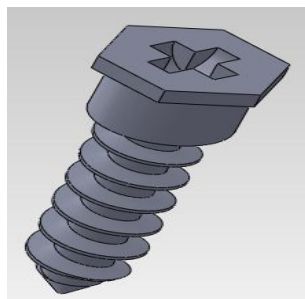


Figure 4.4: Screw with hexagonal head. The image shows a standard screw with a hexagonal head, which fits into a complementary hexagonal hole in the plate.

#### 4.4 Conceptual Final Design

Based on the analysis of the various alternative designs, the best option to pursue as the final design for this project was the reverse expansion screw. To further improve the design, several

modifications were proposed for the screw. For instance, increasing the screw head or modifying the shape and size of the trough could make it easier to manufacture. More specifically, the screw could be machined more easily by widening the angle of the trough in the screw head and of the ridge in the plate. Furthermore, the addition of rough surfaces on the screw head would increase friction between the plate and the screw, thus achieving a more secure lock. Another proposed modification would be to include a groove around the outside of the head to aid in the deformation of the screw. This would reduce the force necessary to install the screw, making it easier to use. The detailed dimensions of this design were established through proof of concept testing.

It was decided that the best option for making a new testing model was to design a bicortical sternum polyurethane foam model. This model represented the mechanical properties and structure of bone better than standard foam models because of the hard cortex and soft cancellous core. The bone model was manufactured by the world-leader in bone models, Sawbones. The model consisted of 10pcf cancellous core foam polyurethane, surrounded by a 1.5mm thick cortex, 20 pcf cortical layer of the same foam, contrasting the uniform 20pcf standard Sawbone model. An image of the final model can be seen in its bisected form below in Figure 4.5, where the difference between the cortical (white foam) and cancellous layers (pink foam) can clearly be seen. These densities were chosen based on those of bicortical models of other bones currently on the market, while the thickness of the layers were determined based on the anatomy of human sterna.

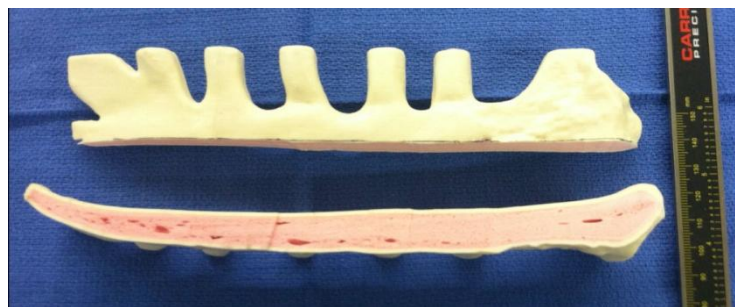


Figure 4.5: Custom Sawbone model, where the pink portion represents cancellous bone, and the white layer represents the cortical bone.

#### 4.5 Feasibility Study and Experiment Setup

After deciding on a tentative final design, the feasibility of it was evaluated. Factors taken into consideration when determining the feasibility of the design were time, and available materials

and machinery. The design also had to be made in a way that made it easily manufactured by KLS Martin. This meant having a simple enough design for their machinery to make efficiently.

When deciding if this design was feasible based upon these factors, as well as if the design concept itself would be effective, we turned to proof of concept testing. To verify the flush fit of the system, rapid-prototyped screws and plate were applied to wood to mimic their real-life application. Upon insertion, the intimate fit between the plastic plate and wood surface were observed. To optimize the deformation of the screw head, finite element analysis (FEA) of the computer-aided design (CAD) model was completed.

#### 4.6 Proof of Concept Testing Results

To test the physical proof of concept of the reverse expansion screw design, a plastic prototype was manufactured. Rapid prototyping was utilized because a metal prototype would have exceeded the time limit and budget for this project. Working with the plastic prototype, the screw was first inserted into the plate as the plate pressed onto a piece of wood. Wood was chosen because it resembles cortical bone due to its ability to splinter easily and because it was readily available. When the first screw was tested at room temperature, it did not show complete deformation into the plate, but demonstrated a friction fit between the plate and the wood, which is shown in Figure 4.6.



Figure 4.6: Flush fit between rapid prototyped fixation system and wooden bone analog.

It was then noted that the plastic should be heated before the next test, making the screw more apt to deform into a stiff plate. For this test, the plastic screw was heated in an oven in the engineering department for approximately 10 minutes at 200°F. Once the screw was hot to the touch, it was pressed into the plastic plate. The screw head then deformed into its appropriate spot in the plate, locking into the plate, shown in Figure 4.7. The screw could also be removed with force, and the deformation seen.

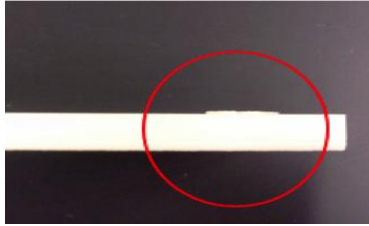


Figure 4.7: Screw head locked into plate.

#### 4.7 Finite Element Analysis Results

While this process showed the basic proof of concept, it was decided that further analysis should be done to optimize multiple parameters and dimensions of the design. To do this, ANSYS software was utilized to test the parameters at which the screw deformed best into the plate. The final design was chosen based on high deformation and equivalent (Von Mises) stress that is less than the yield stress of titanium alloy, which is noted as 930 MPa in the ANSYS program.

While torque is applied to the screw when being inserted into the plate, this was converted to a force when being modeled in ANSYS. This force was then distributed over the four inside edges of the screw, as seen by the red arrows in Figure 4.8. The clamping force formula was used to calculate this force, along with the given values of torque and the major diameter of 191 N mm and 3mm, respectively. The torque used was acquired from a single-blind test conducted to determine the torque that the surgeons felt was appropriate for tightening a screw in a screw-plate system into the human sternum (Ahn, 2009 MQP). A final force per length for each screw edge was calculated to be 24.6 N/mm, based on a net axial force of 318 N. This value is consistent with the magnitude of clamping force empirically determined in a study by Vand et al. (Vand et al, 2008)

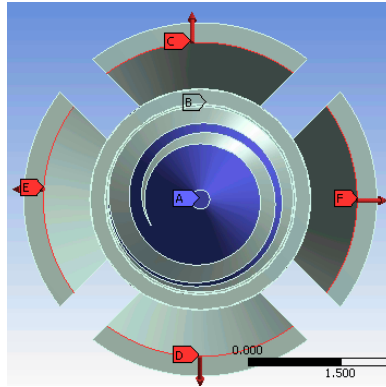


Figure 4.8: Illustration of the reactions forces on the applied edge of the screw. Red arrows represent reaction force on a wing.

With this force, four different parameters of the screw were then modified and tested to determine which would provide the best deformation. The parameters tested include the plate angle, the screw head height, the wing-base thickness, and the screw head radius. These parameters were selected because they were the features that would best optimize the performance of the screws deformation. The dimensions tested were determined based on the tolerances of the machines that would be used to manufacture the screws.

#### 4.7.1 Plate Angle

Different plate angles were analyzed to determine deformation of the angle difference between the plate and the screw. The angle of the plate being altered can be seen in Figure 4.9.

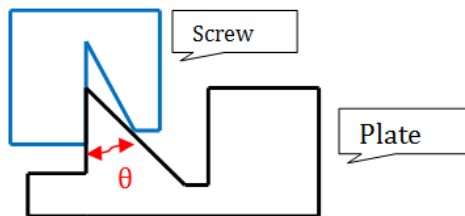


Figure 4.9: 2D cross-sectional view of plate and screw. Angle  $\theta$  shows the parameter that is being changed.

When altering the plate angle, the screw wing angle was kept constant at  $30^\circ$ . The plate angle was tested at  $35^\circ$ , and in increasing increments of 5 degrees, until  $55^\circ$ . These values were chosen because a plate angle smaller than  $35^\circ$  would not be able to apply the necessary force to deform the screw head, as the angle of the plate would be the same size as or smaller than that in the screw. As seen in Table 4.3, as the plate angle increased, the forces and Von Mises

stresses acting on the screw decreased. Shown in Figure 4.10, the maximum deformation occurred at the lowest plate angle, therefore leading to the decision to use this dimension.

Table 4.3: Plate angles and the corresponding force, deformation and stress of the screw head. The optimal dimension is shown in bold.

Plate angle (degrees)	Force acting on screw head due to contact with plate (N)	Maximum deformation (mm)	Maximum Von Mises stress (MPa)
<b>35.0</b>	<b>138</b>	<b>0.0522</b>	<b>1190</b>
40.0	123	0.0454	1010
45.0	112	0.0399	871
50.0	103	0.0353	761
55.0	96.9	0.0313	692

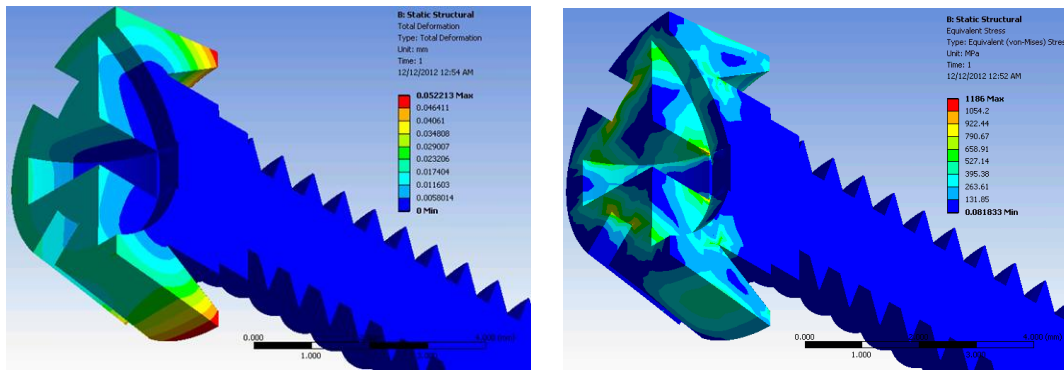


Figure 4.10: Cross-sectional view of deformation of the screw (left) bottom view and stress (right) top view.

#### 4.7.2 Screw Head Height

Another parameter tested was the height of the screw head, as seen in Figure 4.11. When testing the different heights of the screw head, the force corresponding to the chosen plate angle of 35° was used (F=138 N).

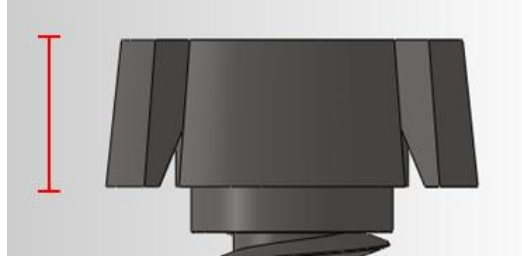


Figure 4.11: Screw head height

Three screw head heights were tested: 2.10 mm, 2.25 mm, and 2.50 mm. As seen in Table 4.4, as the height of the screw head decreased, the deformation increased. With this optimal deformation, there is a consequence of a higher stress. However, as seen in the right portion of Figure 4.12, the maximum stress concentrations are low and are not expected during actual screw insertion due to frictional factors that were not considered during FEA.

Table 4.4: Screw head heights and the corresponding deformation and stresses. The optimal dimension is shown in bold.

Height of the screw head (mm)	Maximum deformation (mm)	Maximum stress (MPa)
2.50	0.0522	1190
2.25	0.0704	1580
<b>2.10</b>	<b>0.0905</b>	<b>1710</b>

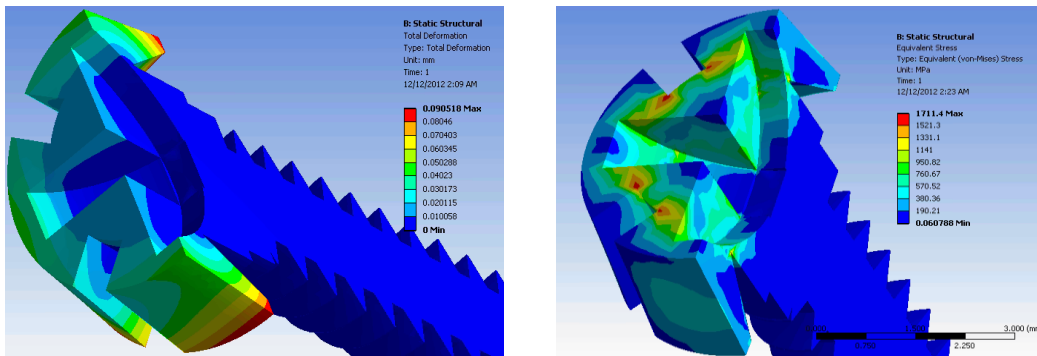


Figure 4.12: Cross-sectional view of screw head height of 2.10mm, showing deformation (left) and stress (right).

### 4.7.3 Wing-Base Thickness

Different thicknesses of the wing base were then tested using the optimal plate angle and screw head height. The wing-base is determined as the outer edges of the screw head that will deform into the plate when inserted, as seen in Figure 4.13.

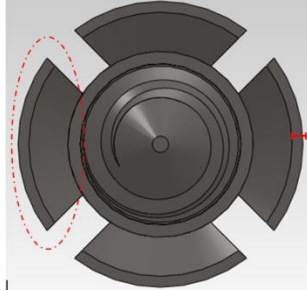


Figure 4.13: Red circle illustrates the wing of the screw and the thickness is the dimension being change

The wing-base thickness was varied between values of 0.138 and 0.318. As seen in Table 4.5, the decrease in thickness of the wing-base lead to increased deformation. Figure 4.14 shows the deformation and stress concentration of the screw. The changes in the deformation and stresses were insignificant, and therefore a value of 0.138 mm wing base was kept.

Table 4.5: Wing-base thicknesses and the corresponding deformation and stresses. The optimal dimension is shown in bold.

Thickness of wing base (mm)	Maximum deformation (mm)	Maximum stress (MPa)
0.318	0.0905	1710
0.210	0.0924	1670
<b>0.138</b>	<b>0.0966</b>	<b>1730</b>

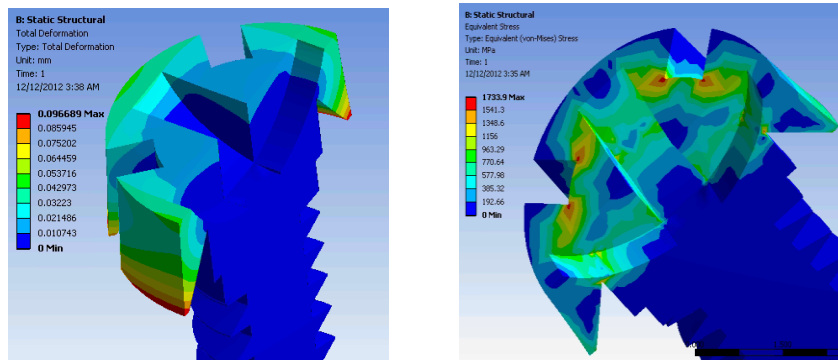


Figure 4.14: Cross-sectional view showing deformation (left) and stress (right)

#### 4.7.4 Screw Head Radius

Finally, the radius of the screw head was varied to maximize deformation. As seen in Figure 4.15, the radius of the screw head was measured as the distance from outer edge of the screw to the center.

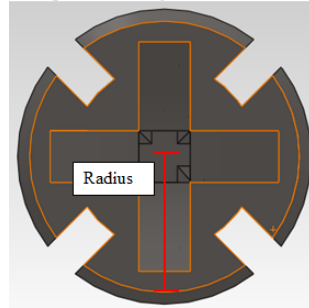


Figure 4.15: Screw head radius

The value of the screw head radius was tested at 2.20 mm, 2.40 mm, and 2.68 mm. As seen in Table 4.6, a decrease in the radius of the screw head led to an increase in deformation, resulting in the selection of a 2.20 mm radius for the screw head. An example of the deformation and stress concentration results from one of these tests can be seen in Figure 4.16.

Table 4.6: Screw head radii and the corresponding deformation and stresses. The optimal dimension is shown in bold.

Screw head radius (mm)	Maximum Deformation (mm)	Maximum Stress (MPa)
2.68	0.0966	1730
2.40	0.106	1650
<b>2.20</b>	<b>0.130</b>	<b>2020</b>

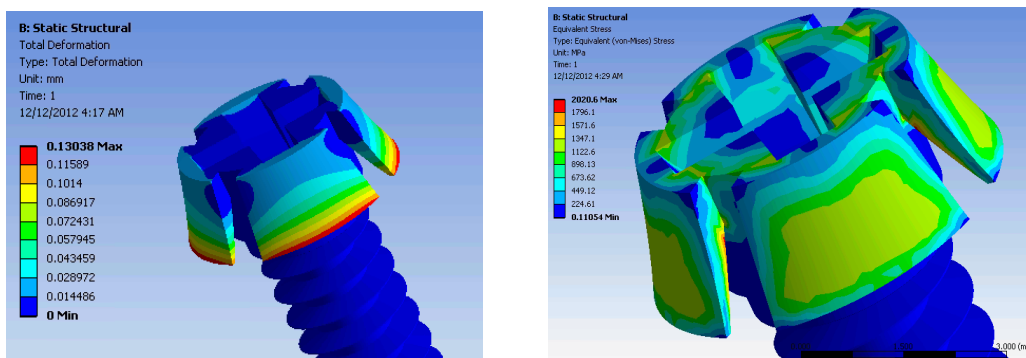


Figure 4.16: Isomeric view of deformation (left) and stress (right)

With the completion of the FEA on the reverse expansion screw and plate system with different plate angles, screw head height, wing-base angle, and screw head radius, the optimal

dimensions for the screw-plate system were devised. The final design included a plate with an angle of 35°, and a reverse expansion screw with a head height and radius of 2.10 mm and 2.30mm, respectively, as well as a wing-base of 0.138 mm. The complete FEA done in ANSYS can be seen in Appendix D, while a CAD drawing of the final design with all corresponding dimensions can be seen in Appendix E.

#### 4.7.5 FEA Validation

In order to validate the finite element analysis conducted, two different screw heads were rapid prototype on a larger scale using ABS plastic. A set of FEA tests was conducted to compare the values predicted by the model to the physical observations in order to evaluate the validity of the FEA model. To complete the test, two screw heads of different diameters were tested, and the results were compared to the FEA. Figure 4.17 shows an example of the rapid prototyped screw head.

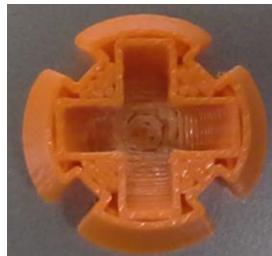


Figure 4.17: ABS plastic prototyped screw head.

The prototypes were cemented and a compressive force was applied to one of the wings using an Instron machine, as seen in Figure 4.18. The displacement was then measured at different forces.



Figure 4.18: Cemented screw head. The red arrow represents the compressive force applied.

The validation tests showed very little difference in displacement between the two models. This is illustrated by the graph below which shows the displacement as a function of force.

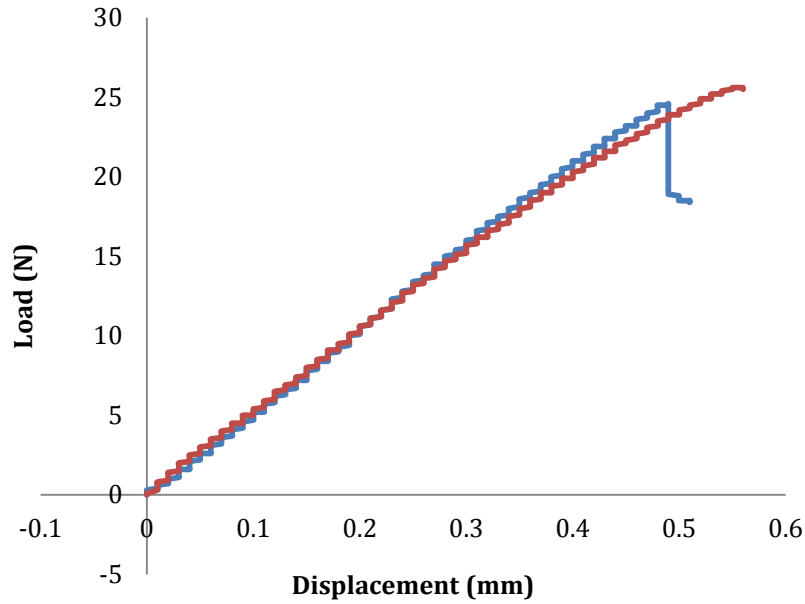


Figure 4.19: This graph depicts the load withstood at certain displacements with screw heads of two different radii.

FEA was used to compare the physical results of this test to what the ANSYS program predicted would happen. Each model was tested using three different continuous forces. The way that the load was applied in the model is indicated by the red arrow in Figure 4.20. Table 4.7 shows the measured and predicted displacements.

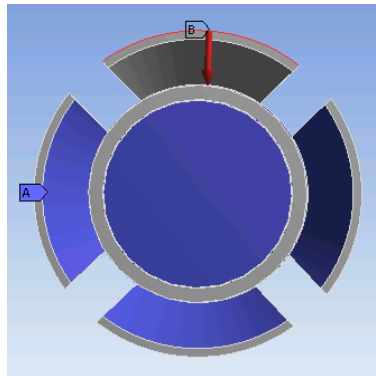


Figure 4.20: FEA showing the compressive force applied.

Table 4.7: Measured and predicted displacements

Load (N)	16.08mm head diameter		13.2mm head diameter	
	Observed Displacement (mm)	Predicted Displacement (mm)	Observed Displacement (mm)	Predicted Displacement (mm)
2	0.04	0.001	0.03	0.002
13	0.24	0.006	0.25	0.018
24	0.47	0.009	0.50	0.070

While the displacements were similar between the two different screw heads when physically tested, the FEA showed a much greater displacement in the smaller screw head. Overall, the validation of the FEA was inconclusive, as the FEA model and rapid prototype were not identical due to the inaccuracy of the 3D printer with intricate designs, such as the screw head.

## Chapter Five: Design Verification

With the completion of initial design verification of the screw-plate system using finite element analysis, the design was submitted to KLS Martin for professional manufacturing and will be tested as a future project. As additional verification for the need of a lag-lock screw and plate system, cyclic loading testing was performed. This test was conducted on sternal models with a screw and plate system flush to the bone, as well as with a gap between the sternal plate and bone model, mimicking premature screw lockage into the plate.

In addition, the custom sternal models had to be verified as a viable bone analog, and characterized with respect to its properties. This was done through testing against a standard sternum model in axial and lateral pullout tests using locking and non-locking screws in unicortical and bicortical purchase.

### 5.1 Testing Models

To characterize the custom bone model, they were tested against standard models of uniform density, which can be seen in Figure 5.1.

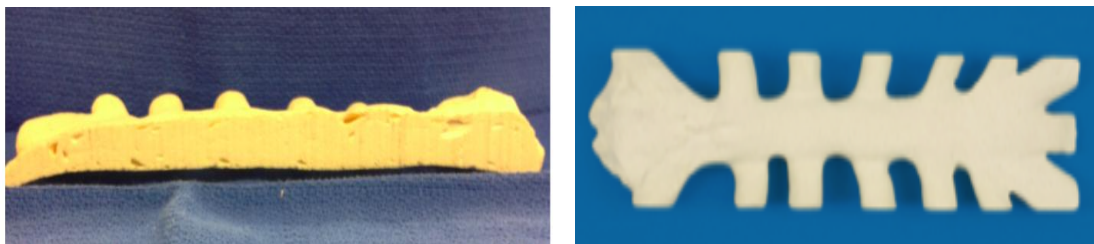


Figure 5.1: Standard Sawbone model. (a) Cross sectional view of uniform density Sawbone model (b) Arial view of uniform density Sawbone model.

The standard screw-plate systems used to complete classification testing on the bone model consisted of a 28 mm Ti-6Al-4V straight plate with a thickness of 2.0mm, as well as 2.3 x 9 mm, 2.3 x 13 mm, 2.3 x 17mm Ti-6Al-4V locking and non-locking cortical bone screws. Images of the sternal plate, as well as the locking screws of length 9mm, 13mm, and 17mm are shown in Figure 5.2, respectively. It is important to note that the non-locking screws' distinctive features could not easily be identified from the locking screws to the naked eye with screws of this scale.

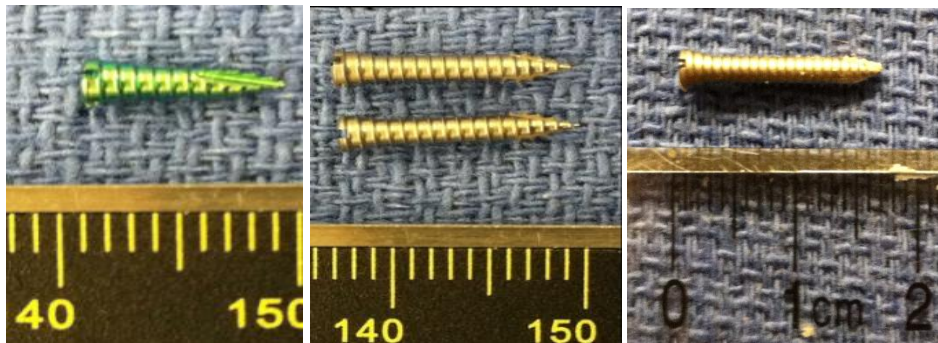


Figure 5.2: Standard screw and plate systems manufactured by KLS Martin. (a) 4-hole straight 28mm Titanium alloy plate (b) 2.3 x 9 mm Titanium alloy locking screw (c) 2.3 x 13 mm Titanium alloy locking screw (d) 2.3 x 17 mm Titanium alloy locking screw.

## 5.2 Testing

Cyclic loading testing was conducted to assess screw loosening and demonstrate the difference in screw displacement between systems with the sternal plate flush to the bone versus those not flush. The test was designed to replicate the loading experienced by the sternum due to respiration by using consistent force, frequency, and number of cycles. The parameters of the cyclic loading testing were prepared for use with the Instron using Wavematrix software. The following parameters were used:

- 0-50N load
- 15000 cycles
- 2 Hz rate

The Sawbones models were prepared for cyclic testing by first being cut to isolated rib pairs. These ribs were scored with a scalpel to allow for more secure potting. The rib pairs were then

bisected along the midline, as they would be in a sternotomy. A single screw was inserted into the sternal plate 6mm from the midline cut. Samples were also prepared with screws being inserted and locked into sternal plates 2mm from the surface of the bone model. These set-ups can be seen in Figure 5.3.



Figure 5.3: Schematic of cyclic loading testing. (a) Set-up of cyclic loading tests with plate flush to the bone model (b) Set-up of cyclic loading tests with plate 2mm above the bone model.

These specimens were then placed into a custom fixture filled with prepared Bondo, a two part epoxy putty, and aligned using specialized guiderails to be sure the specimen was placed with the sternal plate centered in the fixture. Once the putty had been allowed to harden for at least two hours, a custom grip was attached to the free end of the sternal plate so that the sample could be gripped by the Instron. Finally, 2-inch C-clamps were secured at opposite sides of the fixture to prevent the putty from slipping. An image of this final set-up can be seen in Figure 5.4, while the detailed protocol for this procedure can be found in Appendix F.



Figure 5.4: Prepared specimen for cyclic and tensile testing.

Specific and intricate directions were then used to calibrate an Instron Electropulse E-1000 uniaxial testing device for cyclic testing. The final set-up for this testing can be seen in Figure 5.5. When running the cyclic loading test, the Bluehill and Wavematrix software were utilized. Tensile forces ranging from 0 to 50N at a rate of 2Hz were applied to the testing specimen using

the 2kN load cell for 15,000 cycles. The complete protocol for the cyclic loading tests is found in Appendix G.

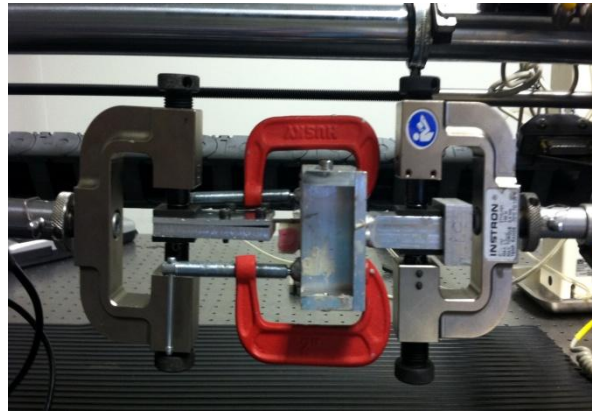


Figure 5.5: Cyclic loading testing set-up.

Screw loosening due to cyclic loading was measured by recording the displacement of the screw using the Instron's extension measurement system. This was chosen in place of an Extensometer because of the negative effects of the Extensometer on the mechanical integrity of the Sawbones model when inserted for use. These tests were completed in the custom-made bone model.

To determine the mechanical properties of the sternum model, it was tested in axial and lateral pullout. For axial pullout testing, a standard cortical bone screw was inserted cortically (9mm) or bicortically (approximately 14mm) into pieces of the Sawbone sternum models. The samples were secured onto a metal plate set-up used for all screw-pull out tests on the Instron machine. A corresponding piece was fastened around the screw-head and attached to the top grip of the Instron machine. This set-up can be seen in Figure 5.6. The screw was then pulled along its vertical axis at a rate of 5mm/min until the recorded data showed a drop in the resistance force, indicating failure. The complete protocol for this procedure can be found in Appendix H.

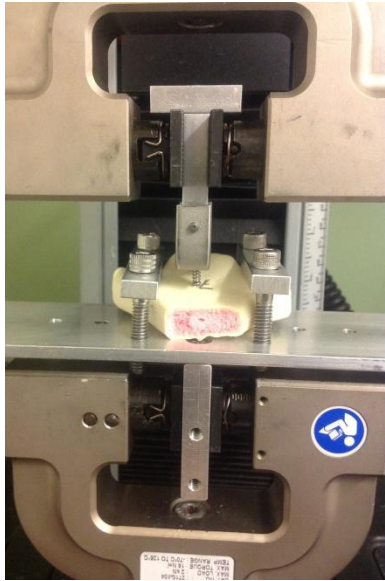


Figure 5.6: Axial pullout testing set-up.

During lateral pullout testing, the same set-up as cyclic testing was utilized, with the sternal plate flush against the bone model. The sternal plate was pulled using the Instron machine at a rate of 5mm/min. The test was run until failure occurred, and the maximum force was recorded. An image of this test set-up can be seen in Figure 5.7, while a more detailed description of this protocol is located in Appendix I.

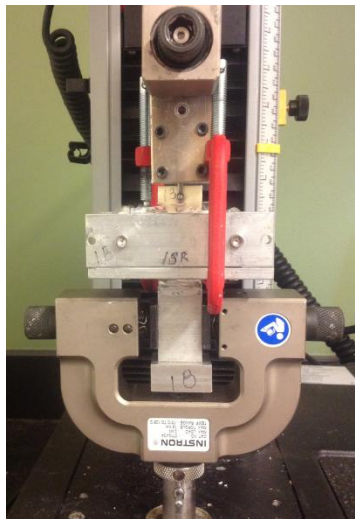


Figure 5.7: Lateral pullout testing set-up.

### 5.3 Testing Results

The cyclic loading tests demonstrated the need for a lag-lock screw, such as the reverse expansion screw that was designed as a result of this study. The testing of the custom Sawbone model demonstrated that it is a suitable replacement for regular Sawbones because its behavior was more indicative of what is expected of bone.

#### 5.3.1 Demonstration of Need for Lag-Lock Screw and Plate

Cyclic testing showed a significant difference in the maximum displacement of the samples whose plates had a flush fit with the bone model and of the samples with a 2mm gap between the plate and bone model. The samples with a flush fit had a maximum displacement of  $0.0735 \pm 0.0315$  mm, while the maximum displacement of samples with the gap was  $0.211 \pm 0.125$  mm. The graph below illustrates the displacements of both as a function of cycles elapsed, while the summarized data of these tests can be found in Appendix J.

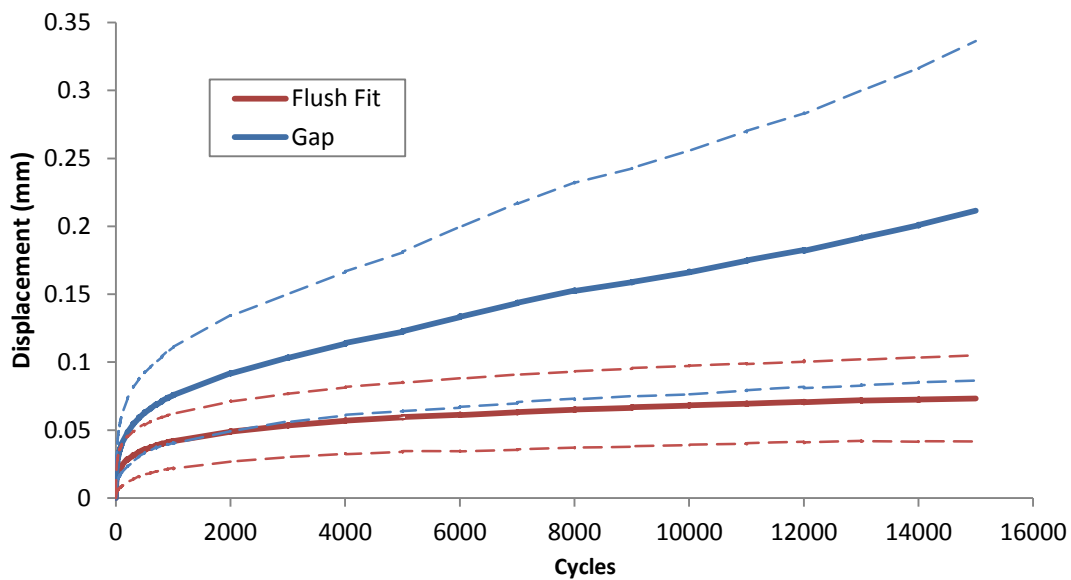


Figure 5.8: Displacement over elapsed cycles. The graph shows the mean peak displacement of the samples with a flush fit to the bone (red) and those with a gap between the plate and bone (blue). The dashed lines represent the error for each case.

#### 5.3.2 Characterization of the Bicortical Sawbones Model

In unicortical purchase, the pullout strength of the regular Sawbones was  $99.3 \pm 6.00$  N, compared to  $96.8 \pm 11.3$  N of the custom Sawbones and  $52.7 \pm 7.39$  N of the cancellous portion

of the bicortical bone model. In bicortical purchase, the pullout strength of the regular Sawbones had nearly tripled to  $304 \pm 74.5$  N, while that of the custom Sawbones approximately doubled to  $172 \pm 42.4$  N. The use of one-way ANOVA ( $\alpha=0.05$ ) showed that the pullout strength of the screws in unicortical purchase in both the custom and regular models were approximately the same, but that the other differences seen were statistically significant. Figure 5.9 shows the summary of the results, including the maximum force measured during each test (excluding outliers, defined as two standard deviations away from the mean), as well as the mean and standard deviation for each type of Sawbone, while the complete summary of this data can be found in Appendix K.

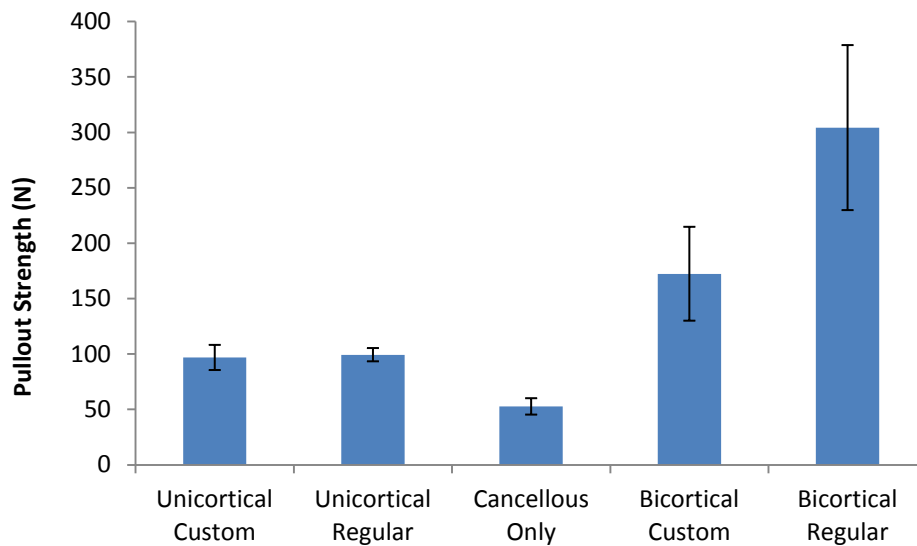


Figure 5.9: Axial pullout testing results. This bar graph shows the pullout strength (in Newtons) of the different bone models when axial pullout was performed with a cortical bone screw. The first three bars represent the cases when the screw was only inserted 9mm into the bone model (unicortical purchase), and the last two represent the cases when the screws achieved a bicortical purchase. The standard deviations for each group are indicated by the black whiskers. The large standard deviations in the bicortical tests can be attributed to the variations in the thickness of the models.

In addition to the axial pullout tests, the Sawbones were also tested in lateral pullout to characterize their performance under conditions comparable to how they would be loaded *in vivo*. For these tests, locking and non-locking screws of three different lengths were compared. A series of one and two-way ANOVAs ( $\alpha=0.05$ ) were performed to analyze the data. The results showed no statistical difference in the pullout strength of the standard Sawbone when the length of the screw was varied. However, the custom models failed at a significantly higher force when 17mm screws were used than they did for the 9mm and 13mm screws, which

performed very similarly to each other. Moreover, the difference between locking and non-locking screws was more pronounced in the standard Sawbones model than the bicortical one. The graph below summarizes these findings.

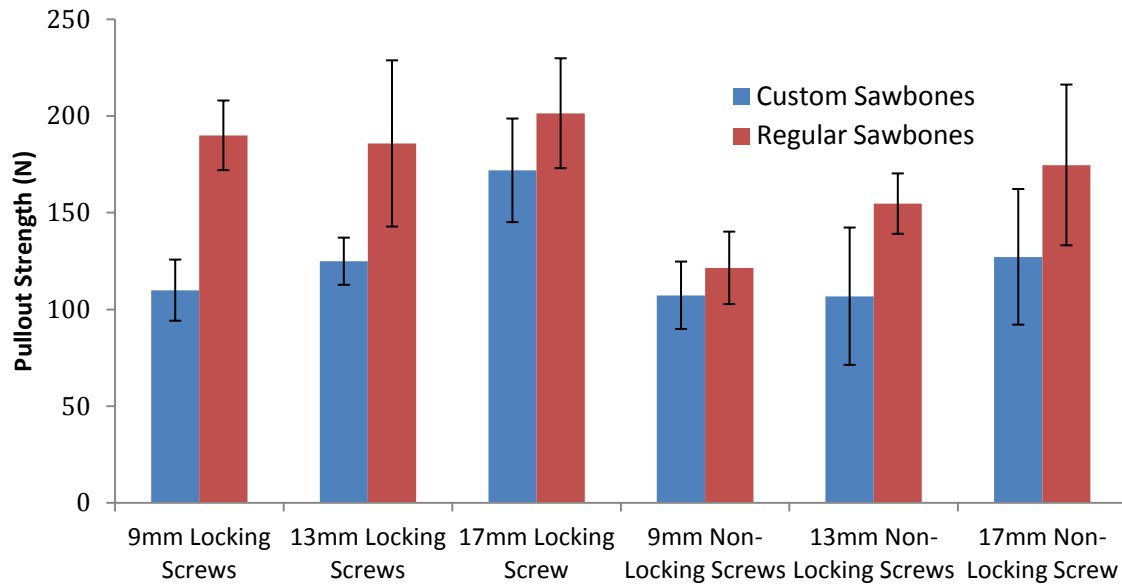


Figure 5.10: Lateral pullout testing results. This graph summarizes the mean maximum force withstood by the custom sawbones (blue) and the standard models (red) in various lateral pullout tests. The three groups on the left are the values obtained when testing locking screws, and the three on the right are those from non-locking screws. The error bars indicate one standard deviation.

## Chapter Six: Discussion

For this study, a novel sternal fixation device was designed and optimal specifications for it were determined so that it could be manufactured by KLS Martin. The need for such a screw was demonstrated through cyclic testing. In addition, a more accurate bone model was designed and characterized in axial and lateral pullout.

### 6.1 Reverse Expansion Screw and Plate Design

The main goal of designing a clinical scale lag-lock screw was achieved, and the need for such a screw was demonstrated using physical testing that replicated the loads exerted on the sternum during respiration. The design, which was optimized using FEA, was sent to KLS Martin for manufacturing and will arrive in time for another group to test against existing locking screw and plate systems. They are expected to outperform the control group based on the results of the cyclic testing completed. The reverse expansion screw eliminates the possibility of locking into the plate prematurely, a situation that was shown to cause excessive displacement and variation when the plate is loaded in a manner that replicates rapid breathing. The differences in displacement observed in the cyclic loading test can be attributed to the added freedom of movement that the gap between the plate and bone model provided the system. The greater distance between the part of the screw being loaded and the Sawbone resisting the motion increased the moment, causing greater displacements at the same force. Based on this, lag-lock screws such as the design completed during this study, should have significantly lower displacements than typical locking screws, which tend to lock prematurely.

### 6.2 Bicortical Bone Model

The axial and lateral pullout tests allowed for the characterization of the new Sawbones model. This testing was necessary because there are currently no bicortical sternal models on the market, and therefore the mechanical properties and behavior of the new model are unknown. While human bone was not tested, its structural properties have been previously explored, and this knowledge allowed for its comparison to the two bone models.

### 6.2.1 Axial Pullout Testing

From Figure 5.9, it is apparent that the pullout strength of the uniform density model and the bicortical model in unicortical purchase was the same, which is supported by the statistical analysis. The similar strengths of the models indicate that the thin outer cortex of the custom bone model takes on most of the load. The significantly lower strength of the cancellous core of the custom model further supports this, as at half the density of the cortex, it failed at half the load. However, in bicortical purchase, there were major differences in strength between the two models. The maximum load withstood by the custom model almost doubled because the amount of material resisting the load doubled as a result of the screw penetrating the second cortex of the model. This behavior is indicative of how human bone would be expected to behave in a similar test because bone also has different layers, with the interior being very weak. On the other hand, the regular model tripled in strength with the use of a bicortical screw, as the amount of material resisting the load increased by much more than a factor of two. This difference in performance implies that the custom model would be more accurate in predicting the behavior of human bone.

### 6.2.2 Lateral Pullout Testing

The results of the lateral pullout tests comparing the use of various locking and non-locking screws in both bone models illustrated significant differences in how the two models behaved under the complex load that sternal fixation devices exert on the sternum *in vivo*. The custom models failed at approximately the same force when 9mm and 13mm screws were used. This is because the cancellous core of the bone is much weaker than the hard cortex that it does not support much of the lateral load. Because the 9mm and 13mm screws do not reach the second cortex, they both rely on the same amount of the stronger material to bear the load, explaining their similar performance across the two shorter length screws. When the screw length was increased to 17mm, there was a significant increase in the amount of force that the model could withstand, which can be attributed to the added support from the second cortex, as these screws were long enough to purchase into the bottom layer of the bone model. This held true for both locking and non-locking screws.

The uniform density Sawbones did not exhibit this property, as there was no significant difference in their performance with locking screws of different lengths. With non-locking screws, the maximum force withstood by the standard model increased incrementally as the length of the screw increased. This effect is a result of the corresponding increase in the amount of the dense material resisting the motion of the screws. Not only does this provide a greater possible reaction force, but it also provides added resistance to the moment caused when the non-locking screw loosens and starts to form an angle with the vertical. From this, it can be understood that the new bicortical model should perform more like human bone than the standard uniform density model. The inner core provides little resistance to force or moment the way the the standard model does, so no changes in the strength of the model are seen until the second cortex is penetrated. As human bone has a similar morphology to the bicortical model, it is expected that testing in human bone should yield similar qualitative behaviors, which were not observed in the regular Sawbones model.

### **6.3 Study Limitations**

This study had several limitations that should be taken into consideration when reviewing the results. First, the time constraints of this project and the lengthy production time limited the scope of the sternal fixation portion of this product to designing and optimizing the reverse expansion screw and plate system. However, this was not a major setback as the major goals of the project were met, and the manufactured device will be available for a future project group to physically validate. In addition, coordinating with KLS Martin, who generously made our custom reverse-expansion screw plate system, proved difficult, as they were completing this project alongside their regular work. In addition, their company is based in Europe and run on a different schedule. Lastly, the variability and limited availability of human sterna meant that the bicortical bone model could not be tested against human bone; however, we can be confident in the hypotheses about how human bone should perform in the tests completed.

### **6.4 Impacts of Device**

As with any new technology, the impacts of the device outside of its primary function were important consideration for these designs.

## **Economics**

These devices are not expected to have a major impact on the economy, however, there is a small portion of society that can be affected financially by this project. The small intricate features of the screw and plate system cost much more to manufacture than systems currently on the market. As a result, production of the device is more expensive for the manufacturer, who would then be forced to charge more for this system than for current systems. This would mean that surgeons, patients, and insurance companies would have to pay more for this system than for competitive products. While it is incredibly important to reduce material costs in the operating room, this device provides the potential for reduced equipment and time costs in the operating room. The device is compatible with standard screwdrivers and does not require any custom tools. In addition, it would reduce the probability of a second surgery, thus severely decreasing the cost for the patient. The bone model should have no impact on the national economy, as it is made by the leading company in the field.

## **Health and Safety**

As with any medical device, the screw and plate system has the potential to have both positive and negative impacts on the health and safety of the user. This novel screw and plate system would decrease the risk of failure and complications in osteoporotic bone, as it is expected to perform better than models currently on the market and because stainless steel wires cannot be used in patients with osteoporosis. The system also poses no risk to the surgeons responsible for its installation. However, there is a slight possibility that the device could fail. In this unlikely event, the screws could damage the bone, and a revision surgery would be required to fix the sternum for a second time.

In addition, the new bone model could have a positive impact on health and safety. Because it more accurately demonstrates the mechanical behavior of bone, testing completed using this model in lieu of existing ones will yield more accurate results. In turn, this will allow designers to make systems that are better suited for sternal fixation.

## **Societal Influence**

The intended impact of the sternal fixation device is to increase the survival rate of the number of patients who experience osteoporosis cannot have normal sternal fixation devices implanted. Patients with this condition are at a higher risk of complication after sternal closure. With this new system, fewer complications may occur, which will then lead to a longer lifespan of those patients. In addition, the bone model will provide more reliable testing results, instilling more confidence in the performance of fixation devices.

## **Ethical Concern**

The ethical concerns for the sternal fixation device mainly stem from its cost and small target population. The cost of manufacturing the screw is extremely high compared to other sternal fixation methods, such as cerclage wires non-locking screw and plate systems. In turn, this gives rise to the issue that it may be more worthwhile to work on a system that would be less expensive and better suited for all patients instead of one that is only required in patients who cannot tolerate cerclage wires. However, past research suggests that such a system would be incredibly difficult to achieve, and that the efforts to develop a system specifically for osteoporotic bone are valid. There are no foreseen ethical concerns pertaining to the bone model.

## **Sustainability**

The screw and plate system are made of titanium alloy (Ti-6Al-4V), using standard methods such as ASTM and ISO. This material has been extensively studied and used *in vivo*. It has been shown to have long-term survival with no negative response. This device is thus considered to be sustainable. The bicortical bone model is made of polyurethane foam, which is used for a variety of materials in numerous fields, from medical products to housing. This wide range of products show that this material has sustained for numerous years in different areas, minimizing the concern of sustainability for this product.

### **Environmental Influence**

This project has no direct environmental impacts. Production of the sternal fixation device does not have a negative impact on the environment, and the device utilizes the natural elements of titanium, aluminum and vanadium, which make up a recyclable titanium alloy used for most medical devices. The bone model material can be recycled and reused in other applications such as insulation boards, furniture, and bedding. The reuse of polyurethane reduces its environmental impact.

### **Political Ramifications**

There are no political ramifications that this project brings about. Implantable medical devices and bone models for testing said devices have been in use for quite some time. Therefore, any past political issues with said systems have since been dealt with.

### **Manufacturability**

The manufacturability of the sternal fixation device was noticeably more difficult than other screw-plate systems. This point was stressed by KLS Martin, the company that manufactured the prototype. New tools were required for manufacturing the small angular indentation in the plate where the screw head deforms, a sizeable investment on the part of the manufacturer. As a result of this difficulty, it was impossible to make the screw head using the same diameter as currently used sternal screws. Instead, the screw head has a diameter 67% larger than other screws. In addition, the manufacturing of the screw was also more difficult than standard screws, as the expandable wings of the screw are considerably more fragile and variable due to their small width and low tolerance for variations in the angle.

Moreover, the bicortical bone model does not present any manufacturing concerns. To make the first prototype, a new mold for the polyurethane was created. This required extra time and money for setup. However, once the mold was made, using it to manufacture new bone models will be much easier. This model was no more complicated than making bicortical models of other bones.

## Chapter 7: Final Design and Validation

### Introduction

Approximately 750,000 median sternotomies are performed each year in the US (Bek, et al, 2010). This procedure involves vertically bisecting the sternum to gain access to the heart. The sternal halves are then fixed together and the chest closed. Failure to do so properly results in complications such as dehiscence with a mortality rate of 14-47% (Martinez et. al., 2005). The standard of care for sternal closure is the use of stainless steel wires, which are inexpensive and easy to use. In osteoporotic patients, the wires often cut through the bone, causing additional complications. Current devices that exist to address this problem include screw and plate systems, but it is uncommon for these systems to achieve flush fit and lock to prevent loosening (Dunn, 2012, personal communication). In addition, there is a need for a better sternal model to test such systems. Current testing is done on human sterna, which are problematic due to biologic variability and difficulty obtaining samples. As an alternative, polyurethane foam models are used, but their uniform density provides results that are unlike human bone. Based on these needs, the two goals for this project were to design a lag-lock screw for sternal fixation and an anatomical sternal model for testing.

### Methods

The selected screw design was a reverse expansion screw, whose head expands when inserted into the plate, increasing friction and locking it into the plate. This function is illustrated by Figure 7.1.

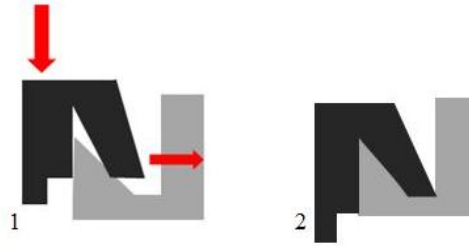


Figure 7.1: Reverse expansion screw concept

The need for this design was demonstrated by cyclic tests using locking screws provided by KLS Martin (Tuttlingen, Germany). A single screw was used to attach a fixation plate to the bone model in one of two ways: flush against the surface of the model or 2mm above it. The plate was then loaded in a cyclic manner to replicate the forces of respiration, as shown in Figure 7.2, and the peak displacement at each cycle was recorded.

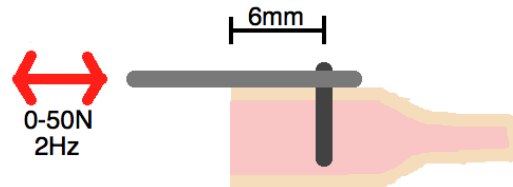


Figure 7.2: Cyclic loading test schematic

Concurrently, a bicortical sternum model was designed and custom ordered from Sawbones (Vashon, WA). The silhouette of the model was chosen to be the same as currently marketed sternum models, which have a uniform density of 20pcf. However, the new model comprised two layers: a 1.5mm thick cortical shell of 20pcf polyurethane foam and a cancellous core of 10pcf polyurethane foam. The material and densities were selected based on what is currently used in bicortical models of other bones. (Pacific Research Laboratories, 2012)

To characterize the new model, two types of tests were performed. The first was axial pullout of a cortical bone screw (ASTM F543-07 Standard). During this experiment, the bicortical bone model was compared to the standard model in cases of both unicortical (9mm into the model) and bicortical (through the entire model) screw purchase. The schematic of this procedure is shown in Figure 7.3.

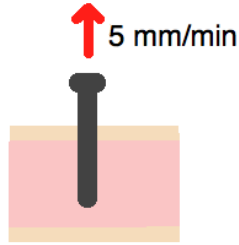


Figure 7.3: Axial pullout test schematic

The second test was a lateral pullout test, in which screw and plate systems were applied to the bone model in a manner similar to that used for cyclic loading. The plate was then loaded at a rate of 5mm/min to find the maximum force at failure. This method is illustrated in Figure 7.4. Both the custom and standard Sawbones were tested using locking and non-locking screws of various lengths.

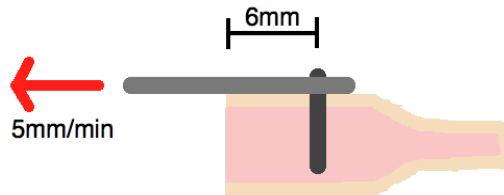


Figure 7.4: Lateral pullout test schematic

## Results

The cyclic loading tests show a significantly greater maximum displacement in those samples with the 2mm gap ( $0.211 \pm 0.125\text{mm}$ ) than those without it ( $0.0735 \pm 0.0315\text{mm}$ ). The following graph shows how the displacement increased with the number of cycles for each case.

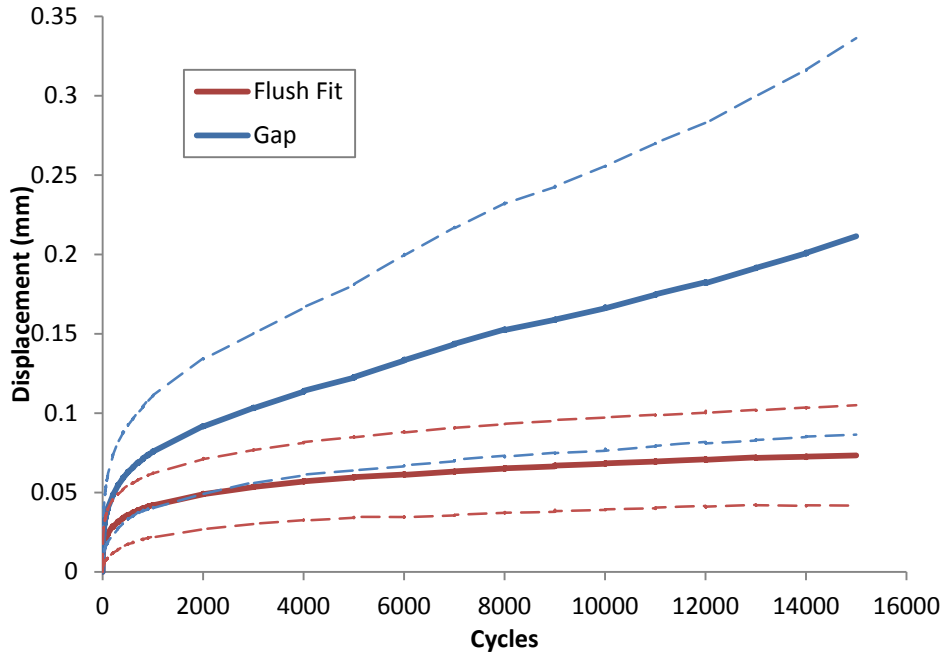


Figure 7.5: Displacement over cycles.

The parameters of the screw and plate were determined by optimizing the deformation of the screw head in FEA. Figure 7.6 shows a representative image of this. The design was then sent to KLS Martin to gain manufacturability perspective. The production and physical validation of the design was infeasible due to the six month lead-time required for production.

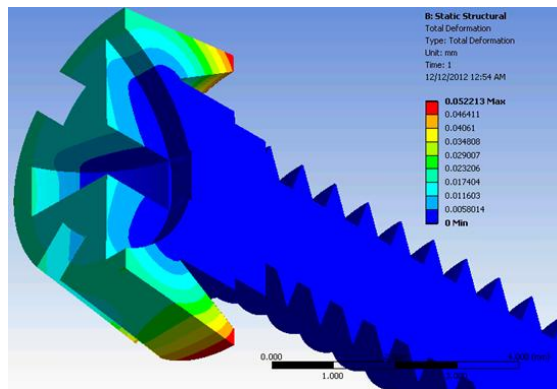


Figure 7.6: Finite element analysis.

The results and analysis from the axial pullout tests show that the pullout strength of the sternal models is dependent on both the model and the purchase of the screw. Figure 7 shows the average pullout strength (N) for each test case.

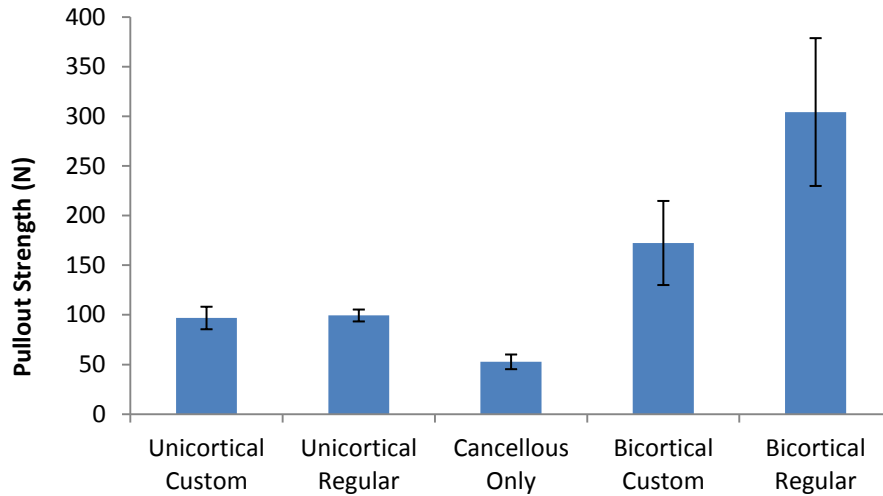


Figure 7.7: Axial pullout strength.

The lateral pullout tests show that the bicortical Sawbones can withstand significantly lower forces than the uniform models. The tests further show that the length of screws is significant only in the custom bone model. The following figure shows the force at failure for each case.

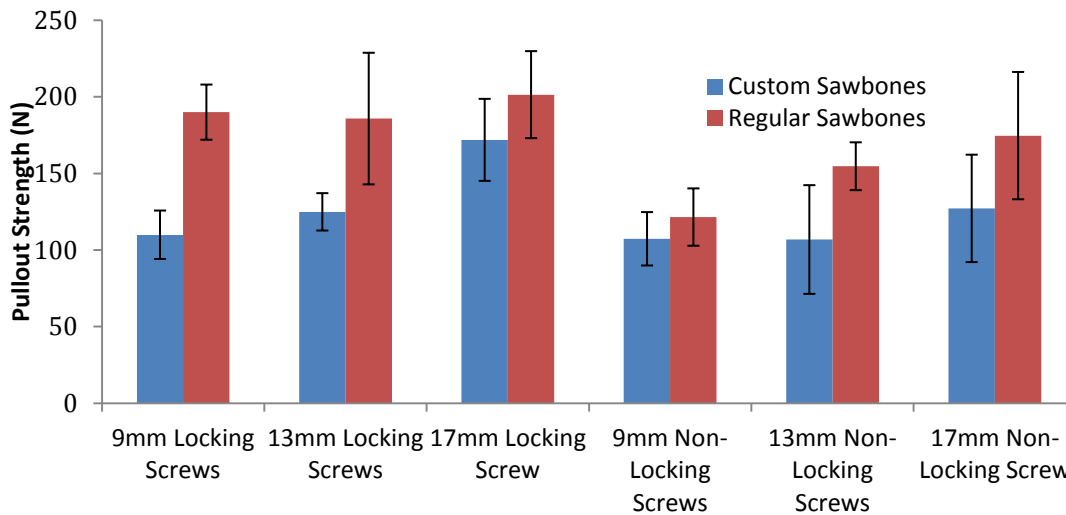


Figure 7.8: Lateral pullout strength.

## Discussion

In cyclic testing, the differences in displacement between the two cases demonstrate the need for a screw and plate system that holds the plate flush to the bone. This will cause less screw movement, and therefore less damage to the bone.

The axial pullout test shows that in unicortical purchase, the custom model withstands a force comparable to that of the standard model, despite only having 1.5mm of purchase in the denser material. However, in bicortical purchase, the pullout strength is significantly less in the custom model compared to that in the standard model.

The differences in lateral pullout performance between the two bone models can be attributed to the differences in their structure. In the custom model, the 9mm and 13mm screws extend into the cancellous core but do not reach the second cortex. Because the core is weaker than the cortex, these screws rely only on the cortical layer of the model for stability. However, when bicortical screws (17mm) are tested, they withstand higher forces. This is expected because the second cortex of the custom model provides added stability. This effect is not seen in standard models, as they have a uniform density throughout. Instead, the force the sample withstands increases incrementally as the screw length increases because the amount of material resisting the movement of the screw also increases. This suggests that the custom model is better suited for analyzing the purchase of sternal screws into bone.

## Chapter Eight: Conclusions and Recommendations

With the results of the cyclic loading test, it was determined that there is a need for a lag-lock screw and plate system that will press the sternal plate flush to the bone before the screw locks into the plate to allow for less screw movement and less damage to the sternum. Such a system was designed and sent to KLS Martin for manufacturing. It is recommended that this design be physically validated in a future project and that lag-lock systems stay the focus of solutions for repairing osteoporotic sternum post-sternotomy.

The axial and lateral pullout testing showed that new sternal model better mimicked how bone would act when mechanically tested and compared to the standard bone models on the market. It is concluded that the new model performs in a manner similar to human bone and is more suited than the standard uniform density models for comparing screw purchase. Although differences between locking and non-locking screws were more pronounced in the standard model than the custom one, there were vast differences in their behavior from what would be expected of human bone. From this, it is recommended that the new models be used to test any new sternal systems where the mechanical properties or screw purchase (thread type, screw length, etc) are being studied.

The performance indicated that the custom sternum models are suitable for testing sternal fixation methods as done in this study; however, certain parameters could have been improved to fully validate the model as a human bone testing substitute. A larger sample size for each test would improve data by reducing variance. Most importantly, we recommend testing in human sterna to fully validate the custom Sawbones models. While the sample size of human sterna would need to be large to allow for reliable and reproducible data, completing the tests in bone using the same protocols that were used for the model would allow for an accurate comparison between real bone and the sternal model.

In addition, better familiarity with the Instron machine and program would have provided the opportunity to conduct more experiments and the ability to eliminate any potential flaws with the testing methods. Furthermore, it is recommended that cyclic testing be completed at a lower frequency that is similar to the normal breathing rate to provide more comparable data to that of human sterna testing.

## References

- American Heart Association. Heart Disease and Stroke Statistics: 2007 Update. *Journal of the American Heart Association*.
- American Heart Association. Heart Disease and Stroke Statistics: 2009 Update. *Journal of the American Heart Association*.
- Ahn, J., Christakis, A., Diselman, J., & Sandefer, A. (April 2009). *Design of an optimized rigid fixation system for the osteoporotic sternum*. (Major Qualifying Project Report). Worcester, Massachusetts: Worcester Polytechnic Institute.
- An, Y. H. (Ed.). (2002). *Internal fixation in osteoporotic bone* (1st ed.) Thieme.
- Baciewicz, J., Frank A. (2011). Sternal fixation device failure? *The Annals of Thoracic Surgery*, 91(4), 1307-1308. doi: 10.1016/j.athoracsur.2010.11.052
- Bakalova et al. (2010). Development of a Bilateral Rigid Sternum Closure Testing System. Worcester Polytechnic Institute.
- Bek, E. L., Yun, K. L., Kochamba, G. S., & Pfeffer, T. A. (2010). Effective median sternotomy closure in high-risk open heart patients. *The Annals of Thoracic Surgery*, 89(4), 1317-1318. doi: 10.1016/j.athoracsur.2009.05.057
- BiometMicrofixation. *SternaLock® Blu: Primary Closure System*. Retrieved September/19, 2012, from <http://www.biometmicrofixation.com/product.php?item=20&cat=7>
- Buckley, D., Mukhanov, S., & Sebastian, H. (April 2012). *Design of a unicortical screw-plate system for the optimization of sternal fixation*. (Major Qualifying Project Report). Worcester, MA: Worcester Polytechnic Institute.
- Chao, J., Voces, R., & Peña, C. (2011). Failure analysis of the fractured wires in sternal perichronal loops. *Journal of the Mechanical Behavior of Biomedical Materials*, 4(7), 1004-1010. doi: 10.1016/j.jmbbm.2011.02.015
- Cerclage Wire. (n.d.). MedetzSurgical - Quality Instrument Provisions and Repair Services.

- Retrieved September 23, 2012, from  
<http://www.medetzurgical.com/366m10/orthopedic-surgical-instruments/cerclage-wire.html>
- Cohen, C. D. J., & Griffin, L. V. (2002). A biomechanical comparison of three sternotomy closure techniques. *The Annals of Thoracic Surgery*, 73(2), 563-568. doi: 10.1016/S0003-4975(01)03389-6
- Decoteau, D. M., Zec, H. C., Hart, A. R., Flannery, D. L., Billiar, Kristen Faculty advisor -- BE, & Dunn, Raymond Faculty advisor -- BE. (2006). *Comparison of cancellous and critical bone screws for sterna*. Worcester, MA: Worcester Polytechnic Institute.
- Dunn, R. (2012, May 3). Personal Interview.
- Ferguson, M. (2010). *Bone biology primer: An overview bone anatomy and remodeling*. Retrieved 9/13, 2012, from  
<http://www.biometmicrofixation.com/downloads/BoneBiologyPrimer.pdf>
- Gray, H. (2009). *Gray's Anatomy*. Arcturus.
- Herring, W. Retrieved 9/23, 2012, from  
<http://www.learningradiology.com/archives2010/COW%20413-Sternal%20dehiscence/sdcorrect.htm>
- Honguero Martínez, A. F., Arnau Obrer, A., Fernández Centeno, A., Saumench Perramon, R., Estors, M., & Cantó Armengod, A. (2005). Descending necrotizing mediastinitis: Treatment by transcervical thoracic drainage. *Archivos De Bronconeumología ((English Edition))*, 41(5), 293-294. doi: 10.1016/S1579-2129(06)60224-3
- Hosam, F., Alhodaib, N., Mazer, C. D., Harrington, A., Latter, D., Bonneau, D., . . . Mahoney, J. (2009). Sternal plating for primary and secondary sternal closure; can it improve sternal stability? *Journal of Cardiothoracic Surgery*, 4(1), 19. Retrieved from  
<http://www.cardiothoracicsurgery.org.ezproxy.wpi.edu/content/4/1/19>
- KLS Martin: Sternal Talon®. (n.d.). KLS Martin: KLS Martin. Retrieved October 3, 2012, from

<http://www.klsmartin.com/products/implants-and-implant-systems/sternal-closure/sternal-talonR/?L=2>

KLS Martin USA: Sternal Talon. (2008, August 29). KLS Martin USA: Operationsleuchten, OP-Leuchten, Untersuchungsleuchten. Retrieved October 3, 2012, from [http://www.klsmartinusa.com/Sternal\\_Talon](http://www.klsmartinusa.com/Sternal_Talon)

Koeppen, B. & Stanton, B. (2010). *Berne & levy physiology*. Philadelphia: Mosby Elsevier.

Kun, H., & Xiubin, Y. (2009). Median sternotomy closure: Review and update research. *Journal of Medical Colleges of PLA*, 24(2), 112-117. doi: 10.1016/S1000-1948(09)60026-5

Levin, L. S., Miller, A. S., Gajjar, A. H., Bremer, K. D., Spann, J., Milano, C. A., & Erdmann, D. (2010). An innovative approach for sternal closure. *The Annals of Thoracic Surgery*, 89(6), 1995-1999. doi: 10.1016/j.athoracsur.2010.01.089

Losanoff, J. E., Foerst, J. R., Huff, H., Richman, B. W., Collier, A. D., Hsieh, F., . . . Jones, J. W. (2002). Biomechanical porcine model of median sternotomy closure. *Journal of Surgical Research*, 107(1), 108-112. doi: 10.1006/jsre.2002.6488

McGregor, W. E., Payne, M., Trumble, D. R., Farkas, K. M., & Magovern, J. A. (2003). Improvement of sternal closure stability with reinforced steel wires. *Ann Thorac Surg*, 76, 1631-4.

McGregor, W. E., Payne, M., Trumble, D. R., Farkas, K. M., & Magovern, J. A. (2003). Improvement of sternal closure stability with reinforced steel wires. *The Annals of Thoracic Surgery*, 76(5), 1631-1634. doi: 10.1016/S0003-4975(03)00760-4

*National osteoporosis foundation*. (2011). Retrieved 9/13, 2012, from <http://www.nof.org/home>

OrthoHelix Surgical Designs, I. (2012). *MaxLock extreme screws* . Retrieved September, 2012, from <http://www.orthohelix.com/products/maxlock-extreme/screws>

Ozaki, W., Buchman, S. R., Iannettoni, M. D., & Frankenburg, E. P. (1998). Biomechanical study of sternal closure using rigid fixation techniques in human cadavers. *The Annals of Thoracic Surgery*, 65(6), 1660-1665. doi: 10.1016/S0003-4975(98)00231-8

- Ozkaya, N., & Nordin, M. (1998). In D.P. Leger (Ed.), *Fundamentals of biomechanics: Equilibrium, motion, and deformation* (Second ed.). New York, NY: Springer.
- Pacific Research Laboratories, Inc. (2012). Sawbones Worldwide company website. Retrieved March 2013 from <http://sawbones.com>
- Pai, S., Billiar, K. L., Gunja, N. J., Dupak, E. L., McMahon, N. L., Roth, T. P., . . . Pins, G. D. (2005). In vitro comparison of wire and plate fixation for midline sternotomies. *The Annals of Thoracic Surgery*, 80(3), 962-968. doi: 10.1016/j.athoracsur.2005.03.089
- Park, J. B., & Lakes, R. S. (1992). *Biomaterials: An introduction* (2nd ed.) Plenum press.
- Patel PSD, Shepherd DET, Hukins DWL: "Compressive properties of commercially available polyurethane foams as mechanical models for osteoporotic human cancellous bone." *BMC Musculoskeletal Disorders* 2008, 9:137
- Plass, A., Grünenfelder, J., Reuthebuch, O., Vachenauer, R., Gauer, J., Zünd, G., & Genoni, M. (2007). New transverse plate fixation system for complicated sternal wound infection after median sternotomy. *The Annals of Thoracic Surgery*, 83(3), 1210-1212. doi: 10.1016/j.athoracsur.2006.03.0
- Raman, J., Straus, D., & Song, D. H. (2007). Rigid plate fixation of the sternum. *The Annals of Thoracic Surgery*, 84(3), 1056-1058. doi: 10.1016/j.athoracsur.2006.11.045
- Selthofer, R., Nikolie, V., Mrcela, T., Radic, R., Leksan, I., Rudez, I., & Selthofer, K. (2006). Morphometric analysis of the sternum. *Coll. Antropol.*, 30, 43-43-47.
- Song, D., Brunelli, J., Costello, P., & Ford, M. (April 2011). *Design of a screw plate system to minimize screw loosening in sternal fixation*. (Major Qualifying Project Report). Worcester, MA: Worcester Polytechnic Institute.
- Sternum*. (2012). Retrieved 9/13, 2012, from <http://www.britannica.com/EBchecked/topic/565822/sternum>
- Trumble, D. R., McGregor, W. E., & Magovern, J. A. (2002). Validation of a bone analog model for studies of sternal closure. *The Annals of Thoracic Surgery*, 74(3), 739-44.

Tsai, I. C., Lee W. L., Tsao C. R., Chang Y., Chen M. C., Lee T., & Liao W. C. (2008) Comprehensive evaluation of ischemic heart disease using MDCT, *American Journal of Radiology*, 191, 64-72

Vand, E.H., Oskouei, R. H., and Chakherlou, T.N. (2008). An experimental method for measuring clamping force in bolted connections and effect of bolt threads lubrication on its value. *World academy of Science, Engineering, and Technology* (22): pp. 457-460.

Voss, B., et al (2008). Sternal reconstruction with titanium plates in complicated sternal dehiscence. *European Journal of Cardio-Thoracic Surgery*, 34, 139-145

Wall SJ, Soin SP, Knight TA, Mears SC, Belkoff SM. (2010). *Mechanical evaluation of a 4-mm cancellous "rescue" screw in osteoporotic cortical bone: A cadaveric study.*

## Appendix

### Appendix A: Sternal Fixation Device Pairwise Comparison Charts

Table 1: Pairwise Comparison Chart completed by the team

	Effective	Safe	Manufacturable	Easy to use	Total
Effective		0	1	1	2
Safe	1		1	1	3
Manufacturable	0	0		0.5	0.5
Easy to use	0	0	0.5		0.5

Table 2: Pairwise Comparison Chart completed by Advisor Professor Billiar

	Effective	Safe	Manufacturable	Easy to use	Total
Effective		0	1	1	2
Safe	1		1	1	3
Manufacturable	0	0		1	1
Easy to use	0	0	0		0

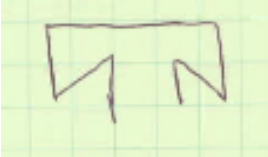
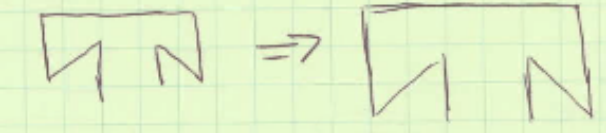
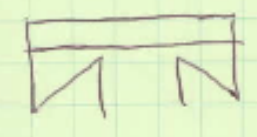
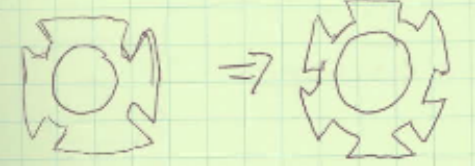
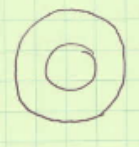
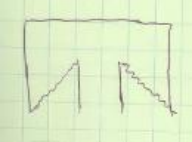
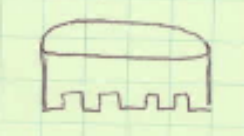
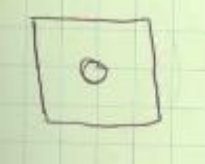
Table 3: Pairwise Comparison Chart completed by client KLS Martin

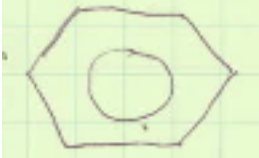
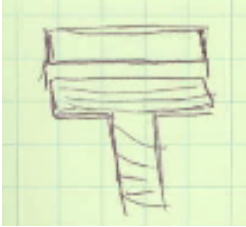
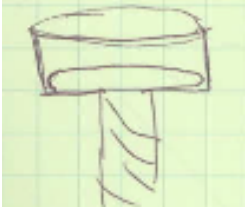
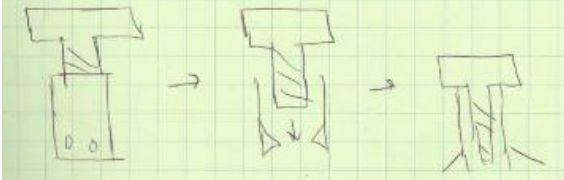
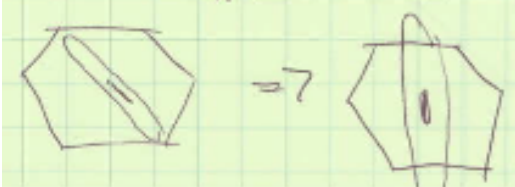
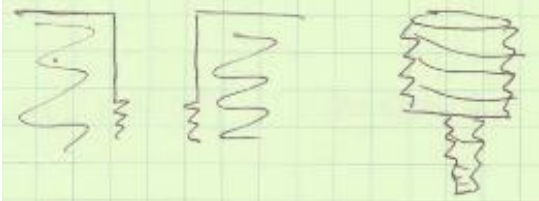
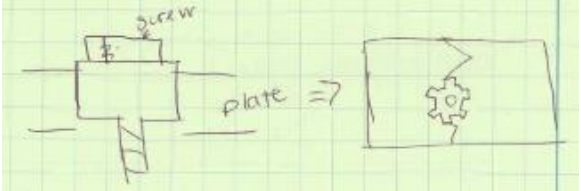
	Effective	Safe	Manufacturable	Easy to use	Total
Effective		0	1	1	2
Safe	1		1	1	3
Manufacturable	0	0		0	0
Easy to use	0	0	1		1

Table 4: Pairwise Comparison Chart completed by client Dr. Raymond Dunn, UMMS

	Effective	Safe	Manufacturable	Easy to use	Total
Effective		0.5	1	1	2.5
Safe	0.5		1	1	2.5
Manufacturable	0	0		1	1
Easy to use	0	0	0		0

## Appendix B: List of Alternative Designs

Design	Sketch
Reverse expansion screw	
Larger screw head or troughs	
Groove around head of screw	
More vertical slits in head	
No vertical slits in head	
Rough surface to increase friction	
Teeth to lock into place	
Square screw head in circular hole	
Circular screw in square hole	

<p>Angled teeth in screw head and plate</p>	
<p>Hexagonal screw in hexagonal hole</p>	
<p>Cap over the screw</p>	
<p>Cap attached to screw head</p>	
<p>Locking sheath around screw</p>	
<p>Hexagonal screw with rotating lock on head</p>	
<p>Lag-threaded plate for locking screw</p>	
<p>Plate attached locking mechanism to secure screw</p>	

## Appendix C: Sternal Fixation Device Design Selection Matrix

	Easy to use	Easy to manufacture	Safe	Effective	Total Points
<b>Weighting based on PCC</b>	<b>0.075</b>	<b>0.075</b>	<b>0.45</b>	<b>0.40</b>	<b>1</b>
<b>Reverse expansion screw and custom plate</b>	8	4	8	9	8.1
<b>Slanted teeth in screw and plate</b>	7	2	8	8	7.475
<b>Lag-lock threaded plate and custom screw</b>	8	6	8	7	7.45
<b>Hexagonal screw head with custom plate</b>	6	7	8	5	6.575
<b>Teeth on screw head</b>	5	3	8	5	6.2
<b>Square screw head, circular hole</b>	5	7	7	4	5.65
<b>Circular screw head, square hole</b>	5	7	7	3	5.25
<b>Attached cap</b>	5	3	6	6	5.7
<b>Rotating lock on screw head</b>	5	2	7	4	5.275
<b>Locking mechanism on plate</b>	6	2	6	6	5.7

## Appendix D: Finite Element Analysis Data

### FEA Calculations

$$\begin{aligned}\tau &= 0.2 * r * F \\ F &= \frac{\tau}{0.2r} \\ F &= \frac{190.66N \cdot mm}{0.2 * 3mm} = 318N\end{aligned}$$

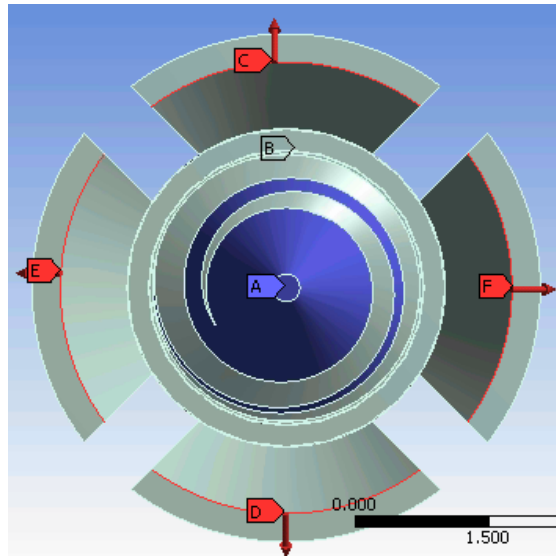


Figure D-1: Illustration of the reactions forces on the applied edge of the screw. Red arrows represent reaction force on a wing.

$$F(\text{per length } h) = \frac{317.767N}{(4)3.23mm} = 25N/mm$$

$$F(\text{applied to one wing}) = Fr = \left(\frac{25N}{mm}\right) * 3.23mm = 79N$$

$$F2\sin\theta - Fr = 0$$

$$F2\sin\theta = Fr = Fy$$

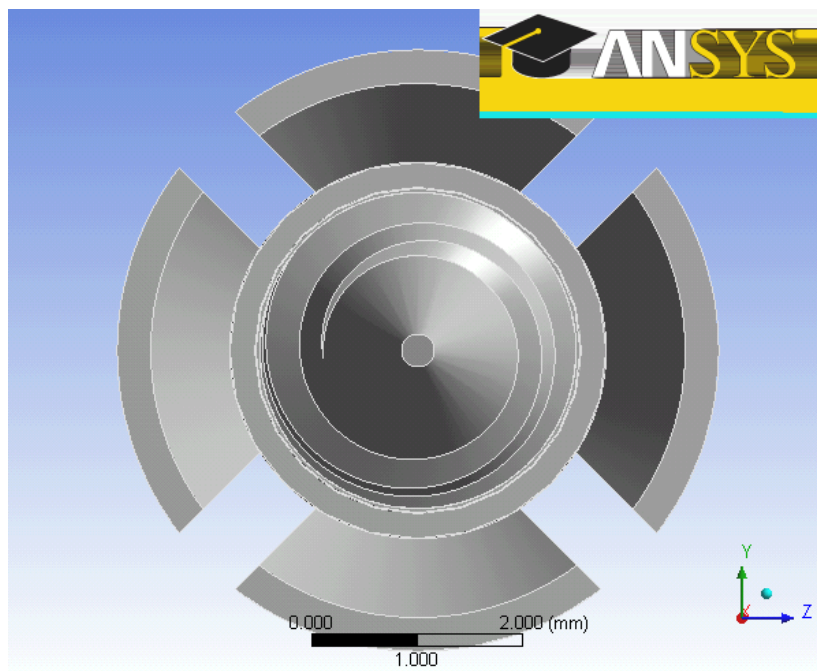
$$F2 = \frac{Fr}{\sin\theta} = \frac{79}{\sin 35} = 138.5 N$$

## FEA Reports



Analysis of 55 degree plate angle

First Saved	Tuesday, December 11, 2012
Last Saved	Tuesday, December 11, 2012
Product Version	13.0 Release



Units

**TABLE 1**

Unit System	Metric (mm, kg, N, s, mV, mA) Degrees rad/s Celsius
Angle	Degrees
Rotational Velocity	rad/s
Temperature	Celsius

Model (B4)

Geometry

**TABLE 2**  
**Model (B4) > Geometry**

Object Name	<i>Geometry</i>
State	Fully Defined
<b>Definition</b>	
Source	C:\Users\bvaaron\Desktop\CAD Designs\Screw Design 2.SLDPRT
Type	SolidWorks
Length Unit	Meters
Element Control	Program Controlled
Display Style	Part Color
<b>Bounding Box</b>	
Length X	15. mm
Length Y	5.7071 mm
Length Z	5.7071 mm
<b>Properties</b>	
Volume	86.246 mm <sup>3</sup>
Mass	3.9846e-004 kg
Scale Factor Value	1.
<b>Statistics</b>	
Bodies	1
Active Bodies	1
Nodes	42265
Elements	22420
Mesh Metric	None
<b>Preferences</b>	
Import Solid Bodies	Yes
Import Surface Bodies	Yes
Import Line Bodies	No
Parameter Processing	Yes
Personal Parameter Key	DS
CAD Attribute Transfer	No
Named Selection Processing	No
Material Properties Transfer	No
CAD Associativity	Yes
Import Coordinate Systems	No
Reader Save Part File	No
Import Using Instances	Yes

Do Smart Update	No
Attach File Via Temp File	Yes
Temporary Directory	C:\Users\bvaaron\AppData\Local\Temp\15771
Analysis Type	3-D
Mixed Import Resolution	None
Enclosure and Symmetry Processing	Yes
Mesh Metric	None

**TABLE 8**  
**Model (B4) > Static Structural (B5) > Loads**

Object Name	<i>Fixed Support</i>	<i>Fixed Support 2</i>	<i>Force</i>	<i>Force 2</i>	<i>Force 4</i>
State	Fully Defined				
<b>Scope</b>					
Scoping Method	Geometry Selection				
Geometry	2 Faces	1 Face	1 Edge		
<b>Definition</b>					
Type	Fixed Support		Force		
Suppressed	No				
Define By	Components				
Coordinate System	Global Coordinate System				
X Component			79.442 N (ramped)	55.626 N (ramped)	
Y Component			0. N (ramped)	-79.442 N (ramped)	79.442 N (ramped)
Z Component			55.626 N (ramped)	0. N (ramped)	

**TABLE 12**  
**Model (B4) > Static Structural (B5) > Solution (B6) > Results**

Object Name	<i>Total Deformation</i>	<i>Equivalent Stress</i>
State	Solved	
<b>Scope</b>		
Scoping Method	Geometry Selection	
Geometry	All Bodies	
<b>Definition</b>		

Type	Total Deformation	Equivalent (von-Mises) Stress
By	Time	
Display Time	Last	
Calculate Time History	Yes	
Identifier		
<b>Results</b>		
Minimum	0. mm	6.1785e-002 MPa
Maximum	3.6425e-002 mm	833.71 MPa
<b>Information</b>		
Time	1. s	
Load Step	1	
Substep	1	
Iteration Number	1	
<b>Integration Point Results</b>		
Display Option		Averaged



Analysis of 45degree plate angle

Mass	3.9846e-004 kg
Centroid X	-4.9375 mm
Centroid Y	8.6454e-004 mm
Centroid Z	1.1365e-003 mm
Moment of Inertia Ip1	8.6197e-004 kg·mm <sup>2</sup>
Moment of Inertia Ip2	7.3469e-003 kg·mm <sup>2</sup>
Moment of Inertia Ip3	7.3468e-003 kg·mm <sup>2</sup>
<b>Statistics</b>	
Nodes	42265
Elements	22420
Mesh Metric	None

**TABLE 8**

**Model (B4) > Static Structural (B5) > Loads**

Object Name	<i>Fixed</i>	<i>Fixed</i>	<i>Force 2</i>	<i>Force 4</i>	<i>Force</i>
-------------	--------------	--------------	----------------	----------------	--------------

	<i>Support</i>	<i>Support 2</i>			
State	Fully Defined				
<b>Scope</b>					
Scoping Method	Geometry Selection				
Geometry	2 Faces	1 Face	1 Edge		
<b>Definition</b>					
Type	Fixed Support		Force		
Suppressed	No				
Define By	Components				
Coordinate System	Global Coordinate System				
X Component	79.442 N (ramped)				
Y Component			-79.442 N (ramped)	79.442 N (ramped)	0. N (ramped)
Z Component			0. N (ramped)		-79.442 N (ramped)



Analysis of 40degree plate angle

**TABLE 8**  
**Model (B4) > Static Structural (B5) > Loads**

Object Name	<i>Fixed Support</i>	<i>Fixed Support 2</i>	<i>Force 2</i>	<i>Force 4</i>	<i>Force</i>
State	Fully Defined				
<b>Scope</b>					
Scoping Method	Geometry Selection				
Geometry	2 Faces	1 Face	1 Edge		
<b>Definition</b>					
Type	Fixed Support		Force		
Suppressed	No				
Define By	Components				

Coordinate System		Global Coordinate System		
X Component		79.442 N (ramped)		
Y Component		-94.674 N (ramped)	94.674 N (ramped)	0. N (ramped)
Z Component		0. N (ramped)		-94.674 N (ramped)

**TABLE 12**

**Model (B4) > Static Structural (B5) > Solution (B6) > Results**

Object Name	<i>Total Deformation</i>	<i>Equivalent Stress</i>
State	Solved	
<b>Scope</b>		
Scoping Method	Geometry Selection	
Geometry	All Bodies	
<b>Definition</b>		
Type	Total Deformation	Equivalent (von-Mises) Stress
By	Time	
Display Time	Last	
Calculate Time History	Yes	
Identifier		
<b>Results</b>		
Minimum	0. mm	7.6742e-002 MPa
Maximum	4.5443e-002 mm	1011.9 MPa
<b>Information</b>		
Time	1. s	
Load Step	1	
Substep	1	
Iteration Number	1	
<b>Integration Point Results</b>		
Display Option		Averaged

Material Data

Titanium Alloy

**TABLE 13**

**Titanium Alloy > Constants**

Density	4.62e-006 kg mm <sup>-3</sup>
Coefficient of Thermal Expansion	9.4e-006 C <sup>-1</sup>
Specific Heat	5.22e+005 mJ kg <sup>-1</sup> C <sup>-1</sup>
Thermal Conductivity	2.19e-002 W mm <sup>-1</sup> C <sup>-1</sup>
Resistivity	1.7e-003 ohm mm

**TABLE 14**

**Titanium Alloy > Compressive Ultimate Strength**

Compressive Ultimate Strength MPa
0

**TABLE 15**

**Titanium Alloy > Compressive Yield Strength**

Compressive Yield Strength MPa
930

**TABLE 16**

**Titanium Alloy > Tensile Yield Strength**

Tensile Yield Strength MPa
930

**TABLE 17**

**Titanium Alloy > Tensile Ultimate Strength**

Tensile Ultimate Strength MPa
1070

**TABLE 18**

**Titanium Alloy > Isotropic Secant Coefficient of Thermal Expansion**

Reference Temperature C
22

**TABLE 19**

**Titanium Alloy > Isotropic Elasticity**

Temperature C	Young's Modulus MPa	Poisson's Ratio	Bulk Modulus MPa	Shear Modulus MPa
---------------	---------------------	-----------------	------------------	-------------------

	96000	0.36	1.1429e+005	35294
--	-------	------	-------------	-------

**TABLE 20**  
**Titanium Alloy > Isotropic Relative Permeability**

Relative Permeability
1



Analysis of 35degree plate angle

Model (B4)

Geometry

**TABLE 2**  
**Model (B4) > Geometry**

Object Name	Geometry
State	Fully Defined
<b>Definition</b>	
Source	C:\Users\bvaaron\Desktop\CAD Designs\Screw Design 2.SLDPRT
Type	SolidWorks
Length Unit	Meters
Element Control	Program Controlled
Display Style	Part Color
<b>Bounding Box</b>	
Length X	15. mm
Length Y	5.7071 mm
Length Z	5.7071 mm
<b>Properties</b>	
Volume	86.246 mm <sup>3</sup>
Mass	3.9846e-004 kg
Scale Factor Value	1.
<b>Statistics</b>	

Bodies	1
Active Bodies	1
Nodes	42265
Elements	22420
Mesh Metric	None
<b>Preferences</b>	
Import Solid Bodies	Yes
Import Surface Bodies	Yes
Import Line Bodies	No
Parameter Processing	Yes
Personal Parameter Key	DS
CAD Attribute Transfer	No
Named Selection Processing	No
Material Properties Transfer	No
CAD Associativity	Yes
Import Coordinate Systems	No
Reader Save Part File	No
Import Using Instances	Yes
Do Smart Update	No
Attach File Via Temp File	Yes
Temporary Directory	C:\Users\bvaaron\AppData\Local\Temp\15771
Analysis Type	3-D
Mixed Import Resolution	None
Enclosure and Symmetry Processing	Yes

**TABLE 3**

**Model (B4) > Geometry > Parts**

Object Name	<i>Screw Design 2</i>
State	Meshed
<b>Graphics Properties</b>	
Visible	Yes
Transparency	1
<b>Definition</b>	

Suppressed	No
Stiffness Behavior	Flexible
Coordinate System	Default Coordinate System
Reference Temperature	By Environment
<b>Material</b>	
Assignment	Titanium Alloy
Nonlinear Effects	Yes
Thermal Strain Effects	Yes
<b>Bounding Box</b>	
Length X	15. mm
Length Y	5.7071 mm
Length Z	5.7071 mm
<b>Properties</b>	
Volume	86.246 mm <sup>3</sup>
Mass	3.9846e-004 kg
Centroid X	-4.9375 mm
Centroid Y	8.6454e-004 mm
Centroid Z	1.1365e-003 mm
Moment of Inertia Ip1	8.6197e-004 kg·mm <sup>2</sup>
Moment of Inertia Ip2	7.3469e-003 kg·mm <sup>2</sup>
Moment of Inertia Ip3	7.3468e-003 kg·mm <sup>2</sup>
<b>Statistics</b>	
Nodes	42265
Elements	22420
Mesh Metric	None

Coordinate Systems

**TABLE 4**

**Model (B4) > Coordinate Systems > Coordinate System**

Object Name	<i>Global Coordinate System</i>
State	Fully Defined
<b>Definition</b>	
Type	Cartesian
Coordinate System ID	0.

Origin	
Origin X	0. mm
Origin Y	0. mm
Origin Z	0. mm
Directional Vectors	
X Axis Data	[ 1. 0. 0. ]
Y Axis Data	[ 0. 1. 0. ]
Z Axis Data	[ 0. 0. 1. ]

Mesh

**TABLE 5**  
**Model (B4) > Mesh**

Object Name	<i>Mesh</i>
State	Solved
Defaults	
Physics Preference	Mechanical
Relevance	0
Sizing	
Use Advanced Size Function	Off
Relevance Center	Coarse
Element Size	0.250 mm
Initial Size Seed	Active Assembly
Smoothing	Medium
Transition	Fast
Span Angle Center	Coarse
Minimum Edge Length	0.250 mm
Inflation	
Use Automatic Inflation	None
Inflation Option	Smooth Transition
Transition Ratio	0.272
Maximum Layers	5
Growth Rate	1.2
Inflation Algorithm	Pre
View Advanced Options	No

<b>Advanced</b>	
Shape Checking	Standard Mechanical
Element Midside Nodes	Program Controlled
Straight Sided Elements	No
Number of Retries	Default (4)
Extra Retries For Assembly	Yes
Rigid Body Behavior	Dimensionally Reduced
Mesh Morphing	Disabled
<b>Defeaturing</b>	
Pinch Tolerance	Please Define
Generate Pinch on Refresh	No
Automatic Mesh Based Defeaturing	On
Defeaturing Tolerance	Default
<b>Statistics</b>	
Nodes	42265
Elements	22420
Mesh Metric	None

Static Structural (B5)

**TABLE 6**  
**Model (B4) > Analysis**

Object Name	<i>Static Structural (B5)</i>
State	Solved
<b>Definition</b>	
Physics Type	Structural
Analysis Type	Static Structural
Solver Target	Mechanical APDL
<b>Options</b>	
Environment Temperature	22. °C
Generate Input Only	No

**TABLE 7**  
**Model (B4) > Static Structural (B5) > Analysis Settings**

Object Name	<i>Analysis Settings</i>
-------------	--------------------------

State	Fully Defined
<b>Step Controls</b>	
Number Of Steps	1.
Current Step Number	1.
Step End Time	1. s
Auto Time Stepping	Off
Define By	Substeps
Number Of Substeps	1.
<b>Solver Controls</b>	
Solver Type	Program Controlled
Weak Springs	Program Controlled
Large Deflection	Off
Inertia Relief	Off
<b>Restart Controls</b>	
Generate Restart Points	Program Controlled
Retain Files After Full Solve	No
<b>Nonlinear Controls</b>	
Force Convergence	Program Controlled
Moment Convergence	Program Controlled
Displacement Convergence	Program Controlled
Rotation Convergence	Program Controlled
Line Search	Program Controlled
Stabilization	Off
<b>Output Controls</b>	
Calculate Stress	Yes
Calculate Strain	Yes
Calculate Contact	No
Calculate Results At	All Time Points
<b>Analysis Data Management</b>	
Solver Files Directory	C:\Users\bvaaron\Desktop\second FEA_files\dp0\SYS\MECH\
Future Analysis	None
Scratch Solver Files Directory	
Save MAPDL db	No

Delete Unneeded Files	Yes
Nonlinear Solution	No
Solver Units	Active System
Solver Unit System	nmm

**TABLE 8**

**Model (B4) > Static Structural (B5) > Loads**

Object Name	<i>Fixed Support</i>	<i>Fixed Support 2</i>	<i>Force 2</i>	<i>Force 4</i>	<i>Force</i>
State	Fully Defined				
<b>Scope</b>					
Scoping Method	Geometry Selection				
Geometry	2 Faces	1 Face	1 Edge		
<b>Definition</b>					
Type	Fixed Support		Force		
Suppressed	No				
Define By	Components				
Coordinate System	Global Coordinate System				
X Component	79.442 N (ramped)				
Y Component			-113.46 N (ramped)	113.46 N (ramped)	0. N (ramped)
Z Component			0. N (ramped)		-113.46 N (ramped)

**FIGURE 1**

**Model (B4) > Static Structural (B5) > Force 2**

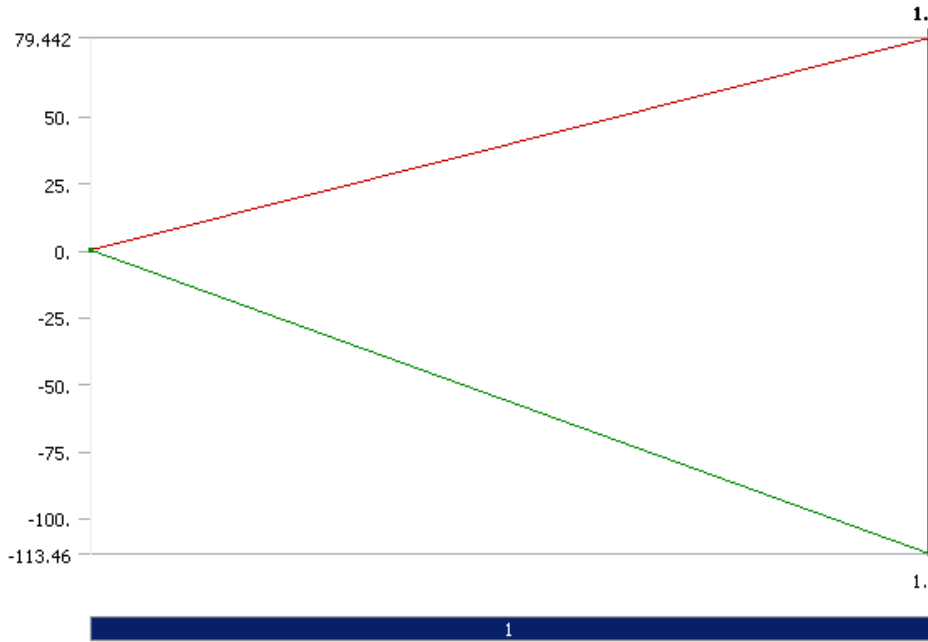


**FIGURE 2**  
**Model (B4) > Static Structural (B5) > Force 4**



**FIGURE 3**  
**Model (B4) > Static Structural (B5) > Force**

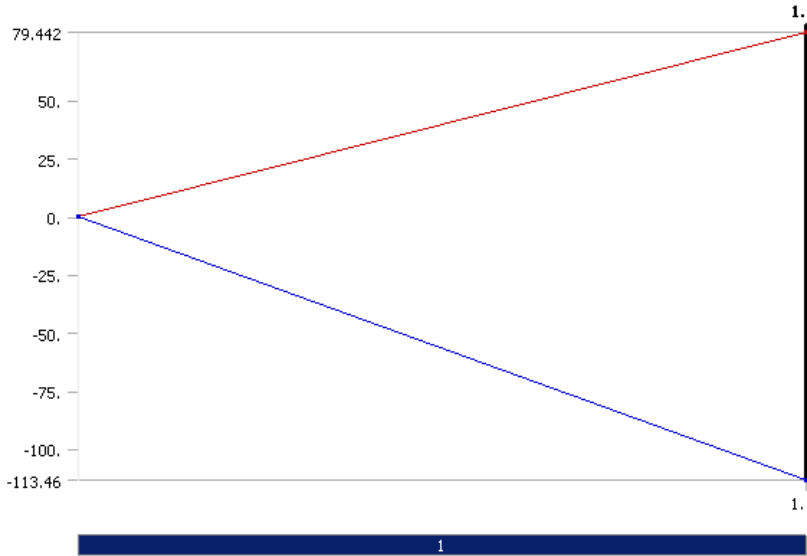
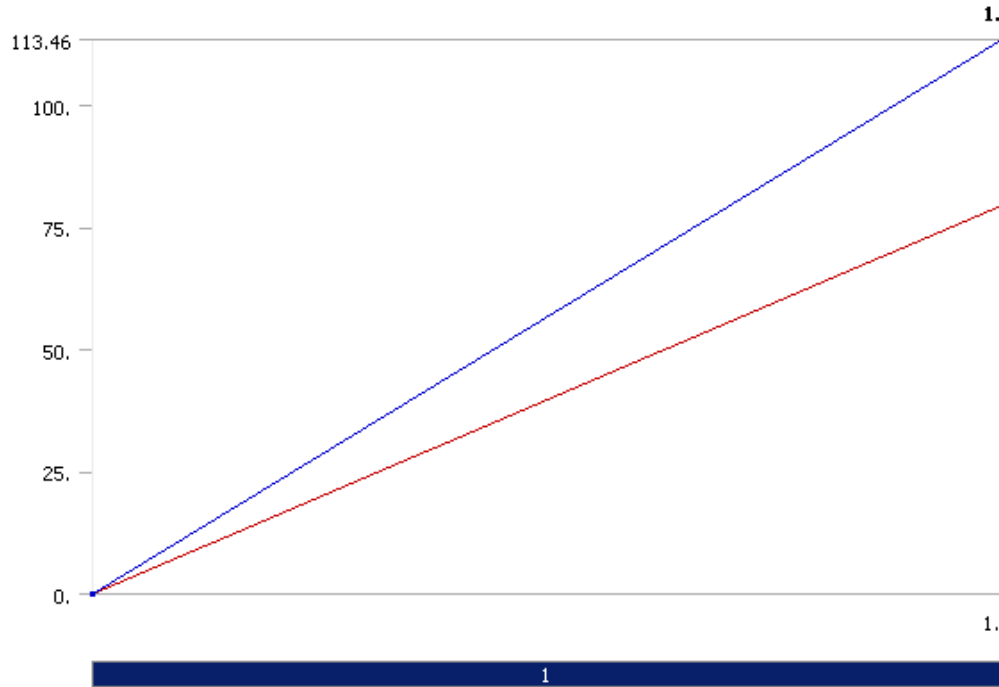


**TABLE 9**  
**Model (B4) > Static Structural (B5) > Loads**

Object Name	<i>Force 5</i>
State	Fully Defined
<b>Scope</b>	
Scoping Method	Geometry Selection
Geometry	1 Edge
<b>Definition</b>	
Type	Force
Define By	Components
Coordinate System	Global Coordinate System
X Component	79.442 N (ramped)
Y Component	0. N (ramped)
Z Component	113.46 N (ramped)
Suppressed	No

**FIGURE 4**  
**Model (B4) > Static Structural (B5) > Force 5**



Solution (B6)

**TABLE 10**  
**Model (B4) > Static Structural (B5) > Solution**

Object Name	<i>Solution (B6)</i>
State	Solved
<b>Adaptive Mesh Refinement</b>	
Max Refinement Loops	1.
Refinement Depth	2.
<b>Information</b>	
Status	Done

**TABLE 11**  
**Model (B4) > Static Structural (B5) > Solution (B6) > Solution Information**

Object Name	<i>Solution Information</i>
State	Solved
<b>Solution Information</b>	
Solution Output	Solver Output
Newton-Raphson Residuals	0
Update Interval	2.5 s

Display Points	All
----------------	-----

**TABLE 12**

**Model (B4) > Static Structural (B5) > Solution (B6) > Results**

Object Name	<i>Total Deformation</i>	<i>Equivalent Stress</i>
State	Solved	
<b>Scope</b>		
Scoping Method	Geometry Selection	
Geometry	All Bodies	
<b>Definition</b>		
Type	Total Deformation	Equivalent (von-Mises) Stress
By	Time	
Display Time	Last	
Calculate Time History	Yes	
Identifier		
<b>Results</b>		
Minimum	0. mm	8.1833e-002 MPa
Maximum	5.2213e-002 mm	1186. MPa
<b>Information</b>		
Time	1. s	
Load Step	1	
Substep	1	
Iteration Number	1	
<b>Integration Point Results</b>		
Display Option	Averaged	



Analysis of 2.25mmscrew head height

**TABLE 11**

**Model (B4) > Static Structural (B5) > Solution (B6) > Solution Information**

Object Name	<i>Solution Information</i>
State	Solved

Solution Information	
Solution Output	Solver Output
Newton-Raphson Residuals	0
Update Interval	2.5 s
Display Points	All

**TABLE 12**

**Model (B4) > Static Structural (B5) > Solution (B6) > Results**

Object Name	Total Deformation	Equivalent Stress
State	Solved	
Scope		
Scoping Method	Geometry Selection	
Geometry	All Bodies	
Definition		
Type	Total Deformation	Equivalent (von-Mises) Stress
By	Time	
Display Time	Last	
Calculate Time History	Yes	
Identifier		
Results		
Minimum	0. mm	7.6007e-002 MPa
Maximum	7.0412e-002 mm	1577.8 MPa
Information		
Time	1. s	
Load Step	1	
Substep	1	
Iteration Number	1	
Integration Point Results		
Display Option	Averaged	



Analysis of 2.10mm screw head height

Model (B4)

Geometry

**TABLE 2**  
**Model (B4) > Geometry**

Object Name	<i>Geometry</i>
State	Fully Defined
<b>Definition</b>	
Source	C:\Users\bvaaron\Desktop\CAD Designs\Screw Design 2-head diameter 2.SLDPRT
Type	SolidWorks
Length Unit	Meters
Element Control	Program Controlled
Display Style	Part Color
<b>Bounding Box</b>	
Length X	15. mm
Length Y	5.7071 mm
Length Z	5.7071 mm
<b>Properties</b>	
Volume	79.557 mm <sup>3</sup>
Mass	3.6755e-004 kg
Scale Factor Value	1.
<b>Statistics</b>	
Bodies	1
Active Bodies	1
Nodes	41957
Elements	22115
Mesh Metric	None
<b>Preferences</b>	
Import Solid Bodies	Yes
Import Surface Bodies	Yes
Import Line Bodies	No
Parameter Processing	Yes
Personal Parameter Key	DS
CAD Attribute Transfer	No

Named Selection Processing	No
Material Properties Transfer	No
CAD Associativity	Yes
Import Coordinate Systems	No
Reader Save Part File	No
Import Using Instances	Yes
Do Smart Update	No
Attach File Via Temp File	Yes
Temporary Directory	C:\Users\bvaaron\AppData\Local\Temp\15771
Analysis Type	3-D
Mixed Import Resolution	None
Enclosure and Symmetry Processing	Yes

**TABLE 3**

**Model (B4) > Geometry > Parts**

Object Name	<i>Screw Design 2-head diameter 2</i>
State	Meshed
<b>Graphics Properties</b>	
Visible	Yes
Transparency	1
<b>Definition</b>	
Suppressed	No
Stiffness Behavior	Flexible
Coordinate System	Default Coordinate System
Reference Temperature	By Environment
<b>Material</b>	
Assignment	Titanium Alloy
Nonlinear Effects	Yes
Thermal Strain Effects	Yes
<b>Bounding Box</b>	
Length X	15. mm

Length Y	5.7071 mm
Length Z	5.7071 mm
<b>Properties</b>	
Volume	79.557 mm <sup>3</sup>
Mass	3.6755e-004 kg
Centroid X	-5.1643 mm
Centroid Y	-1.4949e-003 mm
Centroid Z	-1.4262e-003 mm
Moment of Inertia Ip1	7.3263e-004 kg·mm <sup>2</sup>
Moment of Inertia Ip2	7.031e-003 kg·mm <sup>2</sup>
Moment of Inertia Ip3	7.0309e-003 kg·mm <sup>2</sup>
<b>Statistics</b>	
Nodes	41957
Elements	22115
Mesh Metric	None

**TABLE 12**

**Model (B4) > Static Structural (B5) > Solution (B6) > Results**

Object Name	<i>Total Deformation</i>	<i>Equivalent Stress</i>
State	Solved	
<b>Scope</b>		
Scoping Method	Geometry Selection	
Geometry	All Bodies	
<b>Definition</b>		
Type	Total Deformation	Equivalent (von-Mises) Stress
By	Time	
Display Time	Last	
Calculate Time History	Yes	
Identifier		
<b>Results</b>		
Minimum	0. mm	6.0788e-002 MPa
Maximum	9.0518e-002 mm	1711.4 MPa
<b>Information</b>		
Time	1. s	

Load Step	1	
Substep	1	
Iteration Number	1	
<b>Integration Point Results</b>		
Display Option		Averaged



Analysis of 0.138mm wing base thickness

Model (B4)

Geometry

**TABLE 2**  
**Model (B4) > Geometry**

Object Name	<i>Geometry</i>
State	Fully Defined
<b>Definition</b>	
Source	C:\Users\bvaaron\Desktop\CAD Designs\Screw Design 2-head diameter 2-base width 0.138.SLDPRT
Type	SolidWorks
Length Unit	Meters
Element Control	Program Controlled
Display Style	Part Color
<b>Bounding Box</b>	
Length X	15. mm
Length Y	5.3471 mm
Length Z	5.3471 mm
<b>Properties</b>	
Volume	76.902 mm <sup>3</sup>
Mass	3.5529e-004 kg
Scale Factor Value	1.
<b>Statistics</b>	
Bodies	1

Active Bodies	1
Nodes	41155
Elements	21561
Mesh Metric	None
<b>Preferences</b>	
Import Solid Bodies	Yes
Import Surface Bodies	Yes
Import Line Bodies	No
Parameter Processing	Yes
Personal Parameter Key	DS
CAD Attribute Transfer	No
Named Selection Processing	No
Material Properties Transfer	No
CAD Associativity	Yes
Import Coordinate Systems	No
Reader Save Part File	No
Import Using Instances	Yes
Do Smart Update	No
Attach File Via Temp File	Yes
Temporary Directory	C:\Users\bvaaron\AppData\Local\Temp\15771
Analysis Type	3-D
Mixed Import Resolution	None
Enclosure and Symmetry Processing	Yes

**TABLE 3**  
**Model (B4) > Geometry > Parts**

Object Name	<i>Screw Design 2-head diameter 2-base width 0.138</i>
-------------	--

State	Meshed
<b>Graphics Properties</b>	
Visible	Yes
Transparency	1
<b>Definition</b>	
Suppressed	No
Stiffness Behavior	Flexible
Coordinate System	Default Coordinate System
Reference Temperature	By Environment
<b>Material</b>	
Assignment	Titanium Alloy
Nonlinear Effects	Yes
Thermal Strain Effects	Yes
<b>Bounding Box</b>	
Length X	15. mm
Length Y	5.3471 mm
Length Z	5.3471 mm
<b>Properties</b>	
Volume	76.902 mm <sup>3</sup>
Mass	3.5529e-004 kg
Centroid X	-5.2939 mm
Centroid Y	-1.5631e-003 mm
Centroid Z	-1.47e-003 mm
Moment of Inertia Ip1	6.4306e-004 kg·mm <sup>2</sup>
Moment of Inertia Ip2	6.8051e-003 kg·mm <sup>2</sup>
Moment of Inertia Ip3	6.805e-003 kg·mm <sup>2</sup>
<b>Statistics</b>	
Nodes	41155
Elements	21561
Mesh Metric	None

**TABLE 12**

**Model (B4) > Static Structural (B5) > Solution (B6) > Results**

Object Name	<i>Total Deformation</i>	<i>Equivalent Stress</i>
-------------	--------------------------	--------------------------

State	Solved	
<b>Scope</b>		
Scoping Method	Geometry Selection	
Geometry	All Bodies	
<b>Definition</b>		
Type	Total Deformation	Equivalent (von-Mises) Stress
By	Time	
Display Time	Last	
Calculate Time History	Yes	
Identifier		
<b>Results</b>		
Minimum	0. mm	0. MPa
Maximum	9.6689e-002 mm	1733.9 MPa
<b>Information</b>		
Time	1. s	
Load Step	1	
Substep	1	
Iteration Number	1	
<b>Integration Point Results</b>		
Display Option		Averaged



Analysis of 2.4mm head radius

Model (B4)

Geometry

**TABLE 2**  
**Model (B4) > Geometry**

Object Name	<i>Geometry</i>	
State	Fully Defined	
<b>Definition</b>		

Source	C:\Users\bvaaron\Desktop\CAD Designs\Screw Design 2-head diameter 2-base width 0.138-2.4 radius.SLDPRT
Type	SolidWorks
Length Unit	Meters
Element Control	Program Controlled
Display Style	Part Color
<b>Bounding Box</b>	
Length X	15. mm
Length Y	5.3471 mm
Length Z	5.3471 mm
<b>Properties</b>	
Volume	74.945 mm <sup>3</sup>
Mass	3.4625e-004 kg
Scale Factor Value	1.
<b>Statistics</b>	
Bodies	1
Active Bodies	1
Nodes	40131
Elements	20997
Mesh Metric	None
<b>Preferences</b>	
Import Solid Bodies	Yes
Import Surface Bodies	Yes
Import Line Bodies	No
Parameter Processing	Yes
Personal Parameter Key	DS
CAD Attribute Transfer	No
Named Selection Processing	No
Material Properties Transfer	No
CAD Associativity	Yes

Import Coordinate Systems	No
Reader Save Part File	No
Import Using Instances	Yes
Do Smart Update	No
Attach File Via Temp File	Yes
Temporary Directory	C:\Users\bvaaron\AppData\Local\Temp\15771
Analysis Type	3-D
Mixed Import Resolution	None
Enclosure and Symmetry Processing	Yes

**TABLE 3**  
**Model (B4) > Geometry > Parts**

Object Name	<i>Screw Design 2-head diameter 2-base widgth 0.138-2.4 radius</i>
State	Meshed
<b>Graphics Properties</b>	
Visible	Yes
Transparency	1
<b>Definition</b>	
Suppressed	No
Stiffness Behavior	Flexible
Coordinate System	Default Coordinate System
Reference Temperature	By Environment
<b>Material</b>	
Assignment	Titanium Alloy
Nonlinear Effects	Yes
Thermal Strain Effects	Yes
<b>Bounding Box</b>	
Length X	15. mm
Length Y	5.3471 mm

Length Z	5.3471 mm
<b>Properties</b>	
Volume	74.945 mm <sup>3</sup>
Mass	3.4625e-004 kg
Centroid X	-5.4126 mm
Centroid Y	-1.6608e-003 mm
Centroid Z	-1.5083e-003 mm
Moment of Inertia Ip1	5.6598e-004 kg·mm <sup>2</sup>
Moment of Inertia Ip2	6.573e-003 kg·mm <sup>2</sup>
Moment of Inertia Ip3	6.5728e-003 kg·mm <sup>2</sup>
<b>Statistics</b>	
Nodes	40131
Elements	20997
Mesh Metric	None

Static Structural (B5)

**TABLE 12**

**Model (B4) > Static Structural (B5) > Solution (B6) > Results**

Object Name	Total Deformation	Equivalent Stress
State	Solved	
<b>Scope</b>		
Scoping Method	Geometry Selection	
Geometry	All Bodies	
<b>Definition</b>		
Type	Total Deformation	Equivalent (von-Mises) Stress
By	Time	
Display Time	Last	
Calculate Time History	Yes	
Identifier		
<b>Results</b>		
Minimum	0. mm	8.6533e-002 MPa
Maximum	0.10584 mm	1651.1 MPa
<b>Information</b>		
Time	1. s	

Load Step	1	
Substep	1	
Iteration Number	1	
<b>Integration Point Results</b>		
Display Option		Averaged



Analysis of 0.138 base thickness and 2.2 head radius

Geometry

**TABLE 2**  
**Model (B4) > Geometry**

Object Name	<i>Geometry</i>	
State	Fully Defined	
<b>Definition</b>		
Source	C:\Users\bvaaron\Desktop\CAD Designs\Screw Design 2-head diameter 2-base width 0.138-2.2 radius.SLDPRT	
Type	SolidWorks	
Length Unit	Meters	
Element Control	Program Controlled	
Display Style	Part Color	
<b>Bounding Box</b>		
Length X	15. mm	
Length Y	5.3471 mm	
Length Z	5.3471 mm	
<b>Properties</b>		
Volume	73.27 mm <sup>3</sup>	
Mass	3.3851e-004 kg	
Scale Factor Value	1.	
<b>Statistics</b>		

Bodies	1
Active Bodies	1
Nodes	38805
Elements	20187
Mesh Metric	None
<b>Preferences</b>	
Import Solid Bodies	Yes
Import Surface Bodies	Yes
Import Line Bodies	No
Parameter Processing	Yes
Personal Parameter Key	DS
CAD Attribute Transfer	No
Named Selection Processing	No
Material Properties Transfer	No
CAD Associativity	Yes
Import Coordinate Systems	No
Reader Save Part File	No
Import Using Instances	Yes
Do Smart Update	No
Attach File Via Temp File	Yes
Temporary Directory	C:\Users\bvaaron\AppData\Local\Temp\15771
Analysis Type	3-D
Mixed Import Resolution	None
Enclosure and Symmetry Processing	Yes
<b>Material</b>	

Assignment	Titanium Alloy
Nonlinear Effects	Yes
Thermal Strain Effects	Yes
<b>Bounding Box</b>	
Length X	15. mm
Length Y	5.3471 mm
Length Z	5.3471 mm
<b>Properties</b>	
Volume	73.27 mm <sup>3</sup>
Mass	3.3851e-004 kg
Centroid X	-5.5189 mm
Centroid Y	-1.7292e-003 mm
Centroid Z	-1.5429e-003 mm
Moment of Inertia Ip1	5.06e-004 kg·mm <sup>2</sup>
Moment of Inertia Ip2	6.371e-003 kg·mm <sup>2</sup>
Moment of Inertia Ip3	6.3708e-003 kg·mm <sup>2</sup>
<b>Statistics</b>	
Nodes	38805
Elements	20187
Mesh Metric	None

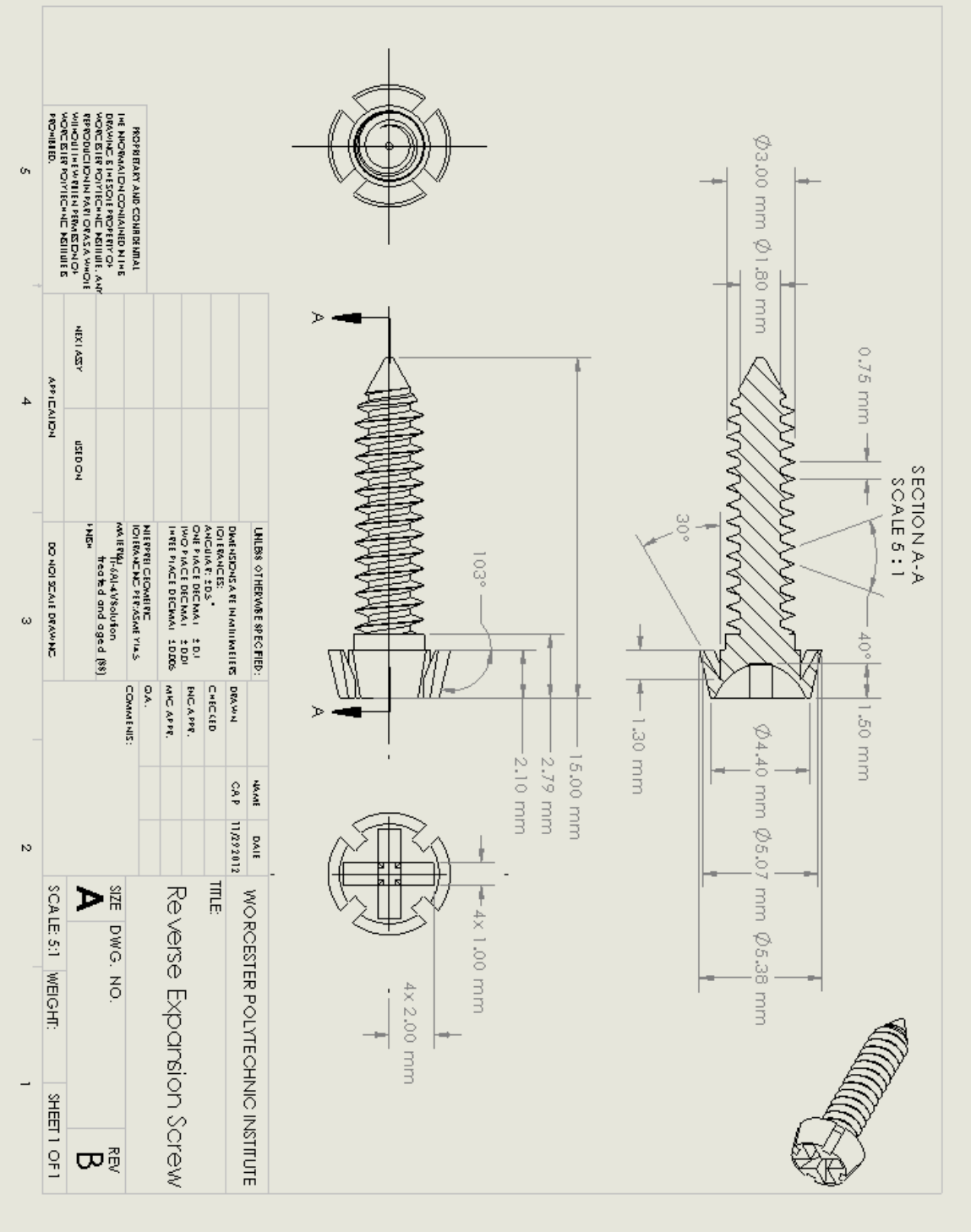
**TABLE 12**

**Model (B4) > Static Structural (B5) > Solution (B6) > Results**

Object Name	<i>Total Deformation</i>	<i>Equivalent Stress</i>
State	Solved	
<b>Scope</b>		
Scoping Method	Geometry Selection	
Geometry	All Bodies	
<b>Definition</b>		
Type	Total Deformation	Equivalent (von-Mises) Stress
By	Time	
Display Time	Last	
Calculate Time History	Yes	
Identifier		

<b>Results</b>		
Minimum	0. mm	0.11054 MPa
Maximum	0.13038 mm	2020.6 MPa
<b>Information</b>		
Time	1. s	
Load Step	1	
Substep	1	
Iteration Number	1	
<b>Integration Point Results</b>		
Display Option		Averaged





PROPRIETARY AND CONFIDENTIAL  
 ALL INFORMATION CONTAINED HEREIN IS UNCLASSIFIED EXCEPT WHERE SHOWN OTHERWISE. ANY REPRODUCTION IN PART OR AS A WHOLE WITHOUT THE WRITTEN PERMISSION OF WORCESTER POLYTECHNIC INSTITUTE IS PROHIBITED.

APPLICATION		DO NOT SCALE DRAWING		SCALE 5:1		SHEET 1 OF 1	
NEXT ASY		DESIGN		DATE		REV	
				11/29/2012		A	
				CAP		B	
				DRAWN		NO.	
				CHECKED		DWG. NO.	
				ENC APP.		A	
				MFC APP.		B	
				DATE		NO.	
				11/29/2012		A	
				CAP		B	
				DRAWN		NO.	
				CHECKED		DWG. NO.	
				ENC APP.		A	
				MFC APP.		B	
				DATE		NO.	
				11/29/2012		A	
				CAP		B	
				DRAWN		NO.	
				CHECKED		DWG. NO.	
				ENC APP.		A	
				MFC APP.		B	
				DATE		NO.	
				11/29/2012		A	
				CAP		B	
				DRAWN		NO.	
				CHECKED		DWG. NO.	
				ENC APP.		A	
				MFC APP.		B	
				DATE		NO.	
				11/29/2012		A	
				CAP		B	
				DRAWN		NO.	
				CHECKED		DWG. NO.	
				ENC APP.		A	
				MFC APP.		B	
				DATE		NO.	
				11/29/2012		A	
				CAP		B	
				DRAWN		NO.	
				CHECKED		DWG. NO.	
				ENC APP.		A	
				MFC APP.		B	
				DATE		NO.	
				11/29/2012		A	
				CAP		B	
				DRAWN		NO.	
				CHECKED		DWG. NO.	
				ENC APP.		A	
				MFC APP.		B	
				DATE		NO.	
				11/29/2012		A	
				CAP		B	
				DRAWN		NO.	
				CHECKED		DWG. NO.	
				ENC APP.		A	
				MFC APP.		B	
				DATE		NO.	
				11/29/2012		A	
				CAP		B	
				DRAWN		NO.	
				CHECKED		DWG. NO.	
				ENC APP.		A	
				MFC APP.		B	
				DATE		NO.	
				11/29/2012		A	
				CAP		B	
				DRAWN		NO.	
				CHECKED		DWG. NO.	
				ENC APP.		A	
				MFC APP.		B	
				DATE		NO.	
				11/29/2012		A	
				CAP		B	
				DRAWN		NO.	
				CHECKED		DWG. NO.	
				ENC APP.		A	
				MFC APP.		B	
				DATE		NO.	
				11/29/2012		A	
				CAP		B	
				DRAWN		NO.	
				CHECKED		DWG. NO.	
				ENC APP.		A	
				MFC APP.		B	
				DATE		NO.	
				11/29/2012		A	
				CAP		B	
				DRAWN		NO.	
				CHECKED		DWG. NO.	
				ENC APP.		A	
				MFC APP.		B	
				DATE		NO.	
				11/29/2012		A	
				CAP		B	
				DRAWN		NO.	
				CHECKED		DWG. NO.	
				ENC APP.		A	
				MFC APP.		B	
				DATE		NO.	
				11/29/2012		A	
				CAP		B	
				DRAWN		NO.	
				CHECKED		DWG. NO.	
				ENC APP.		A	
				MFC APP.		B	
				DATE		NO.	
				11/29/2012		A	
				CAP		B	
				DRAWN		NO.	
				CHECKED		DWG. NO.	
				ENC APP.		A	
				MFC APP.		B	
				DATE		NO.	
				11/29/2012		A	
				CAP		B	
				DRAWN		NO.	
				CHECKED		DWG. NO.	
				ENC APP.		A	
				MFC APP.		B	
				DATE		NO.	
				11/29/2012		A	
				CAP		B	
				DRAWN		NO.	
				CHECKED		DWG. NO.	
				ENC APP.		A	
				MFC APP.		B	
				DATE		NO.	
				11/29/2012		A	
				CAP		B	
				DRAWN		NO.	
				CHECKED		DWG. NO.	
				ENC APP.		A	
				MFC APP.		B	
				DATE		NO.	
				11/29/2012		A	
				CAP		B	
				DRAWN		NO.	
				CHECKED		DWG. NO.	
				ENC APP.		A	
				MFC APP.		B	
				DATE		NO.	
				11/29/2012		A	
				CAP		B	
				DRAWN		NO.	
				CHECKED		DWG. NO.	
				ENC APP.		A	
				MFC APP.		B	
				DATE		NO.	
				11/29/2012		A	
				CAP		B	
				DRAWN		NO.	
				CHECKED		DWG. NO.	
				ENC APP.		A	
				MFC APP.		B	
				DATE		NO.	
				11/29/2012		A	
				CAP		B	
				DRAWN		NO.	
				CHECKED		DWG. NO.	
				ENC APP.		A	
				MFC APP.		B	
				DATE		NO.	
				11/29/2012		A	
				CAP		B	
				DRAWN		NO.	
				CHECKED		DWG. NO.	
				ENC APP.		A	
				MFC APP.		B	
				DATE		NO.	
				11/29/2012		A	
				CAP		B	
				DRAWN		NO.	
				CHECKED		DWG. NO.	
				ENC APP.		A	
				MFC APP.		B	
				DATE		NO.	
				11/29/2012		A	
				CAP		B	
				DRAWN		NO.	
				CHECKED		DWG. NO.	
				ENC APP.		A	
				MFC APP.		B	
				DATE		NO.	
				11/29/2012		A	
				CAP		B	
				DRAWN		NO.	
				CHECKED		DWG. NO.	
				ENC APP.		A	
				MFC APP.		B	
				DATE		NO.	
				11/29/2012		A	
				CAP		B	
				DRAWN		NO.	
				CHECKED		DWG. NO.	
				ENC APP.		A	
				MFC APP.		B	
				DATE		NO.	
				11/29/2012		A	
				CAP		B	
				DRAWN		NO.	
				CHECKED		DWG. NO.	
				ENC APP.		A	
				MFC APP.		B	
				DATE		NO.	
				11/29/2012		A	
				CAP		B	
				DRAWN		NO.	
				CHECKED		DWG. NO.	
				ENC APP.		A	
				MFC APP.		B	
				DATE		NO.	
				11/29/2012		A	
				CAP		B	
				DRAWN		NO.	
				CHECKED		DWG. NO.	
				ENC APP.		A	
				MFC APP.		B	
				DATE		NO.	
				11/29/2012		A	
				CAP		B	
				DRAWN		NO.	
				CHECKED		DWG. NO.	
				ENC APP.		A	
				MFC APP.		B	
				DATE		NO.	
				11/29/2012		A	
				CAP		B	
				DRAWN		NO.	
				CHECKED		DWG. NO.	
				ENC APP.		A	
				MFC APP.		B	
				DATE		NO.	
				11/29/2012		A	
				CAP		B	
				DRAWN		NO.	
				CHECKED		DWG. NO.	
				ENC APP.		A	
				MFC APP.		B	
				DATE		NO.	
				11/29/2012		A	
				CAP		B	
				DRAWN		NO.	
				CHECKED		DWG. NO.	
				ENC APP.		A	
				MFC APP.		B	
				DATE		NO.	
				11/29/2012		A	
				CAP		B	
				DRAWN		NO.	
				CHECKED		DWG. NO.	
				ENC APP.		A	
				MFC APP.		B	
				DATE		NO.	
				11/29/2012		A	
				CAP		B	
				DRAWN		NO.	
				CHECKED		DWG. NO.	
				ENC APP.		A	
				MFC APP.		B	
				DATE		NO.	
				11/29/2012		A	
				CAP		B	
				DRAWN		NO.	

## Appendix F: Protocol for Cyclic Loading and Failure Testing Preparation

Cut between rib pairs, perpendicular to the median line of the Sawbone, using a band saw.



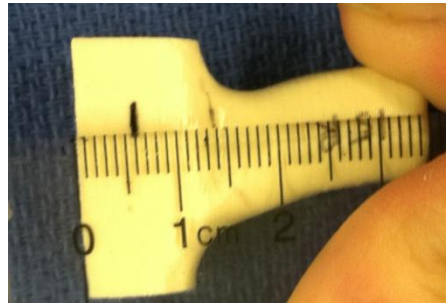
Bisect each pair along the median line using a band saw.



Working with the four middle rib pairs on the Sawbone, score the sides of each of the ribs with a scalpel.



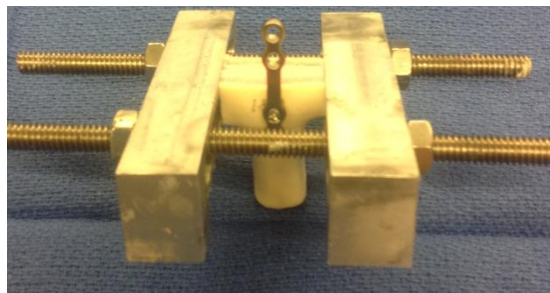
Measure and mark a location 6mm from the median cut on each rib, centered between the superior and inferior cuts.



To attach the plate to the sample, line up end of the plate with the above line, insert a screw into one of the outer holes in the plate and screw it into the sample at the marked location.

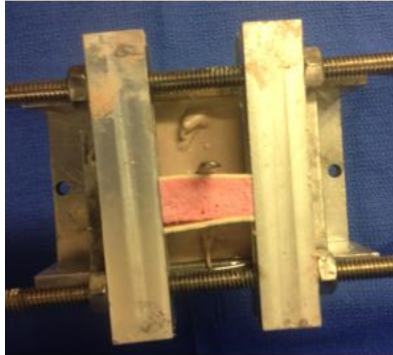


Place the sample between the guide rails for the potting fixture so that the median cut is level with the top of the guide rails, the plate is centered, and the plate remains vertical.

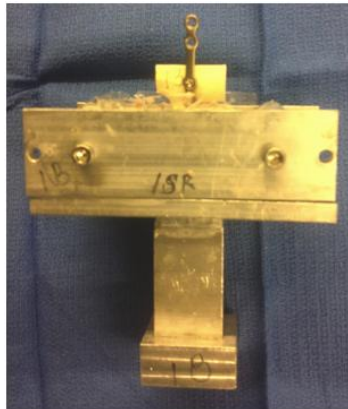


Mix one and a half scoops of Bondo putty according to the package instructions and insert in potting fixture lined with packing tape.

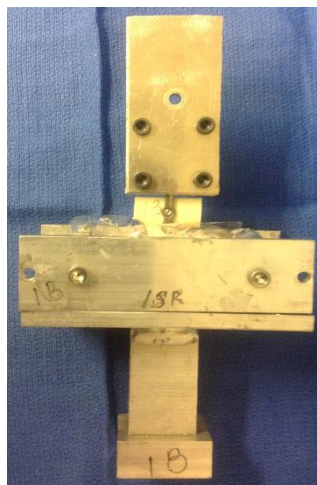
Insert the sample into the putty, using the guiderails to position. Spread putty up the back of the sample to better hold it in place, and leave guiderails in place while the putty hardens.



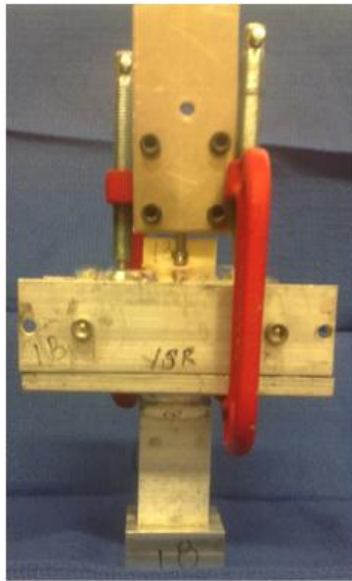
Once hardened, remove the guide rails.



Clamp the plate into the custom grip by inserting between the two pieces of metal, and then tightening the 4 screws.



Clamp C clamps onto diagonal edges of the potting fixture, pressing against the putty and bottom of the fixture.



## Appendix G: Protocol for Cyclic Loading

Turn the Instron machine on and log into the computer. Adjust the ElectroPulse length.

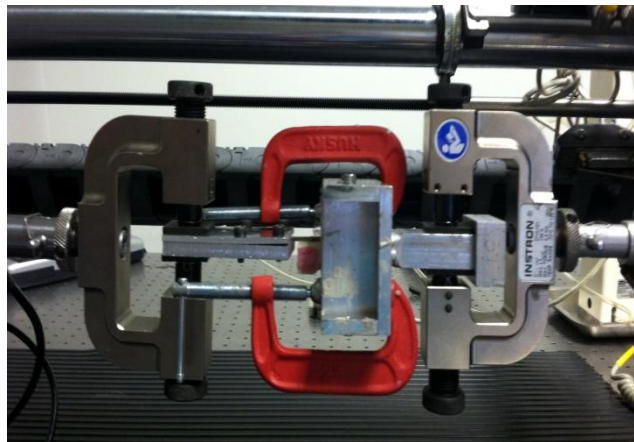
Attach the 2000N load cell onto the Instron machine.

Open the Instron Console Software. Calibrate the load with no grips attached to the Instron.

Adjust the load cell limits to under positive or negative 25 mm.

Attach grips onto the Instron. Balance the load.

Load sample.



Tune the sample and start preliminary testing at a ramp time of 5 seconds, and using increments of 25 and 50 N.

Start cyclic preliminary testing at a frequency of 1 Hz and 2Hz, and forces of 25N and 50N.

Arm the limits of the Instron machine.

Open the Instron WaveMatrix Software.

Open the prepared procedure for sternal cyclic testing and start the test.

## Appendix H: Protocol for Axial Pullout Testing

Working with the remaining end pieces of Sawbones after the middle rib pairs have been removed, simultaneously number the pieces for tracking in the lab notebook.



Insert a small hole onto the surface of the middle of the exposed Sawbone surface using a simple drill bit.



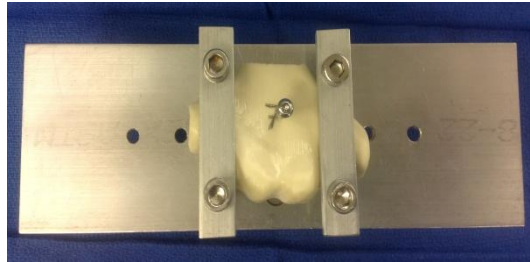
Mark a cortical bone screw at 9mm from the screw tip for cortical testing.



Insert the bone screw into the Sawbone at the hole started by the drill bit, up to the marking on the screw for cortical, or through both sides of the model for bicortical (approximately 14 mm).



Tighten each piece onto the standard plate using the plate's corresponding screws and bars.



Turn the Instron machine on and log into the Bluehill software program.

Load the system onto the Instron machine. Attach a standard Instron tool used to pull the screw out of the Sawbone to the upper grip of the Instron machine and lower it around the screw.



Open the prepared procedure for pull out testing.

Enter the rate of 5mm/min, with the dimensions of a length of 100mm, width of 2 mm, and a height of 3mm.

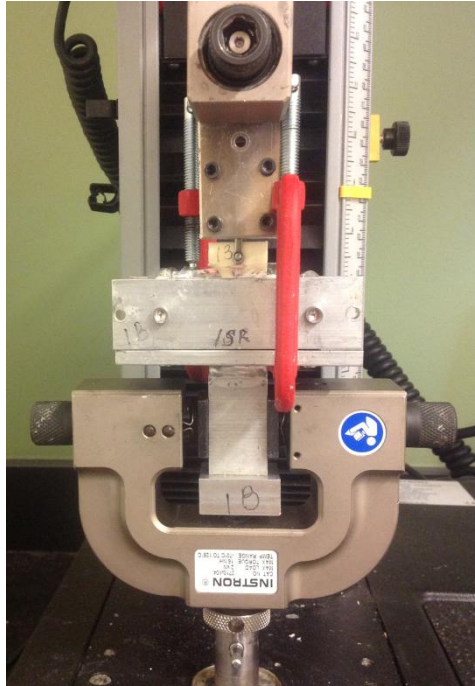
Balance the load of the Instron machine and place the load at an approximate force of 1N using the fine precision knob.

Calibrate the extension and start the test.

## Appendix I: Protocol for Lateral Pullout Testing

Turn the Instron machine on and log into the Bluehill software program.

Using the prepared Sawbones from the previous protocol, secure the custom potting fixture onto the bottom grip of the Instron machine, while also securing the custom plate onto the top grip of the Instron.



Open the prepared procedure for tensile testing in the Bluehill program.

Enter the rate of 5mm/min into the system.

Balance the load of the Instron machine and place the load at an approximate 1 N force using the fine precision knob.

Calibrate the extension and start the test.

## Appendix J: Cyclic Testing Displacement at Each Cycle

Cycles	Displacement (mm)		
	Flush Fit	Gap	Difference
200	0.0288	0.0478	0.0190
400	0.0338	0.0587	0.0249
600	0.0374	0.0657	0.0283
800	0.0400	0.0711	0.0311
1000	0.0421	0.0758	0.0336
2000	0.0488	0.0919	0.0430
3000	0.0535	0.103	0.0498
4000	0.0571	0.114	0.0563
5000	0.0596	0.122	0.0627
6000	0.0616	0.133	0.0715
7000	0.0631	0.143	0.0803
8000	0.0651	0.153	0.0876
9000	0.0665	0.159	0.0923
10000	0.0680	0.166	0.0979
11000	0.0696	0.175	0.105
12000	0.0708	0.182	0.112
13000	0.0722	0.191	0.119
14000	0.0723	0.201	0.128
15000	0.0733	0.211	0.138

## Appendix K: Axial Pullout Testing Maximum Force Sustained

Sample	Unicortical			Bicortical	
	Custom Sawbones	Regular Sawbones	Cancellous only	Custom Sawbones	Regular Sawbones
1	102	96.2	56.6	127	253.7
2	93.8	84.9	48.3	133	374
3	101	86.4	63.8	223	292
4	92.7	97.7	40.3	247	280
5	110	87.8	43.7	188	215
6	102	100	55.7	176	227
7	116	93.1	64.0	133	134
8	91.0	122	54.3	127	352
9	77.9	104	49.9	142	364
10	81.4	118	50.1	197	393
11	96.4	102	52.9	202	463
Mean	96.8 ± 11.3	99.3 ± 6.00	52.7 ± 7.39	172 ± 42.4	304 ± 74.5

## Appendix L: Lateral Pullout Testing Summary Data

Locking Screws:

Sample #	Custom Sawbones			Regular Sawbones		
	9mm	13mm	17mm	9mm	13mm	17mm
1	131	110	212	171	214	165
2	93.0	140	155	205	225	231
3	110	125	162	205	131	215
4	106	125	158	178	173	196
mean	110	125	172	190	186	201
st dev	15.8	12.2	26.8	18.0	43.0	28.4

Non-Locking Screws:

Sample #	Custom Sawbones			Regular Sawbones		
	9mm	13mm	17mm	9mm	13mm	17mm
1	127	158	93.0	114	159	142
2	91.5	101	171	124	174	207
3	117	92.7	139	146	138	136
4	93.6	76.0	106	101	147	214
mean	107	107	127	121	155	175
st dev	17.4	35.5	35.0	18.7	15.6	41.5